NASA CR 5-4812
AGC 8800-59

DEVELOPMENT OF LO_2/LH_2 GAS GENERATORS FOR THE M-1 ENGINE

By

I. Ito

Prepared for

National Aeronautics and Space Administration

Contract NAS 3-2555

AEROJET-GENERAL CORPORATION

SACRAMENTO, CALIFORNIA

Requests for copies of this report should be referred to:

National Aeronautics and Space Administration
Office of Scientific and Technical Information
Attention: AFSS-A
Washington, D. C. 20546

NASA CR-54812
AGC 8800-59

TECHNOLOGY REPORT

DEVELOPMENT OF LO_2/LH_2 GAS GENERATORS FOR THE M-1 ENGINE

Prepared for

NATIONAL AERONAUTICS AND SPACE ADMINISTRATION

1 June 1966

CONTRACT NAS3-2555

Prepared by:

AEROJET-GENERAL CORPORATION
LIQUID ROCKET OPERATIONS
SACRAMENTO, CALIFORNIA

AUTHOR: J. I. Ito

APPROVED: S. C. Datsko
Manager
M-1 Thrust Chamber Project

Technical Management:

NASA LEWIS RESEARCH CENTER
CLEVELAND, OHIO

TECHNICAL MANAGER: A. Fortini

APPROVED: W. W. Wilcox
M-1 Project Manager

ABSTRACT

27739

The current technology for a 120,000 horsepower liquid oxygen/liquid hydrogen gas generator that was successfully designed and tested for the M-1 Engine Program is summarized in this report. Nominal gas generator operating conditions for the 8.125-in. diameter and 20-in. long chamber were: 1145 psia chamber pressure, 110.4 lbm/sec flowrate, and 0.80 mixture ratio. A successful coaxial injector design achieved 98% of theoretical combustion efficiency. Local gas temperature at the chamber exit varied from 900°F to 1300°F. Limited test data with unbaffled injectors indicated injection velocity ratios (fuel injection velocity/oxidizer injection velocity) of approximately 10 might suppress high frequency combustion instability. Low frequency combustion oscillations, which occurred with a low amplitude during the turbopump development tests with gas generator drive, are also discussed in this report.

TABLE OF CONTENTS

		Page
I.	SUMMARY	1
II.	INTRODUCTION	2
III.	TECHNICAL DISCUSSION	5
	A. LARGE THRUST PER ELEMENT GAS GENERATOR ASSEMBLY	5
	B. MULTI-ORIFICE GAS GENERATOR ASSEMBLY	8
	C. COAXIAL GAS GENERATOR ASSEMBLY DESIGN	12
	D. COAXIAL GAS GENERATOR PERFORMANCE AND COMBUSTION GAS TEMPERATURE DISTRIBUTION	28
	E. HIGH FREQUENCY AND LOW FREQUENCY COMBUSTION STABILITY OF M=1 GAS GENERATOR ASSEMBLIES	42
IV.	CONCLUSIONS	69
V.	RECOMMENDATIONS	70
	BIBLIOGRAPHY	72

LIST OF TABLES

No.	Title	Page
I	Large-Thrust-per-Element Gas Generator Assembly Test Results	9
II	Nomenclature and Symbols	27
III	Coaxial Gas Generator Performance	30
IV	Gas Generator Single Injection Element Chugging Data	60

LIST OF FIGURES

No.	Title	Page
1	Serial Number 013 Large-Thrust-per-Element Gas Generator Assembly Injector Face, Pre-Test Run No. 1.2-02-EHG-011	6
2	Serial Number 013 Large-Thrust-per-Element Gas Generator Assembly Injector Face, Post-Test Run No. 1.2-02-EHG-011	7
3	Serial Number 003 Multi-Orifice Gas Generator Assembly Injector Face, Post-Test Run No. 1.2-02-EHG-009	10
4	Serial Number 004 Multi-Orifice Gas Generator Assembly Injector Face, Post-Test Run No. 1.2-02-EHG-005	11
5	Serial Number 007 Multi-Orifice Gas Generator Assembly Injector Face, Post-Test Run No. 1.2-02-EHG-016	13
6	Serial Number 004A Multi-Orifice Gas Generator Assembly Injector Face, Post-Test Run No. 1.2-03-EHG-007	14
7	Coaxial Gas Generator Schematic	15
8	Gas Generator Coaxial Injection Elements (2 Sheets)	16
9	Serial Number 015 Coaxial Gas Generator Assembly Injector Face	18
10	Serial Number 017 Coaxial Gas Generator Assembly Injector Face with Acoustical Liner Installed, Post-Test Run No. 1.2-04-EHG-001	19
11	Serial Number 017A Coaxial Gas Generator Assembly Injector Face, Post-Test Run No. 1.2-04-EHG-010	20

LIST OF FIGURES (Cont'd)

No.	Title	Page
12	Serial Number 018 Coaxial Gas Generator Assembly Injector Face, Post-Test Run No. 1.2-04-EHG-007	21
13	Serial Number 020 Coaxial Gas Generator Assembly Injector Face with Acoustical Liner Installed	22
14	Typical Injector Face Patterns (Serial Numbers 022, 025, and 026)	23
15	Gas Generator Chamber Film Temperature Versus Axial Length of Chamber (Typical)	29
16	Gas Generator Development Test Schematic and Instrumentation	32
17	Gas Generator Chamber Pressure Versus Axial Length of Chamber (Typical)	33
18	Mean Combustion Gas Exit Temperature Versus Gas Generator Mixture Ratio - Serial Number 022 Type Gas Generator Assembly	34
19	Combustion Efficiency of Serial Number 022 Gas Generator Assembly Versus Mixture Ratio and Chamber Pressure	37
20	Typical Gas Generator Assembly Exit Temperature Distribution	38
21	Typical Radial Combustion Gas Temperature Distributions Downstream of Serial Number 022 Type Gas Generator Assembly	39
22	Fuel Turbopump Development Test Schematic with Gas Generator Drive	41
23	Estimated M-1 Gas Generator High Frequency Combustion Instability Zones	44
24	Injector Manifold and Gas Generator Chamber Pressure Versus Time for Test No. 1.2-03-EHG-003 with Serial Number 007 Multi-Orifice Gas Generator Assembly (Over-all Test)	48
25	Injector Manifold and Gas Generator Chamber Pressure Versus Time for Test No. 1.2-03-EHG-006 with Serial Number 015 Coaxial Gas Generator Assembly (Over-all Test)	50

LIST OF FIGURES (Cont'd)

No.	Title	Page
26	Pressures, Injection Velocities, and Velocity Ratio at Spontaneous Initiation of High Frequency Combustion Instability of Serial Number 015 Coaxial Gas Generator Assembly During Test No. 1.2-03-EHG-006 (Typical)	51
27	Pressures, Injection Velocities, and Velocity Ratio at Spontaneous Termination of High Frequency Combustion Instability of Serial Number 015 Coaxial Gas Generator Assembly During Test No. 1.2-03-EHG-006 (Typical)	52
28	Injector Manifold and Gas Generator Chamber Pressure Versus Time for Test No. 1.2-03-EHG-007 with Serial Number 004A Multi-Orifice Gas Generator Assembly (Over-all Test)	55
29	Injector Manifold and Gas Generator Chamber Pressure Versus Time for Test No. 1.2-04-EHG-011 with Serial Number 020 Coaxial Gas Generator Assembly (Over-all Test)	56
30	Fuel Injector Manifold Temperature and Injection Velocity Ratio Effect on High Frequency Combustion Instability	58
31	Injection Velocity Ratio Effect on Gas Generator Single Injection Element Chugging	61
32	Oxidizer Injection Velocity Effect on Gas Generator Single Injection Element Chugging	62
33	Oxidizer Injector Pressure Drop Effect on Gas Generator Single Injection Element Chugging	63

I. SUMMARY

The M-1 gas generator development program was initiated to provide a source of high pressure, homogeneous combustion gases to drive the fuel and oxidizer turbopump turbines during the operation of the M-1 engine. Both the fuel and oxidizer turbines were to be driven in series with a single gas generator. The fuel turbine was designed to deliver 90,000 hp and the oxidizer turbine 27,000 hp. The turbines drive their respective fuel and oxidizer pumps which, in turn, supply high pressure liquid hydrogen and liquid oxygen to the engine thrust chamber assembly as well as to the gas generator.

To achieve the turbine horsepower requirements, the gas generator was nominally designed for 110.4 lbm/sec total propellant flowrate at a mixture ratio of 0.8 to supply 1000°F combustion gases. Gas generator chamber pressures (Pc) were recorded from 750 to 1145 psia. Peripheral tests were conducted for mixture ratio excursions from 0.6 to 1.0 at steady-state conditions. Approximately 98% of theoretical combustion efficiency was achieved with the final coaxial injector design based upon characteristic exhaust velocity calculations. Typical combustion gas exit temperatures measured at the gas generator outlet ranged from 900 to 1300°F at nominal mixture ratio.

A coaxial injection element injector design with a cylindrical fuel film-cooled combustion chamber proved to be successful and was selected as the prototype gas generator from three basic injector concepts. Other concepts evaluated were the multi-orifice type injector and a pentad, large-thrust-per-element injector design.

Severe injector face and combustion chamber wall erosion occurred during the initial test of the large-thrust-per-element injector concept. Although design modifications could have solved the gas generator erosion problem, no further development was attempted because of the long combustor mixing length that would have been required to achieve homogeneous gas temperature in front of the turbine inlet.

Minor injector face erosion occurred with all pattern variations of the multi-orifice injector design. Of the multi-orifice injector patterns tested, the uniformly spaced, like-on-like impinging doublet with radially aligned fuel-oxidizer-fuel impingement fans encountered the least face erosion. It was indicated from work with the J-2 and RL-10 thrust chambers as well as with various NASA Lewis Research Center injectors that favorable combustion performance and stability was being obtained with coaxial injection element designs for the liquid oxygen/liquid hydrogen propellant combination. Therefore, it was assumed that a coaxial gas generator could be developed in less time and at lower cost, and further development effort with the multi-orifice designs was terminated.

During gas generator development tests of unbaffled injector designs, tangential modes of high frequency combustion instability occurred in four tests. Two of these tests were with multi-orifice injectors and the remaining two tests were with serial numbers 015 and 020 coaxial injector gas generator assemblies. High frequency

combustion instability spontaneously occurred in all four tests during the start transient when the injection velocity ratio (fuel injection velocity/oxidizer injection velocity) was less than four. Because of a shift in the test conditions during all four unstable, unbaffled injector tests, the injection velocity ratio exceeded the normal steady-state values. When the injection velocity ratio exceeded approximately 9 in the three tests with the first tangential mode and when it exceeded 5.7 in the test with the second tangential mode, the high frequency combustion instability was spontaneously suppressed during all four tests. Thereafter, combustion continued with only the normal combustion noise until the end of the tests. Based upon observations during these four unbaffled injector tests, it was suspected that a correlation existed between injection velocity ratios and the occurrence or disappearance of high frequency combustion instability. The stabilizing effect of injection velocity ratio appears to be primarily caused by liquid phase mixing and liquid oxygen droplet vaporization phenomena. Liquid oxygen combustion dynamics are suspected of being the primary cause of high frequency combustion instability.

Several coaxial injection gas generator element designs, one of which was selected for the prototype gas generator, were evaluated by using a single element injector test apparatus. Several element designs with nominal injection velocity ratios from 15 to 20 were rejected because of their severe chugging characteristics. A nominal velocity ratio of 10 was selected for the prototype gas generator assemblies. This lower value was achieved by decreasing the oxidizer injection area to obtain a higher oxidizer injection velocity, thus resulting in a lower fuel/oxidizer velocity ratio.

Throughout the initial gas generator development test series, excellent low frequency combustion stability characteristics were demonstrated by the prototype coaxial gas generator assembly. The measured injector pressure drops of 215 psia and 240 psia for the fuel and oxidizer, respectively, were obtained during nominal gas generator operation. When the gas generator exhaust duct downstream of the sonic gas generator stabilizing nozzle was replaced with the turbopump turbine inlet test manifold, attempts were made to maintain all other test facility and hardware systems intact and follow earlier successfully demonstrated test procedures. However, when the turbopump development test series with gas generator drive was initiated, a persistent low frequency combustion oscillation phenomena was experienced. However, the steady-state amplitude of the oscillations ($\pm$ 30 psi at 1145 P_c, 120 cps) were not detrimental to turbopump operation. Seven oxidizer turbopump and two fuel turbopump development tests were conducted with gas generator drive. The nature and origin of low frequency combustion oscillations is not yet fully understood.

II. INTRODUCTION

The development of the M-1 gas generator assembly for the M-1 Engine Program is delineated in this report. Development testing of the M-1 gas generator assembly was conducted at the Aerojet-General Corp., Sacramento, California during the period

May 1963 to December 1965 for the NASA Lewis Research Center, Cleveland, Ohio under Contract NAS3-2555.

Some liquid oxygen/liquid hydrogen gas generator test data was available at Aerojet-General and from the J-2 gas generator but it was largely limited to multi-orifice type injectors. However, a coaxial injection element gas generator had been tested at NASA/LeRC[1] on a smaller scale. The NASA gas generator was typical of most applicable liquid oxygen/liquid hydrogen gas generator designs prior to the M-1 gas generator assembly development effort. It operated a single 1000 hp turbopump whereas a single M-1 gas generator assembly operates both a 90,000 hp fuel turbopump in series with a 27,000 hp oxidizer turbopump. The NASA gas generator assembly total flowrate of 0.890 lbm/sec had to be extrapolated to 110.4 lbm/sec to satisfy M-1 gas generator assembly requirements. The lowest mode transverse combustion instability frequency of the 2.00-in. diameter NASA gas generator assembly chamber was 19,000 cps and baffles were not required. Previously, the only possible screeching modes for gas generators were of the longitudinal variety. The 4500 cps first tangential combustion instability frequency of the 8.125-in. diameter M-1 gas generator assembly chamber was experienced and eventually required the use of injector baffles. Hardware erosion may not have been as severe a problem with previous gas generators because of their lower chamber pressures and consequently, their lower erosive heat fluxes.

The purpose of the gas generator development program was to provide a gas generator to power the fuel and oxidizer pumps for the prototype M-1 engine configuration. The initial phase of the program consisted of design, fabrication, and testing of three basic injector concepts with the expectation that the first design of the three to be successful would be selected for further refinement. The three injector concepts were the drilled multi-orifice, the large-thrust-per-element, and coaxial injector designs. The three types of gas generator assemblies were designed, fabricated, and tested. Development of the large-thrust-per-element injector was terminated because of severe injector face and chamber wall erosion as well as significant thermal striations in the combustion gas stream that resulted from poor mixing. Development of the J-2 and RL-10 injectors as well as research work being conducted at NASA/LeRC indicated that satisfactory combustion performance and stability data were being obtained from liquid oxygen/liquid hydrogen with coaxial injection element injectors. Although both the J-2 and RL-10 were thrust chamber injectors operating at higher mixture ratios, it was assumed the coaxial injection element data would also be applicable to the M-1 gas generator assembly. Therefore, continued testing and development effort was undertaken with the coaxial injector design only.

Prior to discontinuing the multi-orifice development effort, three unbaffled

---

[1] Sekas, N. J. and Acker, L. W., Design and Performance of a Liquid-Hydrogen, Liquid-Oxygen Gas Generator for Driving a 1000-Horsepower Turbine, NASA TN D-1317, 1962

M-1 gas generator assembly injectors had experienced high frequency combustion instability. Two of the injectors were multi-orifice and the other was of a coaxial type. It had previously been observed that high frequency combustion instability was more likely for liquid oxygen/liquid hydrogen at low hydrogen injection temperatures. One method of quantitatively rating the "screech margin" of an injector had been to conduct tests with successively lower hydrogen injection temperatures until screeching was encountered. Because the M-1 engine was being designed for deep space applications, the low hydrogen temperature was unavoidable. The M-1 gas generator assembly operated with 40 to 60°R hydrogen temperature.

During mid-1964 it was disclosed that liquid oxygen/liquid hydrogen injector research work being performed at NASA/LeRC indicated a possible injection velocity ratio effect upon screeching. Re-analysis of data from all three unstable, unbaffled M-1 gas generator assembly tests upon this same basis also inferred a like relationship. Review of the data also indicated that among other momentary shifts in test conditions with these normally low injection velocity ratio injectors, high frequency combustion instability was spontaneously suppressed when the injection velocity ratio exceeded approximately 10.

A critical need existed for an operable gas generator assembly for impending turbopump development tests and a review of available technological data was conducted in November 1964 for all liquid oxygen/liquid hydrogen coaxial injection elements. As a result, the features incorporated into S/N 022 gas generator assembly were a relatively high injection velocity ratio, baffles, a counterbored-showerhead oxidizer element, oxidizer element recess, adequate chamber and baffle film cooling, a porous faceplate, improved injector and injection element structural design. Serial No. 022 gas generator assembly was fabricated and successfully tested in early February 1965. Excellent performance and combustion stability data were obtained.

The first test of S/N 022 gas generator assembly with prototype gas generator valves on the turbopump development test stand resulted in chugging instability during the start transient. This was caused by low mixture ratio and low oxidizer $\triangle P$ resulting from the flow characteristic of the new valve. Previous tests were conducted with interim (modified Titan) valves. Gaseous helium augmentation of the oxidizer system during the start transient eliminated all traces of chugging during the next three tests by increasing the oxidizer $\triangle P$. The chugging problem was considered solved. However, chugging was encountered during subsequent turbopump development tests even with gaseous helium augmentation. There are aspects of the chugging problem that still are not fully understood. No adverse effects to turbopump development tests were attributable to gas generator chugging and the turbopump development testing was completed.

Some of the problems encountered during the M-1 gas generator assembly development tests were unique to the gas generator component development test conditions. The primary difference occurred in the propellant pressurization transient with tank-fed systems as compared to the transient predicted for the engine with turbo-

pump pressurization. Differences in development facility feed systems and hot gas system from the final planned engine configuration must also be expected to result in differences with engine gas generator performance.

III. TECHNICAL DISCUSSION

A. LARGE-THRUST-PER-ELEMENT GAS GENERATOR ASSEMBLY

The large-thrust-per-element injector consisted of four quadrants of pentad elements. Each pentad element had an oxidizer orifice in the center with four impinging fuel jets (see Figure No. 1). The oxidizer stream was directed axially and each fuel stream impinged at a 30 degree included half-angle. The injector faceplate was made of 0.19-in. thick solid plate stainless steel except for the porous plate disc at the center. The porous plate was transpiration cooled by hydrogen.

Severe injector face and combustion chamber wall erosion occurred during the only large-thrust-per-element gas generator test conducted (see Figure No. 2). The dense, large diameter oxidizer stream did not permit adequate liquid phase mixing of the propellants prior to combustion and resulted in localized high combustion mixture ratios.

At a design mixture ratio of 0.80, the M-1 gas generator assembly operates at one-tenth of stoichiometric conditions. Twenty moles of hydrogen and one mole of oxygen are injected under cryogenic conditions to be combusted. When initially reacted, the combustion products yield two moles of water (whose stoichiometric reaction temperature exceeds 6000°F) and 18 moles of excess hydrogen. It is only after the two moles of water and 18 moles of hydrogen reach thermal equilibrium that the design homogeneous gas temperature of 1000°F is attained. By concentrating the total oxidizer flow through only four injection orifices with the large-thrust-per-element injector design, the core of each pentad element remains oxidizer-rich and thus nearly at stoichiometric temperature regardless of the excess hydrogen around each element.

By injecting the total propellant flowrate through four discrete points on the injector face, high mass injection momentum is achieved directly under each pentad element. However, there is zero injection momentum on the remainder of the injector face. When combustion occurred downstream of the injection elements, local static pressures in the combustion zone exceeded the static injector face pressures in the zero injection momentum areas and caused the combustion gas flow to recirculate back toward the injector face. The flame recirculation pattern can be determined by closely inspecting its erosive action upon the injector face shown in Figure No. 2.

The pentad element produces a four-pointed flame pattern with the points oriented between the fuel injection elements. Sets of three fuel film coolant holes were drilled at each flame point. Coolant holes drilled adjacent to the chamber

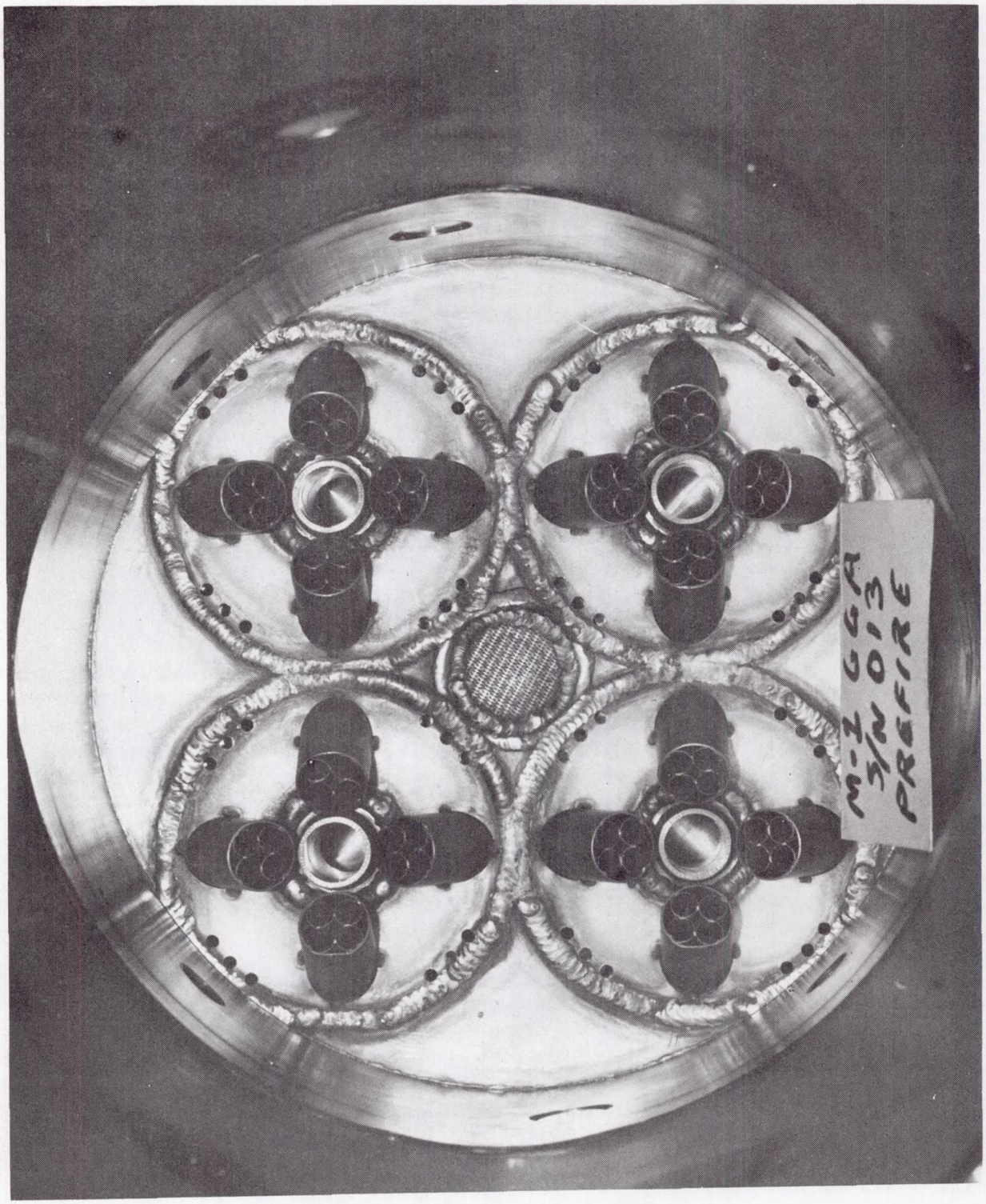

Figure 1

Serial Number 013 Large-Thrust-per-Element Gas Generator

Assembly Injector Face, Pre-Test Run No. 1.2-02-EHG-011

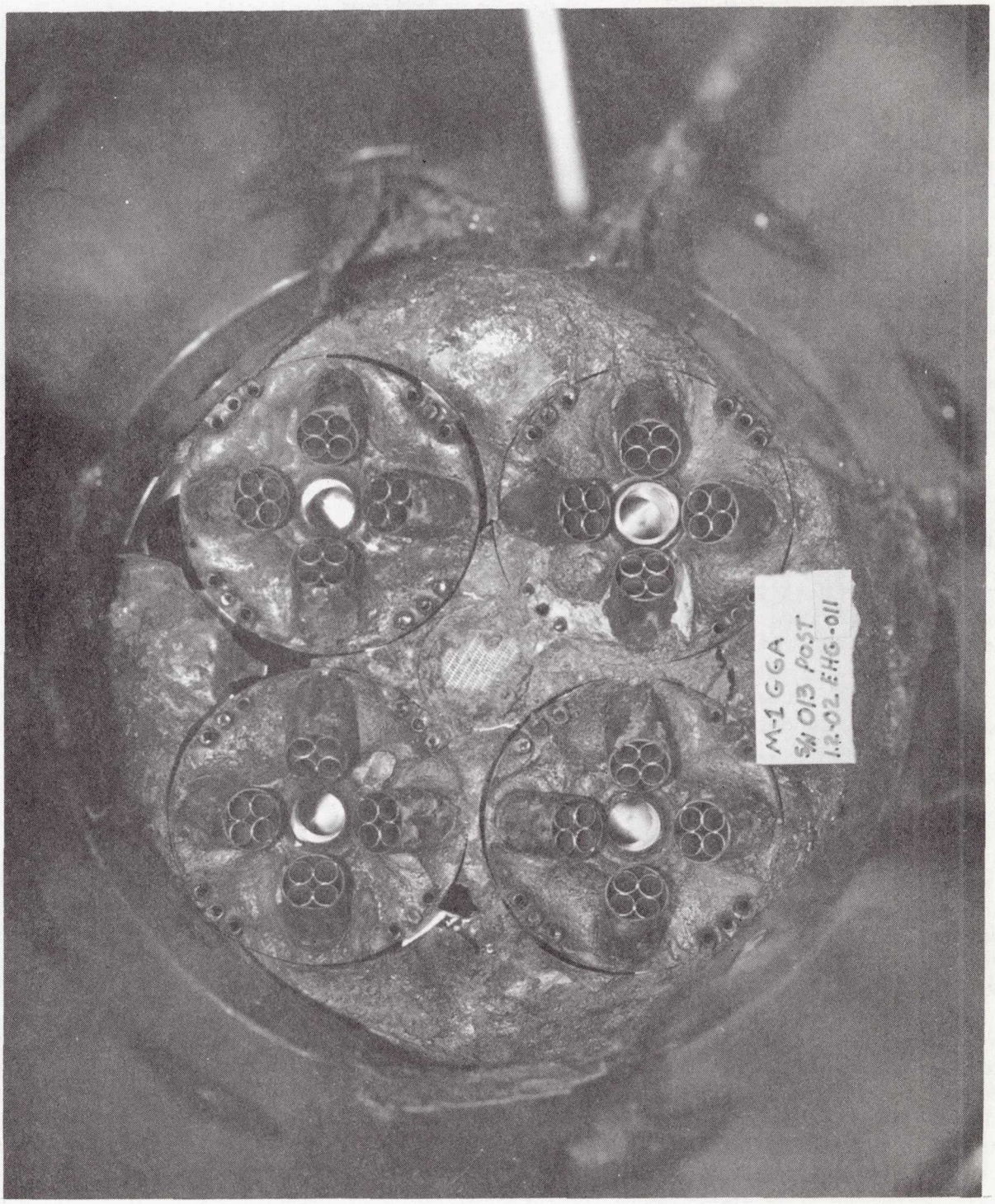

Figure 2

Serial Number 013 Large-Thrust-per-Element Gas Generator Assembly Injector Face, Post-Test Run No. 1.2-02-EHG-011

wall were effective in protecting the wall against erosion even though the flame was close to the wall. Fuel coolant flows at points removed from the chamber wall were dispersed by the flame and were not effective. The severely eroded areas along the chamber wall occurred along the combustion flame points.

The hydrogen-cooled porous plate disc at the axis of the injector was free from erosion. It appeared that a porous faceplate injector could be designed to solve the face erosion problem. Additional fuel film cooling injected along the chamber wall could probably have protected the chamber wall against erosion. However, combustion gas temperature distribution data, shown in Table I indicated that excessive mixing length would have been required to produce homogeneous gas temperatures before entering the turbine. All of the large-thrust-per-element injector concept development effort was terminated.

B. MULTI-ORIFICE GAS GENERATOR ASSEMBLY

The multi-orifice injector design incorporated alternate fuel (four) and oxidizer (three) concentric channels machined into the injector body. Concentric rings were welded over the channels to form the injector faceplate. The rings were then drilled to provide fuel and oxidizer injection orifices. Prior to development of the M-1 gas generator assembly, the bulk of the liquid oxygen/liquid hydrogen data at gas generator mixture ratios had been obtained with multi-orifice injectors.

Fourteen gas generator tests were conducted with multi-orifice injectors and moderate success was achieved. Major development problems were high frequency combustion instability, which was encountered on two occasions, and minor injector faceplate erosion, which occurred with all of the assemblies tested.

Serial No. 003 gas generator assembly injector pattern consisted of alternate channels of showerhead oxidizer orifices and impinging pairs of fuel orifices (see Figure No. 3). Impinging orifice pairs produce a fan of propellant normal to their line of impingement. Baffles were used to divide the injector into four quadrants. Faceplate erosion occurred because of combustion gas recirculation. The worst areas of erosion were around the showerhead oxidizer orifices, between the oxidizer and fuel channels, and in the void areas between fuel injection pairs.

Serial No. 004 gas generator assembly utilized a like-on-like injector pattern with both oxidizer and fuel self-impinging pairs as shown in Figure No. 4. Four-bladed injector baffles similar to those used on S/N 003, were used. The areas where the least face erosion occurred were where an impinging oxidizer pair was radially aligned with fuel impinging pairs along both the inner and outer channels. The baffles were eroded downstream of the outermost oxidizer channel.

Serial No. 007 gas generator assembly was designed upon the basis of test results with S/N 004. The four-bladed baffle was eliminated to more effectively utilize the available injector face area and to avoid further baffle erosion problems. Oxidizer pairs were aligned radially with fuel pairs in adjacent channels.

TABLE I

LARGE-THRUST-PER-ELEMENT GAS GENERATOR ASSEMBLY TEST RESULTS

Gas Generator Assembly Serial Number:	013
Injector Type:	LT/E, Pentad
Test No.:	1.2-02-EHG-011
Test Duration:	3.4 sec
PcGG (3½-in. from Injector Face):	755 psia
$\dot{w}$tGG:	98.8 lb/sec
MRGG:	0.83
Comb. Eff., η :	92%

Hot Gas Temperature Distribution (32-in. from Injector Face):

Parameter	Temperature, (°F)	Radial Distance From Chamber Axis (in.)	Angular Location With Reference To Oxidizer Torus Inlet (Degrees)
TgTS-2A	687	3/4	115
TgTS-2B	1621	1/4	135
TgTS-2C	1258	1 1/4	75
TgTS-2D	731	2 1/4	15
TgTS-2E	1185	3	315
TgTS-2F	236	3 3/4	255

NOTE: TgTS-2A: Gas Temperature, Turbine Simulator, Station 2, Position A; etc.

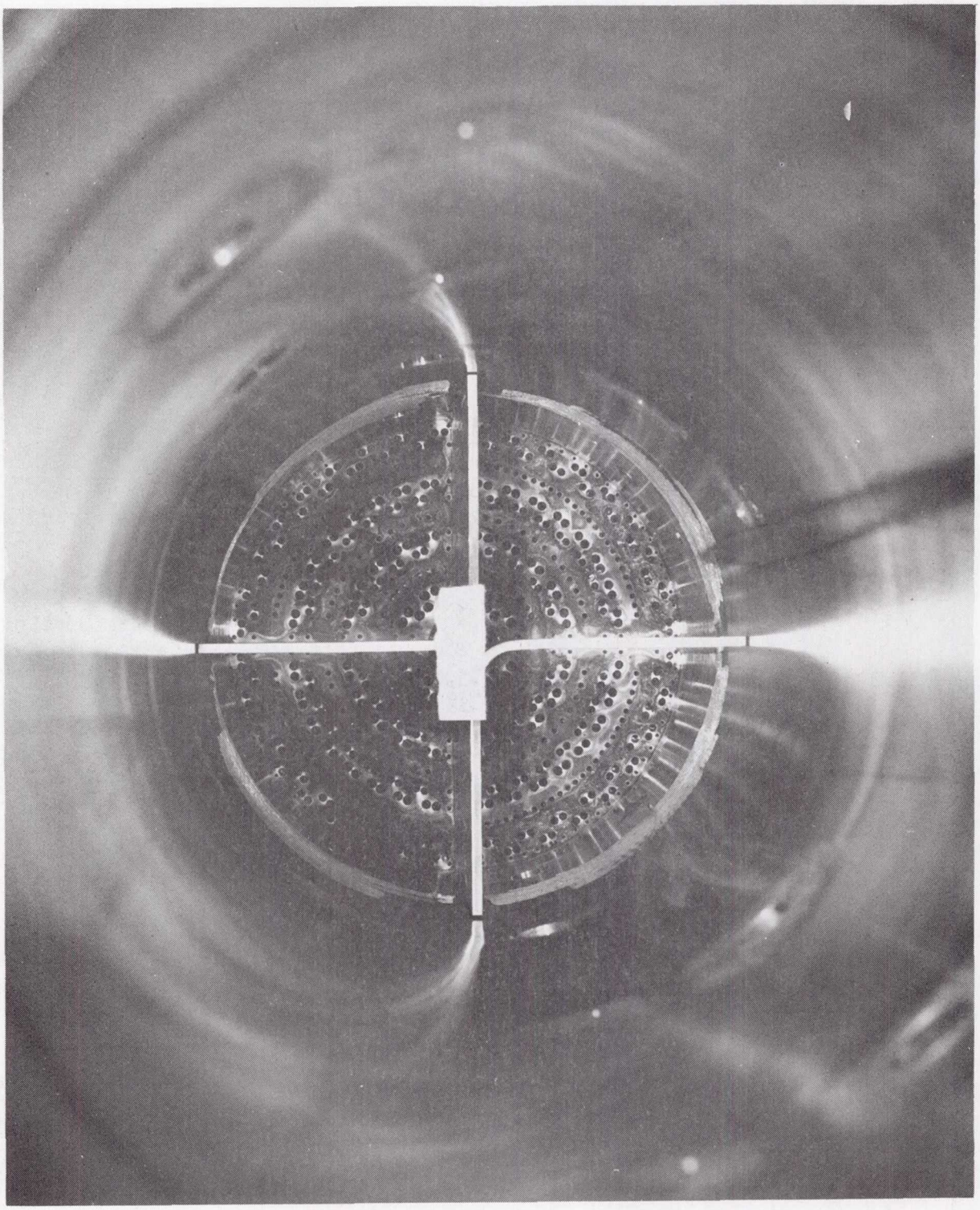

Figure 3

Serial Number 003 Multi-Orifice Gas Generator

Assembly Injector Face, Post-Test Run No. 1.2-02-EHG-009

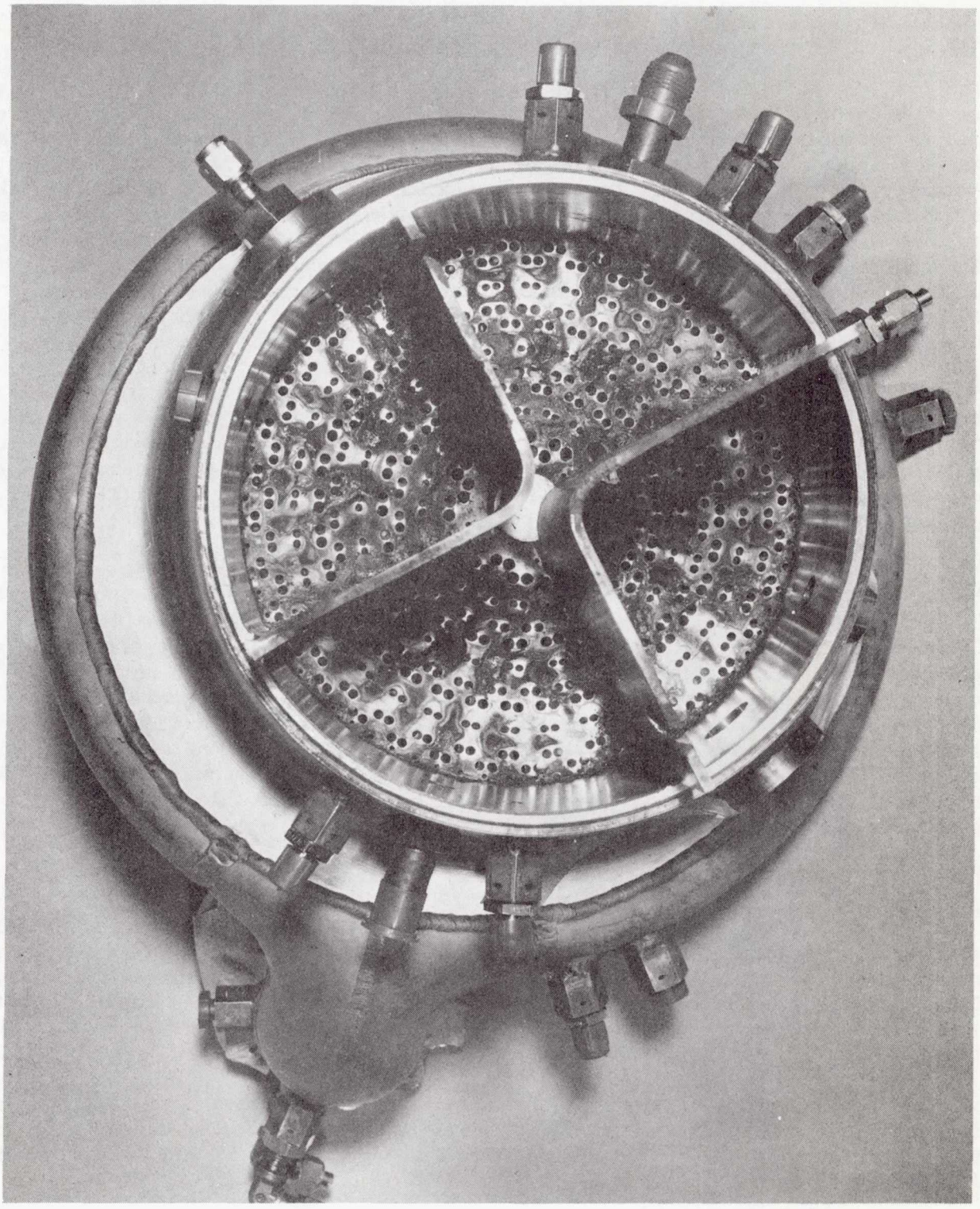

Figure 4

Serial Number 004 Multi-Orifice Gas Generator

Assembly Injector Face, Post-Test Run No. 1.2-02-EHG-005

The pattern was moderately free of face erosion as shown in Figure No. 5. The worst erosion occurred in areas void of injection orifices. The voids were conducive to erosion by recirculatory combustion gases. Although the injector pattern was drilled with six-point symmetry, the face erosion occurred with four-point symmetry. Furthermore, the areas where maximum erosion occurred were under the four oxidizer cross-feed slots to the oxidizer channels. This indicated injector manifolding was at least as significant in determining face erosion characteristics as the injector drill pattern. One instance of high frequency combustion instability occurred during the eighth test of this unbaffled injector assembly. This is discussed in Section III.E.

Serial No. 004 injector was reworked into S/N 004A (Figure No. 6) to incorporate a finer grid that would minimize void injection areas to reduce face erosion between injection orifices. Also, the baffles were removed. The first tangential mode of high frequency combustion instability occurred with this injector pattern. The worst area of face erosion was under the oxidizer channels. The circumferential erosion pattern is typical of first tangential instability modes. The combustion stability characteristics are discussed in Section III.E.

Although it appeared that a successful multi-orifice gas generator could be developed, this effort was discontinued in favor of the coaxial-type injector. It appeared that a coaxial gas generator could be developed in less time and with less expenditure. Successful performance and combustion stability data was being obtained using the liquid oxygen/liquid hydrogen propellant combination with coaxial injection elements. Some of the liquid oxygen/liquid hydrogen rocket engines utilizing the coaxial element were the J-2, RL-10, and various research injectors such as those at the Lewis Research Center. Most of the development work with coaxial elements had been accomplished at higher thrust chamber mixture ratios, but it appeared likely that much of the data would also be applicable at the lower M-1 gas generator mixture ratio.

C. COAXIAL GAS GENERATOR ASSEMBLY DESIGN

A total of 39 tests were conducted with seven coaxial injection element gas generator assemblies. Of these tests, seven oxidizer turbopump assembly tests and two fuel turbopump assembly tests were conducted with gas generator drive. The last three assemblies (S/N 022, 025, and 026) were tested with a common injection element design because of its successful performance. These same assemblies were used for the nine turbopump development tests.

A cross-sectional view of the coaxial gas generator injector and chamber assembly is shown in Figure No. 7. Cross-sections of injection elements tested are shown in Figure No. 8. Injector faces of these coaxial assemblies are included in Figures No. 9 through 14.

The earlier versions of coaxial injection element designs incorporated some type of oxidizer swirler. Its purpose was to induce vorticity to the liquid

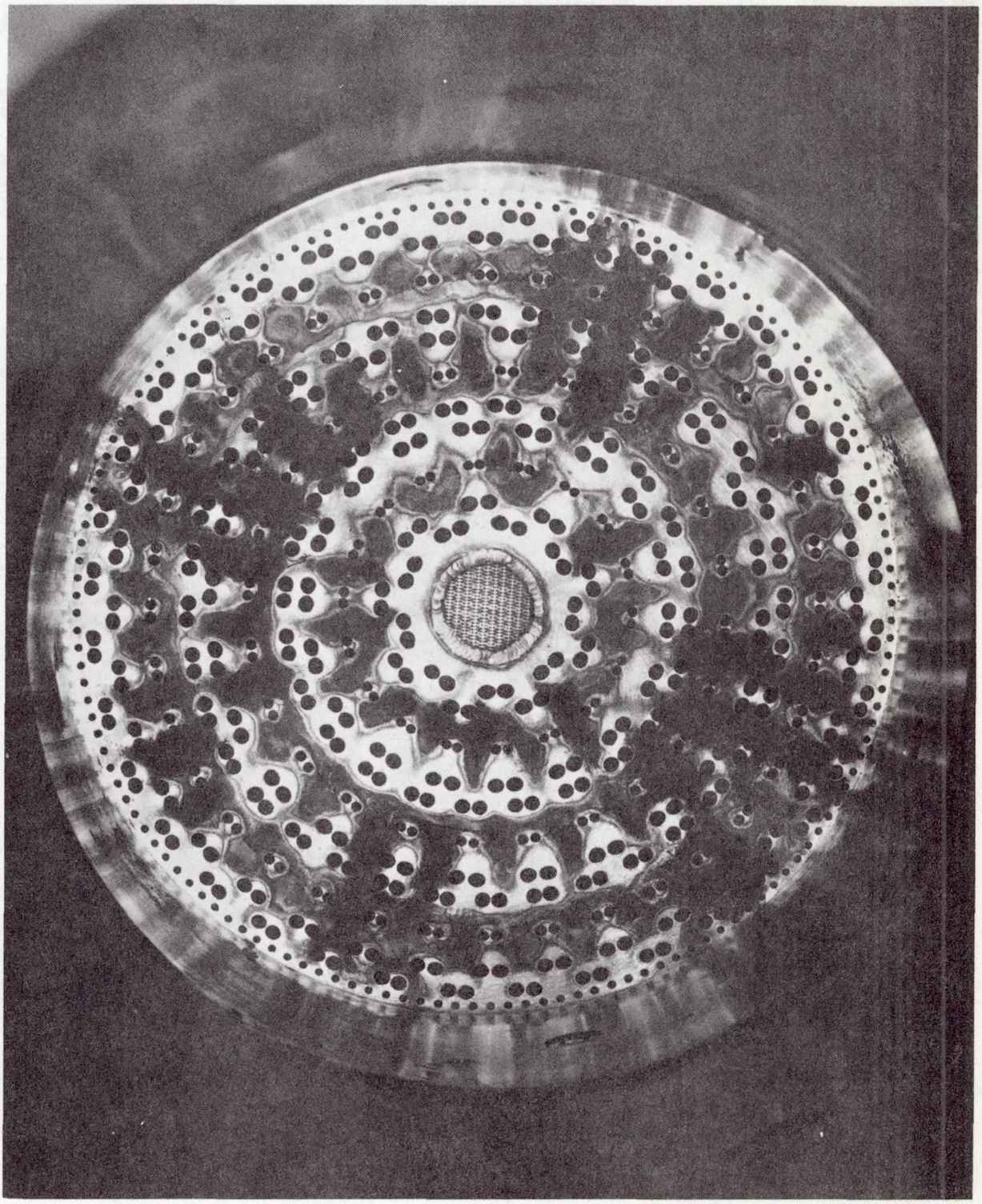

Figure 5

Serial Number 007 Multi-Orifice Gas Generator

Assembly Injector Face, Post-Test Run No. 1.2-02-EHG-016

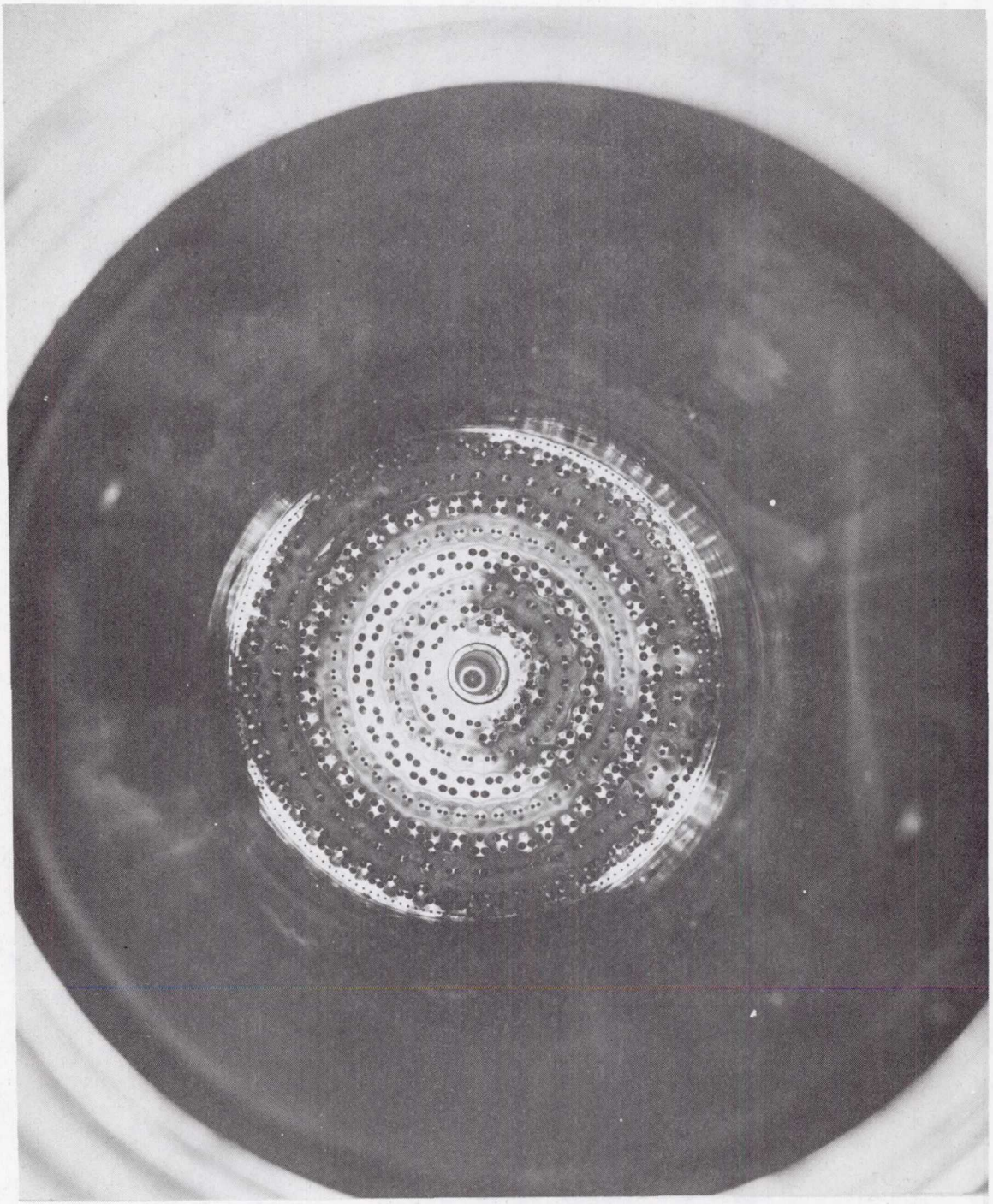

Figure 6

Serial Number 004A Multi-Orifice Gas Generator Assembly Injector Face, Post-Test Run No. 1.2-03-EHG-007

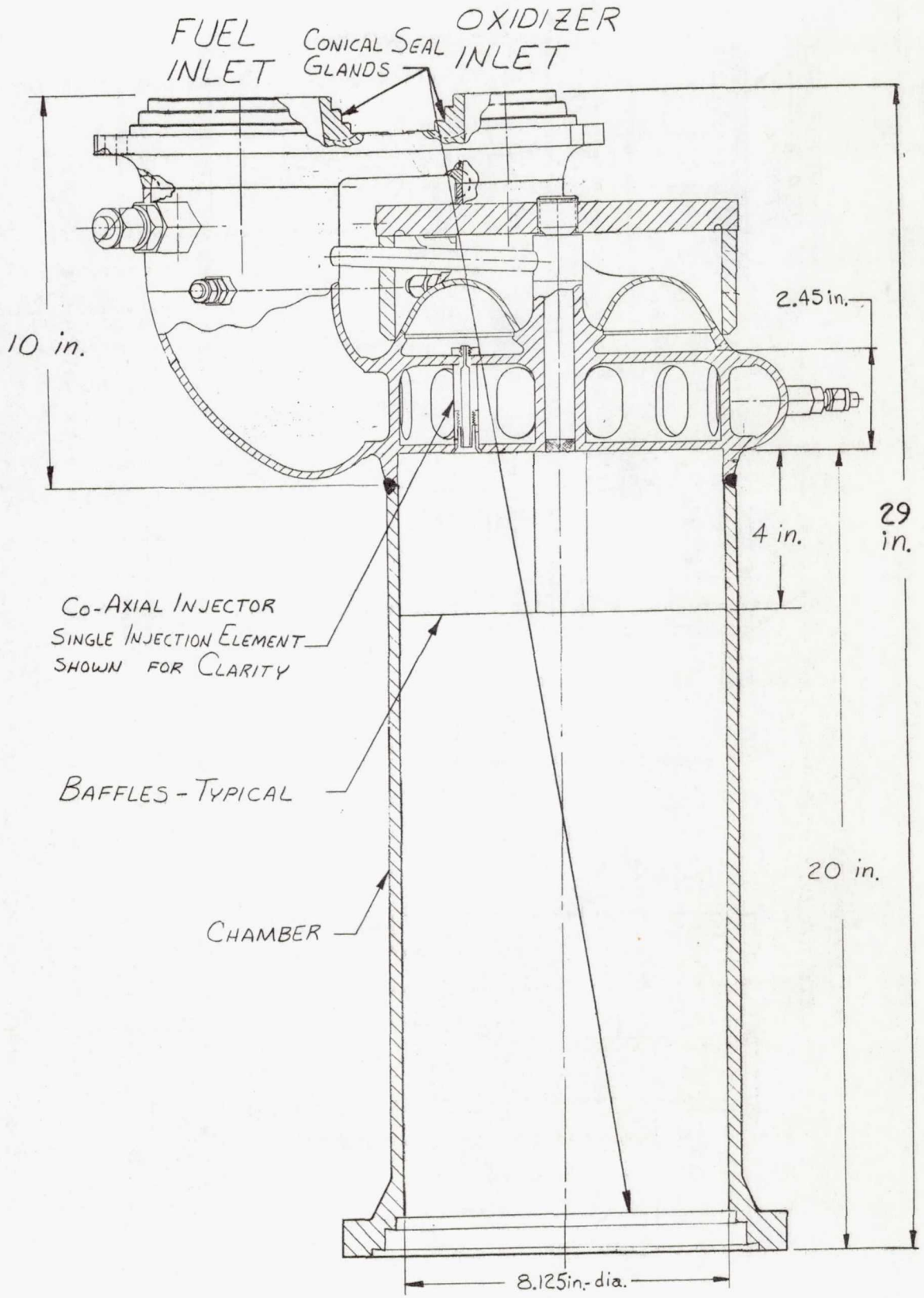

Figure 7

Coaxial Gas Generator Schematic

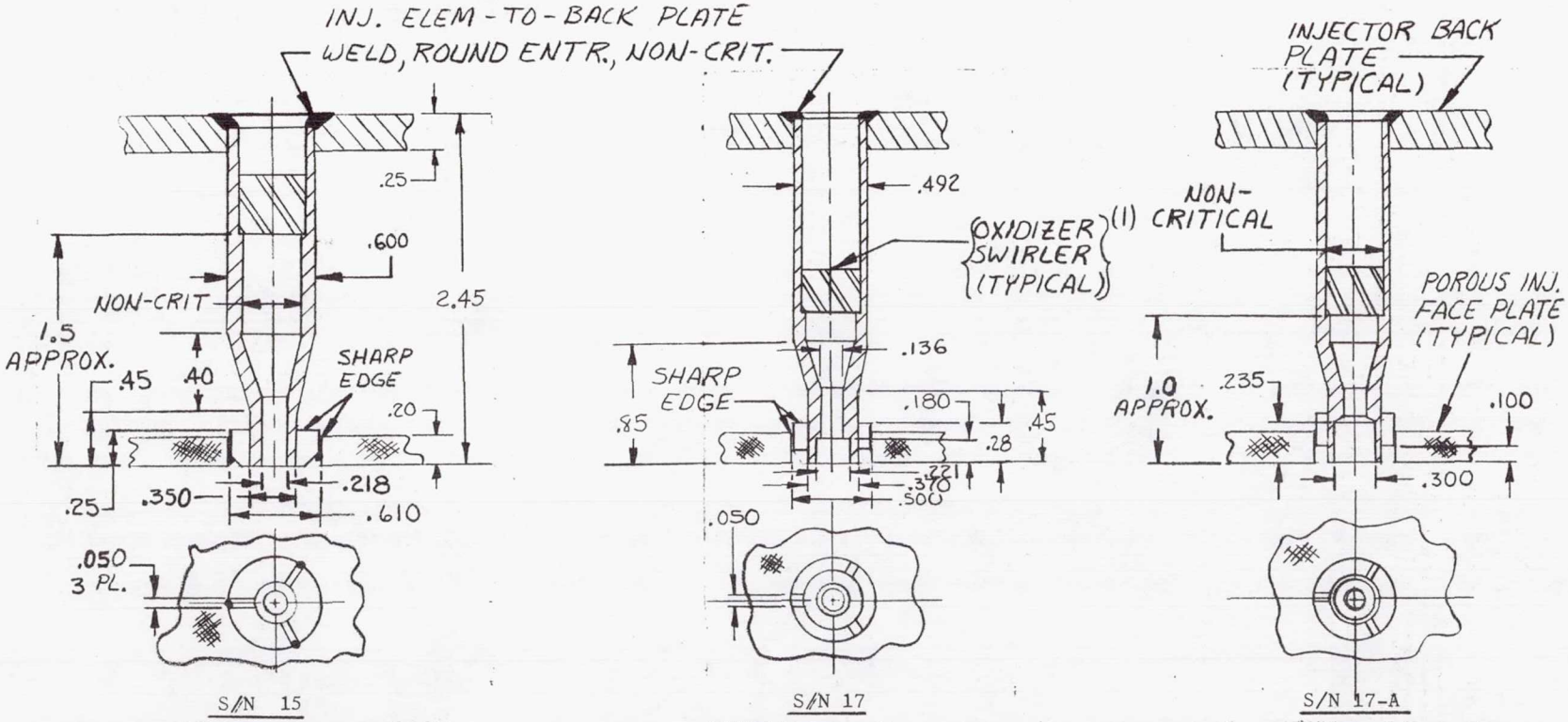

	S/N 15	S/N 17	S/N 17-A
ΔP_f (PSI):	120	165	155
ΔP_o (PSI):	100	145	140
V_f / V_o:	4.0	9.1 (2)	16.7 (2)
P_f / P_o:	.063	.063	.063

(1) OXIDIZER SWIRLER DESIGN DETERMINED EMPIRICALLY WITH HYDRAULIC FLOW MODELS TO ACHIEVE DESIRED ELEMENT PRESSURE DROP AND SPRAY CHARACTERISTICS.

(2) BASED UPON ASSUMED FULL FLOW AT OXIDIZER ELEMENT COUNTERBORE

Figure 8 (Sheet 1 of 2)

Gas Generator Coaxial Injection Elements

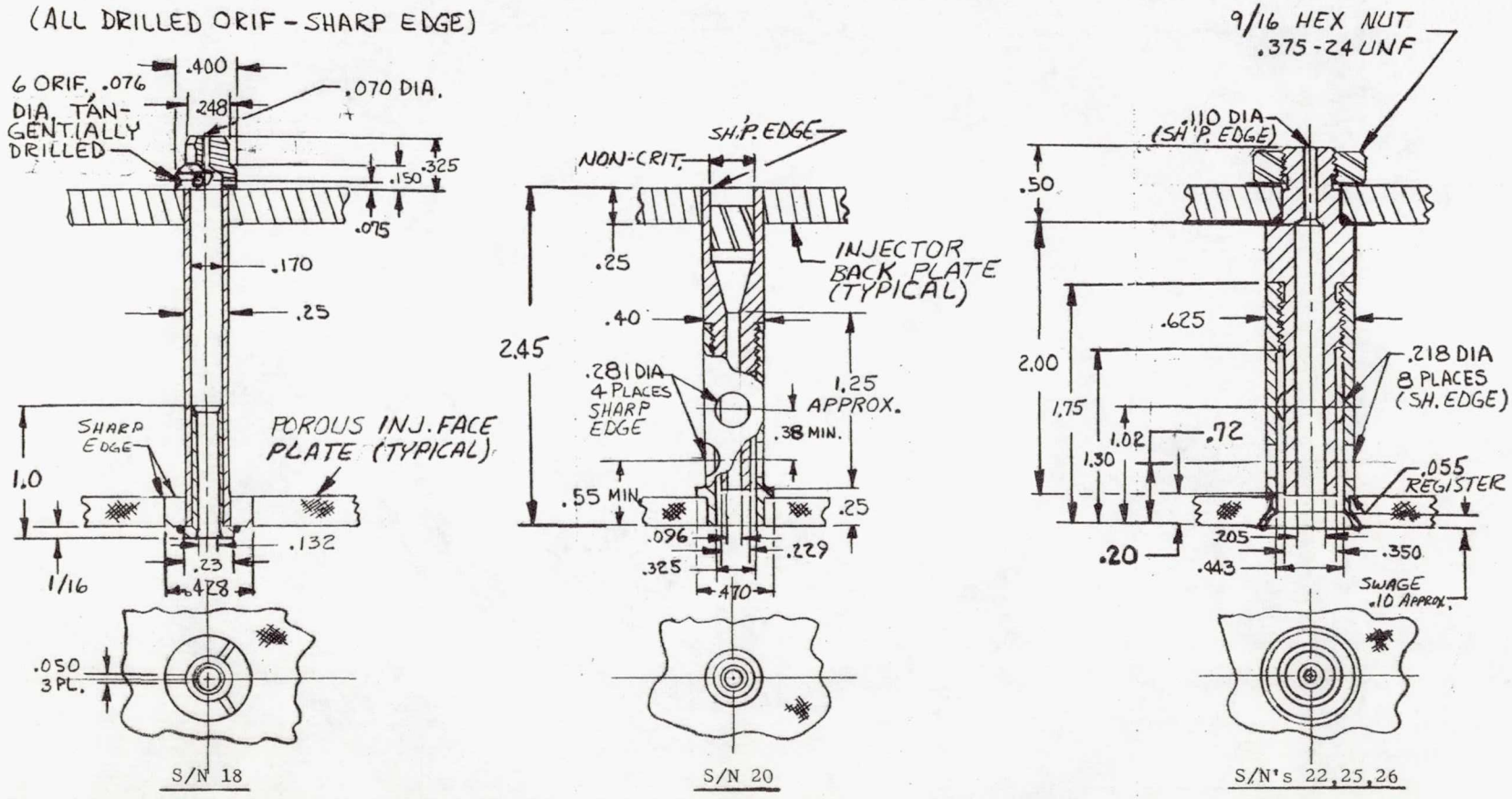

ΔP_f (PSI) :	145	245	215
ΔP_o (PSI) :	160	265	240
V_f/V_o :	3.0	3.2	10.0
ρ_f/ρ_o :	.063	.065	.065

Figure 8 (Sheet 2 of 2)

Gas Generator Coaxial Injection Elements

Figure 9

Serial Number 015 Coaxial Gas Generator Assembly Injector Face

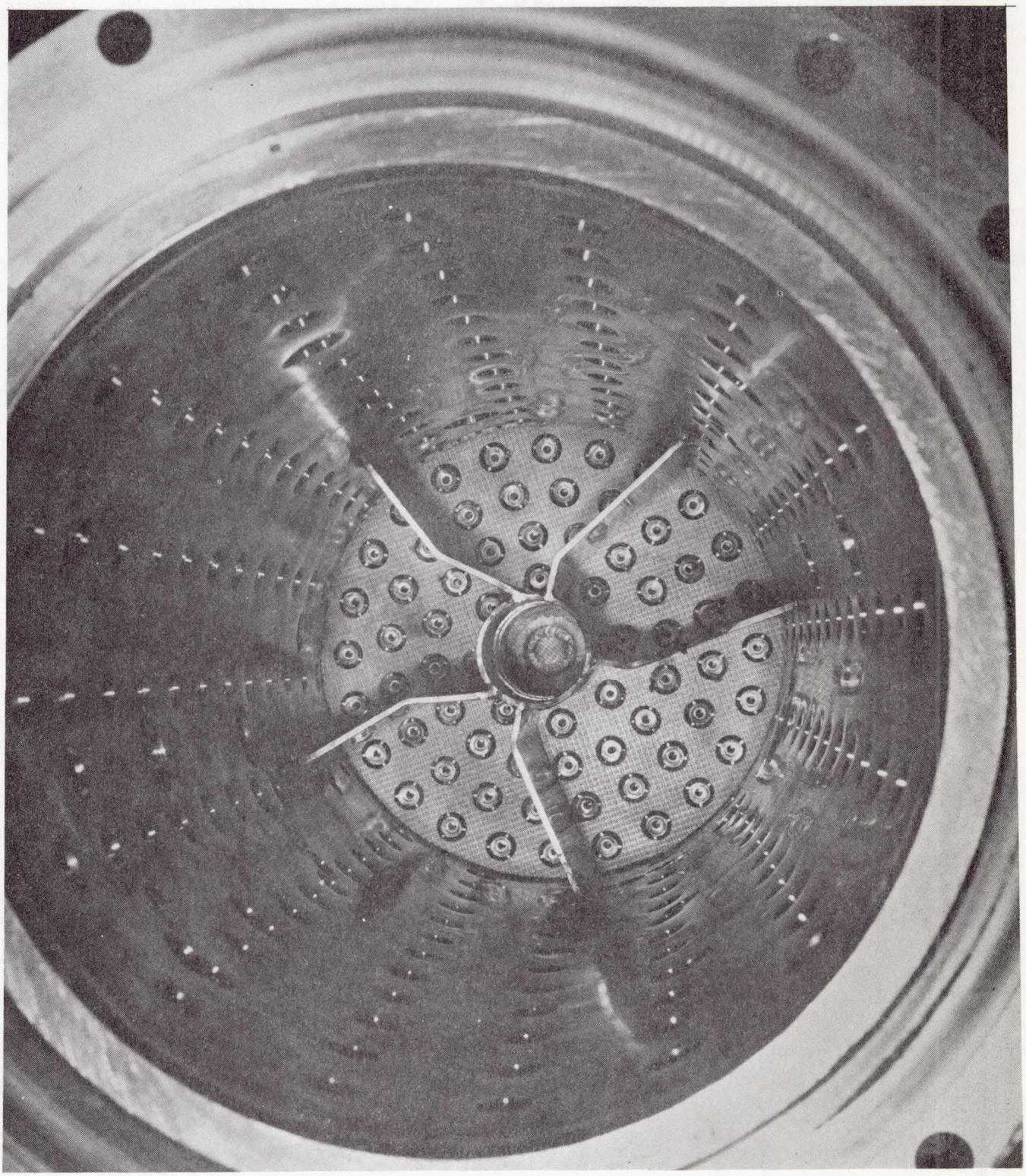

Figure 10

Serial Number 017 Coaxial Gas Generator Assembly Injector Face

with Acoustical Liner Installed, Post-Test Run No. 1.2-04-EHG-001

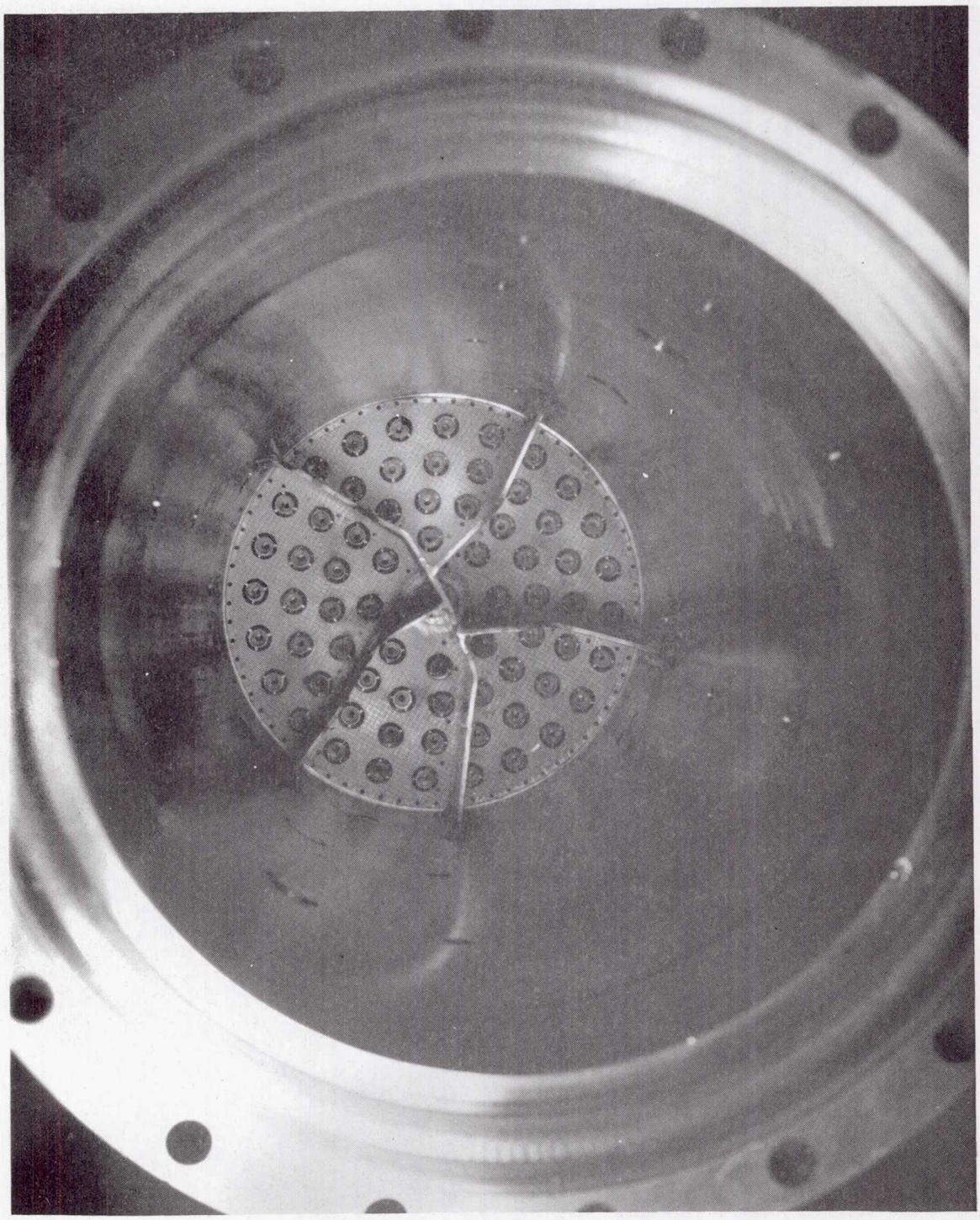

Figure 11

Serial Number 017A Coaxial Gas Generator Assembly

Injector Face, Post-Test Run No. 1.2-04-EHG-010

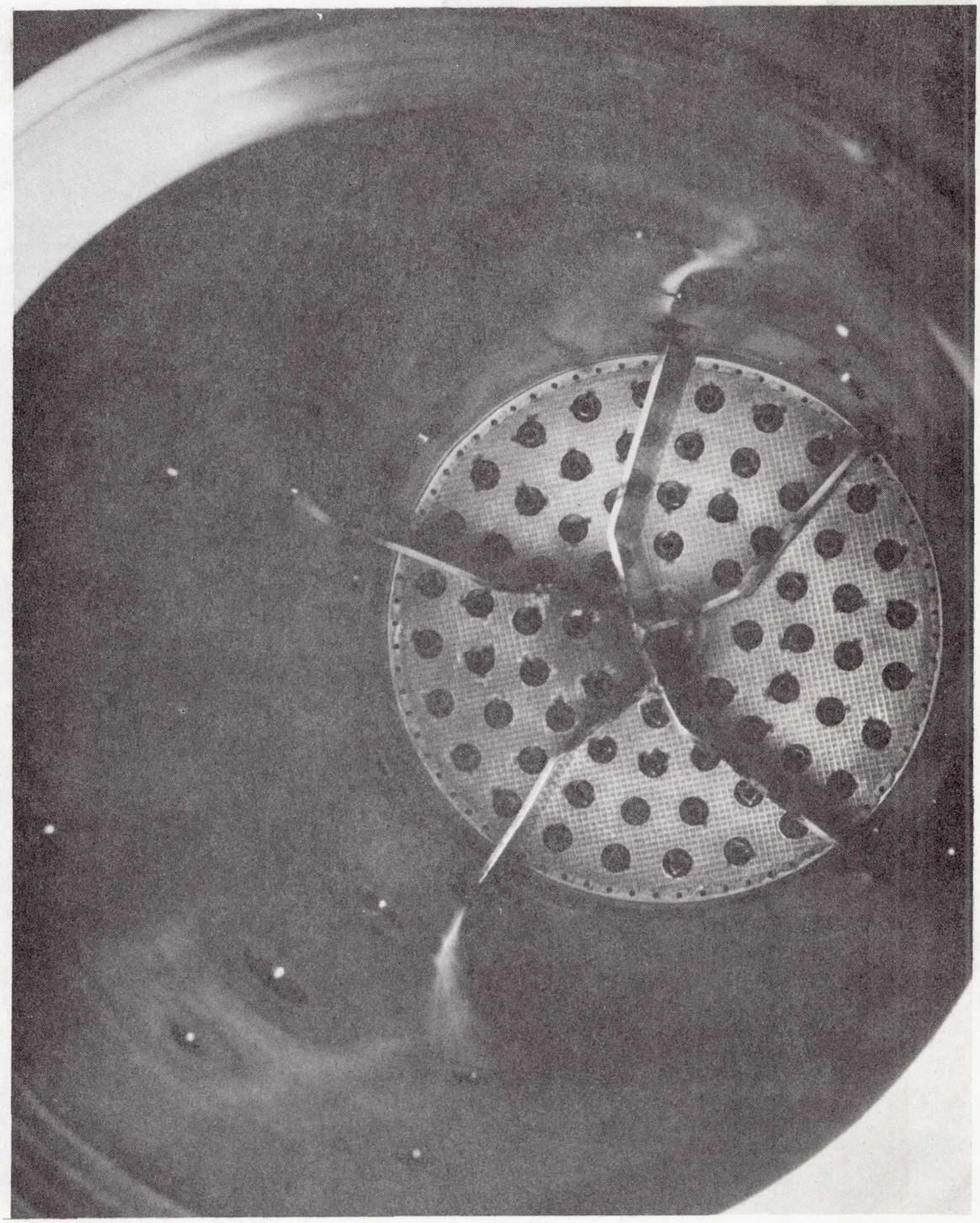

Figure 12

Serial Number 018 Coaxial Gas Generator Assembly

Injector Face, Post-Test Run No. 1.2-04-EHG-007

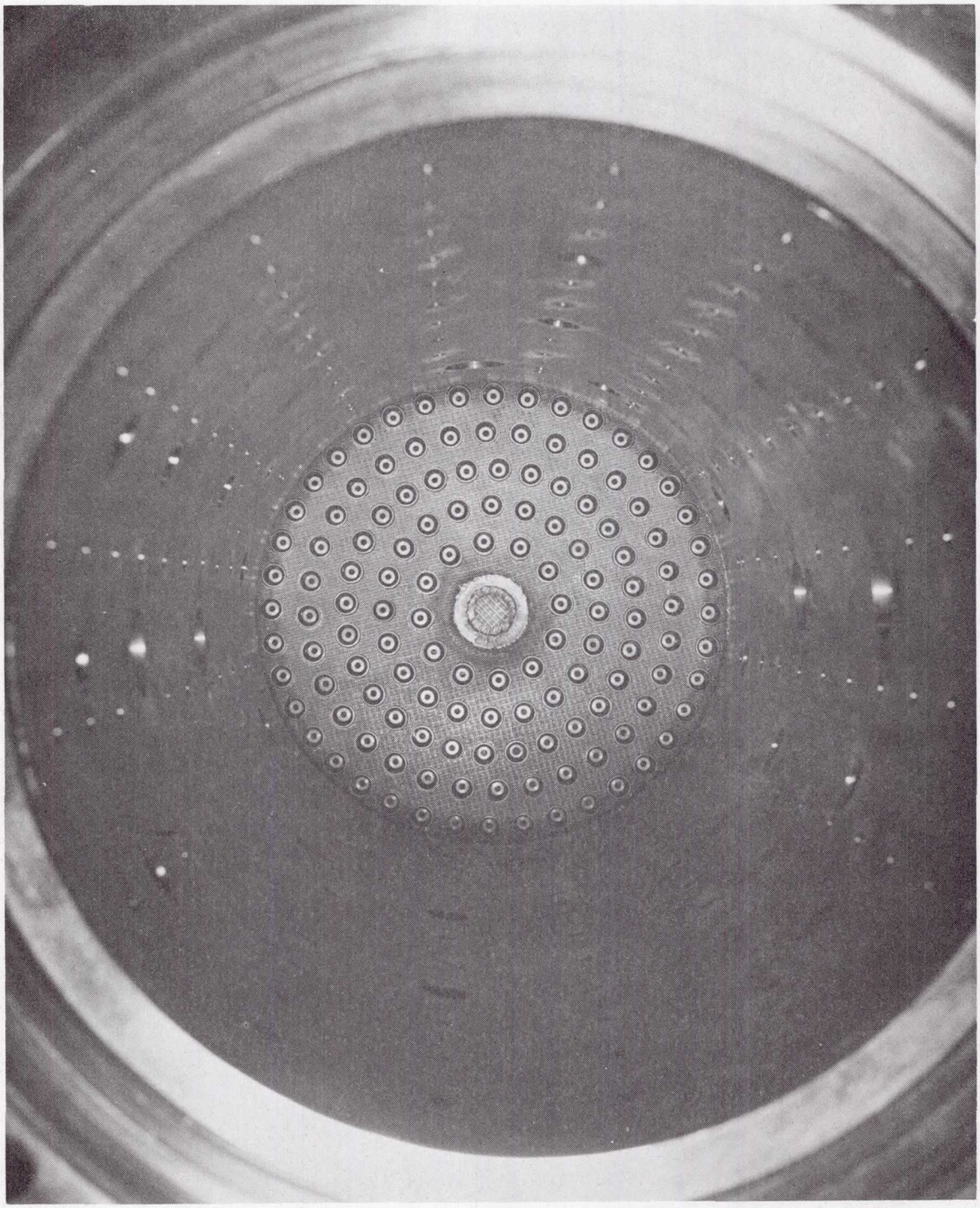

Figure 13

Serial Number 020 Coaxial Gas Generator

Assembly Injector Face with Acoustical Liner Installed

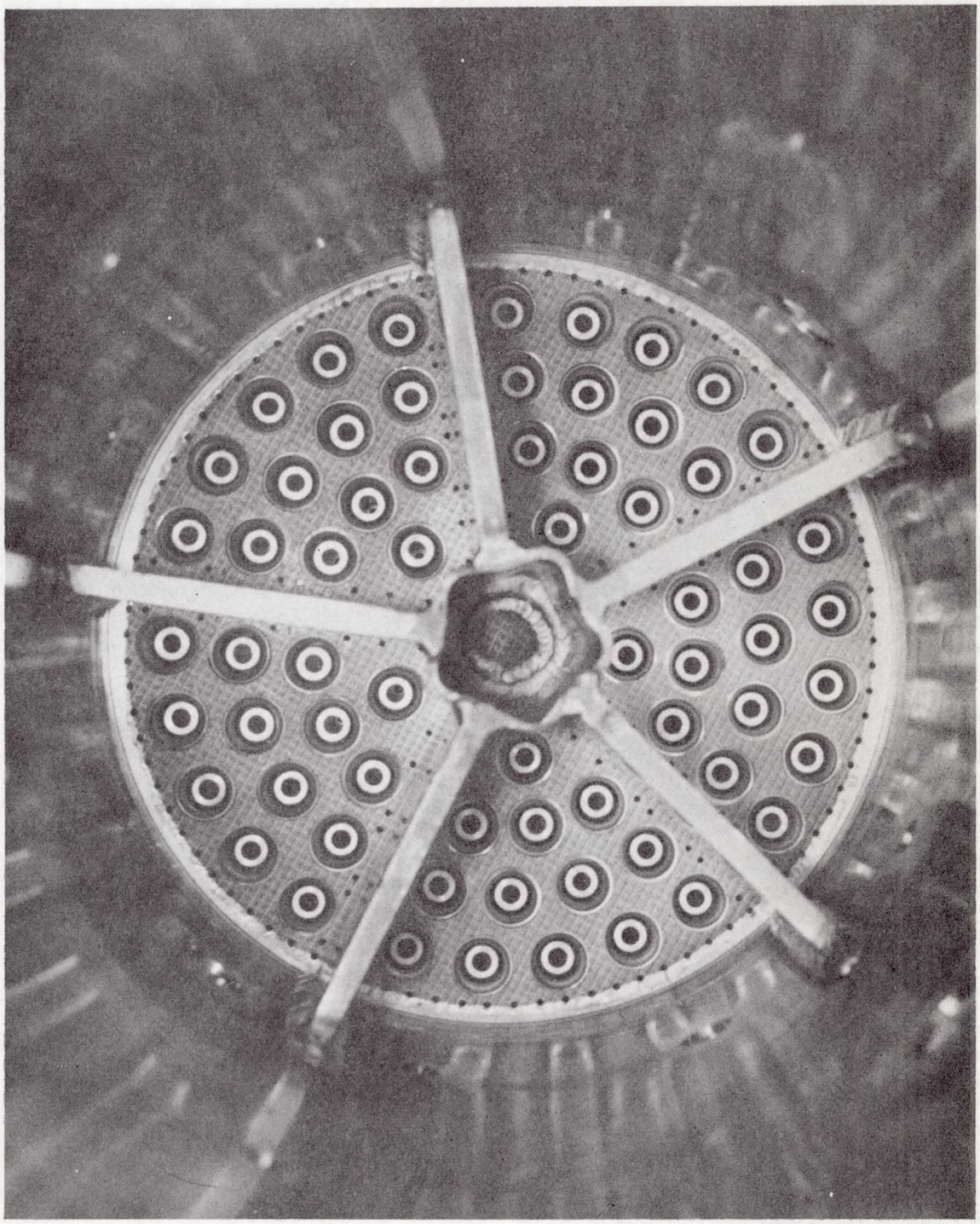

Figure 14

Typical Injector Face Patterns (Serial Numbers 022, 025, and 026)

oxygen so that when injected, the oxidizer stream would form a spray pattern into the outer annulus of liquid hydrogen for improved liquid phase mixing prior to combustion. Two types of swirlers were tested; the mechanical swirler and a tangentially drilled orifice cap.

The mechanical swirler consisted of a helically machined plug installed within the oxidizer element. The oxidizer spray divergence angle, spray droplet size, and fullness of the oxidizer cone could be influenced by the swirler pitch, relative swirler flow area, number of swirler channels, swirler distance from the injector face, and other lesser variables. Hydraulic flow tests of oxidizer swirler design variations were conducted at Aerojet-General to assist in selecting swirlers that produce the desired spray patterns. The second type of swirler (S/N 018) consisted of a tangentially drilled orifice cap. The tangential oxidizer injection velocity created rotational flow through the oxidizer element, forming the spray pattern when injected.

The most successful performance and stability data was obtained from the last injection element design tested. It did not have any oxidizer swirlers. Instead of using an oxidizer spray pattern to provide better propellant mixing, high hydraulic shear stresses were used. The oxidizer injection velocity was decreased by counterboring the tip of the showerhead oxidizer injection element. High fuel injection velocities were maintained to produce high injection velocity ratios (V_f/V_o). The combustion stability aspects of the high velocity ratio design are discussed in Section III,E.

Two concepts of fuel injection element circuits were tested. The simplest design to fabricate consisted of a porous injector faceplate, through which an orifice was drilled, which formed the outer fuel injection annulus. The inner fuel annulus was provided by the oxidizer injection element. Fins, which were an integral part of the injection element, were used to maintain element concentricity within the fuel annulus. Later designs used a separate fuel element tip to form the outer annulus. The separate tip allowed closer control of the fuel annulus areas. The element tip was screwed onto the oxidizer element body to control concentricity and the fins were eliminated. Elimination of the fins could have reduced the local hot spots downstream of each fin location which resulted from local thinning of the fuel flow stream. Inspection of baffle erosion patterns (Figures No. 10, No. 11, and No. 12) indicates that the location of the erosion may have been associated with an adjacent fuel element fin, although not all fins caused baffle erosion. The decrease in baffle erosion that occurred with fuel injection elements with no fins, could have resulted primarily from improved baffle film cooling.

The porous injector faceplate was chamfered about each element and the fuel element tip was swaged after installation of the element on S/N 022, 025, and 026. This afforded better structural support of the porous faceplate, which was otherwise attached to the injector body only by welding at its inner and outer periphery.

The S/N 015 coaxial injection elements were welded to the injector backplate as shown in Figure No. 8. The welded element joint was reinforced by furnace brazing from the reverse (fuel manifold) side on S/N 017 (and S/N 017A) gas generator assembly. The injection elements were brazed to the injector backplates on the remaining coaxial gas generator assemblies. Serial No. 022, 025, and 026 injection element bodies were threaded and a nut was used to attach each to the backplate prior to brazing.

Thermal erosion design problems are present with all liquid oxygen/liquid hydrogen gas generators. As discussed in Section III,A, there is a great disparity between the local stoichiometric reaction zone temperature and homogeneous combustion gas temperature. The prevention of hardware erosion was one of the primary design objectives. This is accomplished by attaining gas thermal equilibrium as rapidly as possible following combustion reaction. The excess unreacted hydrogen should be used to reduce the local reaction zone temperature below that of the material melting temperature of the injector hardware prior to impingement of the gases upon the injector surfaces. The erosive heat flux can be approximated from Bartz' Equation[2] as follows:

$$Q/A = Hg\ (Tg - Tw)$$

$$\text{and } Hg = \frac{0.026}{d_T^{0.2}} \left(\frac{\mu^{0.2} Cp}{Pr^{0.6}} \right)_t \left(\frac{Pc\ \ gc}{C^*} \right)^{0.8} \left(\frac{d_T}{r_c} \right)^{0.1} \left(\frac{A_T}{A_c} \right)^{0.9} \sigma$$

where Q/A = Local Heat Flux, BTU/in.^{2}-sec

Hg = Gas Side Heat Transfer Coefficient, BTU/in.^{2}-sec-°F

Tg = Local Gas Temperature, °F

Tw = Local Wall Temperature, °F

μ = Viscosity, lb_m/ft-sec

Cp = Specific Heat, BTU/lb_m-°R

Pr = Prandtl Number

gc = Gravitational Conversion Factor, ft-lbm/lb_f-sec^2

---

(2) Bartz, D. R., "A Simple Equation for Rapid Estimation of Rocket Nozzle Corrective Heat Transfer Coefficients," Journal of the American Rocket Society, January 1957.

r_c = Throat Radius of Curvature, in.

σ = Dimensionless Factor Accounting for Density and Viscosity Variations Across Boundary Layer

(Also see Table II)

Usually, the local gas temperature is the determining factor in the occurrence of erosion. However, if the local gas temperature is marginal (only slightly exceeds the hardware melting temperature), the heat flux proportionality factor, $P_c^{0.8}$, may become the determining factor in the occurrence of erosion.

The coaxial injection element injector is less likely to encounter thermal erosion than either the multi-orifice or large-thrust-per-element designs because of their more uniform local mixture ratios. Also, the fuel injection annulus is placed outermost and the cooling characteristics of the excess hydrogen are used to the greatest advantage. During liquid oxygen/liquid hydrogen experiments with single coaxial injection elements,[3] noticeably higher performance was observed for mixture ratios greater than 3.5 with the oxidizer annulus situated outermost. Mixture ratios tested ranged from 1.45 to 9. This concept was not used in testing M-1 gas generator assemblies because the slight performance increase with reversed flow at the low mixture ratios did not warrant the greater hazard of faceplate, element tip, baffle, or chamber wall erosion. It was theorized that if the highly volatile, higher momentum, higher velocity hydrogen were injected through the center, it would expand out into the oxidizer annulus forcing combustion to occur in an oxidizer-rich atmosphere near the injector face with greater recirculatory erosion.

The two primary fabrication problems that occurred early in the development program were weld distortion of the hardware and conical seal glands (see Figure No. 7) not being fabricated according to the specifications.

Some of the weld distortion problems occurred when adjacent thick and thin members, with their different heating and cooling rates were welded together. The thin members cooled and set first, and when the heavier more rigid sections cooled, local yielding and distortion resulted. Welding of instrumentation bosses on the chamber and injector assemblies were originally troublesome. Most of the weld problems were minimized by either one or a combination of the following procedures:

1. Intermittent welding of thick and thin members to allow more uniform cooling and shrinkage rates.

2. Wherever possible, all machining was performed after welding.

---

(3) Hersch, M., Effect of Interchanging Propellants on Rocket Combustor Performance with Coaxial Injection, NASA TN D-2169, 1964

TABLE II

NOMENCLATURE AND SYMBOLS

A	Area, $in.^2$
C_d	Discharge Coefficient
c*	Characteristic Exhaust Velocity, ft/sec
d	Diameter, in.
FS_1	Signal for Start of Test
FS_2	Signal for End of Test
GGA	Gas Generator Assembly
GGV	Gas Generator Valve
MR	Mixture Ratio, $\dot{w}o/\dot{w}_f$
P	Pressure, psia
ΔP	Differential Pressure Drop, psi
S/N	Serial Number
T	Temperature, °F or °R
V	Velocity, ft/sec
$\dot{w}$	Propellant Flowrate, lbm/sec
η	Combustion Efficiency, c*actual/c*theoretical

Subscripts

c	Chamber
f	Fuel
J	Injector
o	Oxidizer
GG	Gas Generator
t	Total or Stagnation
T	Throat

3. Additional stress relief cycles were performed between welding operations.

4. Local grinding and fit-up was performed during assembly whenever distortion was unavoidable.

Three sets of double metallic conical seals were used in the M-1 gas generator assembly. Double conical seals are located at the oxidizer injector inlet, fuel injector inlet, and chamber (hot gas) outlet (see Figure No. 7). This seal design is excellent when properly fabricated, installed, and tested. However, the recommended tolerances for seal glands are very stringent (nominal diameter $\pm$ 0.002-in. for gas generator glands) and difficult to achieve. The problem was eventually minimized by performing all welding and stress relief cycles with rough-machined flanges and performing the conical seal gland machining as the final fabrication operation. One known instance of mating conical seal flanges at the gas generator chamber outlet being fabricated that did not adhere to specification requirements resulted from the use of dissimilar materials. The male conical seal gland was machined from a material with a coefficient of thermal expansion that was approximately 10% higher than that for the female flange. After several firings and thermal cycles, including combustion temperature excursions to 1600°F, the joint began leaking at ambient temperature. Inspection of the mating flanges revealed that the male seal gland was permanently "toed-in" approximately 0.015-in. on the diameter and the female seal gland "toed-out" approximately 0.005-in. This distortion was calculated and was apparently the result of the greater rate of thermal expansion of the male flange with local yielding at the elevated temperatures. This condition did not occur, even after repeated firings, when mean combustion temperatures were maintained below approximately 1000°F. The chamber fuel film coolant is still somewhat effective along the length of the chamber, as shown in Figure No. 15. Conversely, it is assumed that if the female flange material had a higher rate of thermal expansion than the male flange, the leakage would have occurred during the test operation period at elevated temperatures, although possibly not at ambient conditions.

D. COAXIAL GAS GENERATOR PERFORMANCE AND COMBUSTION GAS TEMPERATURE DISTRIBUTION

Typical values of M-1 coaxial gas generator injector performances are given in Table III. The combustion efficiency values shown for some of the injectors are only approximate figures because there was a lack of adequate steady-state data with the less successful designs when automatic combustion instability shutdowns occurred during the start transient. Design of the test facility feed system necessitated that the propellant flowmeters, used to measure gas generator flowrate, be situated from 50 to 100 ft upstream of the gas generator assembly. This resulted in questionable transient flowrate data. The performance data from these tests were evaluated at the maximum transient chamber pressure. The mean chamber pressure and flowrates were measured during tests in which chugging occurred.

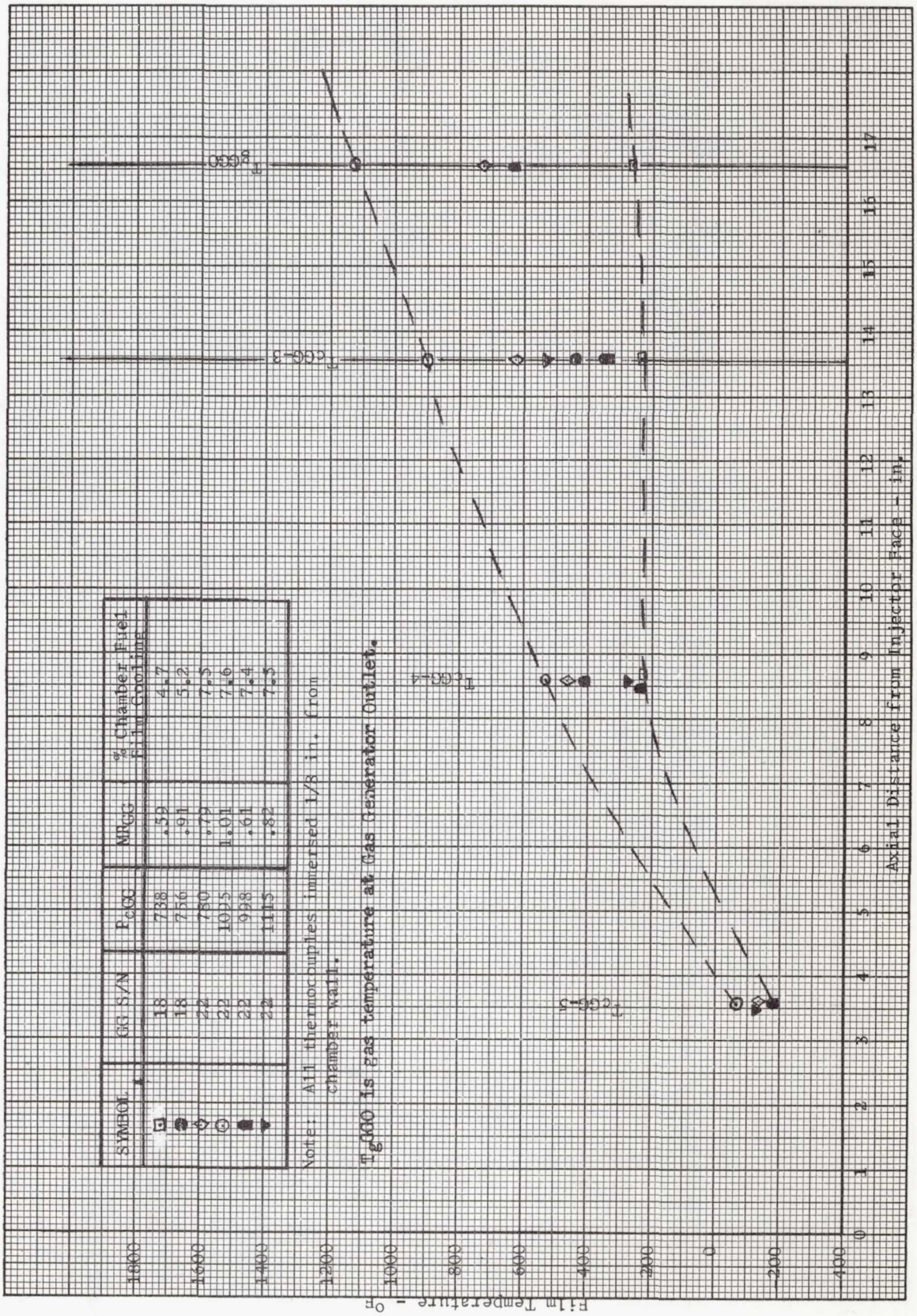

Figure 15

Gas Generator Chamber Film Temperature

Versus Axial Length of Chamber (Typical)

TABLE III

COAXIAL GAS GENERATOR PERFORMANCE

S/N	No. Inj. Elements	No. Tests	Total Run Time, Sec	P_c Range	$(\dot{w}_o + \dot{w}_f)$ Average	M.R. Range	η Avg.(2) (%)	Oxid. Inj. (ΔP) Avg.	Fuel Inj. (ΔP) Avg.	A_T Range	C_d	L* (3) Range
015	34	3(1)	4.2	750 to 1000	108	0.65 to 1.0	88.0	100	120	$\binom{31.5}{26.2}$	$\binom{0.835}{0.745}$	$\binom{205}{278}$
017	68	1	2.0	740	112	0.58	91.9	145	165	31.3	0.833	207
018	68	6	84.0	738 to 768	110	0.59 to 0.91	90.7	160	145	31.3	0.833	207
017A	68	3(1)	4.4	735 to 788	110	0.57 to 0.82	91.3	140	155	31.3	0.833	207
020	132	1(1)	1.2	664	110	0.84	92.8	265	245	30.2	1.0	180
022	65	16	121.1	765 to 1153	110-115	0.61 to 1.01	98.0 $\pm$ 3.0	240	215	$\binom{30.2}{20.3}$	1.0	$\binom{50}{250}$
025	65	4	22.4	1104 to 1137	115-123	0.68 to 0.72	97.8	240	215	$\binom{22.8}{20.3}$	1.0	$\binom{45}{50}$
026	65	5	34.2	986 to 1159	115	0.76 to 0.78	98.6	240	215	20.3	1.0	$\binom{50}{260}$

(1) Includes tests automatically terminated during start transient.

(2) c^* actual $= \dfrac{(P_c GG - 5C)\, g_c\, (C_d A_T)}{\dot{w}_o + \dot{w}_f}$, where g_c = Gravitational Conversion Factor

(3) $L^* = (\text{Chamber Volume})/C_d A_T$

Back pressure for the gas generator development tests was provided by an interchangeable sonic orifice or nozzle installed in the turbine simulator hot gas duct (see Figure No. 16). A sharp-edge orifice was used for all tests up to and including S/N 017A. A convergent entrance flow nozzle was used during all subsequent tests. When the sharp-edge orifice was used, the sonic throat area was taken at the orifice vena contracta. The orifice discharge coefficient was based upon the line-to-orifice contraction diameter ratio and the flow Reynolds number. The line diameter upstream of the orifice was corrected for boundary layer growth. The displacement boundary layer was calculated for axisymmetric pipe flow neglecting the effect of the single right angle bend in the facility gas duct. The gas properties were based upon assumed homogenous combustion products and no attempt was made to account for film cooling. The turbulent boundary layer was assumed to start from the injector face. Further approximations were made that the turbulent boundary layer grew at the same rate as for a flat plate at zero incidence angle and that the velocity profile conformed to the one-seventh power law. The flat plate approximation near the wall was justified by the relative thinness of the boundary layer relative to the pipe radius.

The effect of using PcGG-5c for the chamber plenum pressure value may not have been exact for calculating c*. Typical static chamber pressure distribution along the axial length of the gas generator is shown in Figure No. 17. Static pressure readings below 8-in. indicate that the combustion gas Mach Number is probably constant and combustion is essentially complete. The design chamber Mach Number is approximately 0.3. Inspection of baffle erosion patterns indicated combustion probably started approximately 2-in. downstream of the injector face. Therefore, PcGG-5c is approximately in the middle of the combustion zone. The static pressure reading at PcGG-5c has to be increased by a finite velocity head to correct for combustion that occurs upstream of PcGG-5c. This reading also has to be decreased for combustion losses that may occur downstream of PcGG-5c. When the Mach Number immediately upstream of the sonic nozzle was used to calculate nozzle entrance stagnation pressure for a few typical tests, the values corresponded very closely to PcGG-5c (static). Thus for simplicity, the latter parameter was used in all tests.

There were no attempts to make other corrections to the c* efficiency calculations. Heat conductive losses to the gas duct were neglected as was thermal expansions of the throat diameter. The c* values used in this report are given for comparative purposes only when identical assumptions were made for identical test conditions at the same test facility. Although numerous minor corrections were neglected, if the c* efficiency is taken as the square root of the actual-to-theoretical combustion gas temperature, as shown in Figure No. 18, both methods used to calculate c* indicate approximately 98% of combustion efficiency was achieved with S/N 022, 025, and 026.

When the performance of gas generators S/N 015 through 020 is examined, there is a data trend indicating improved combustion efficiencies when the number of coaxial injection elements per injector is increased (decreased thrust per element). However, because of the few tests involved as well as the lack of

Figure 16

Gas Generator Development Test Schematic and Instrumentation

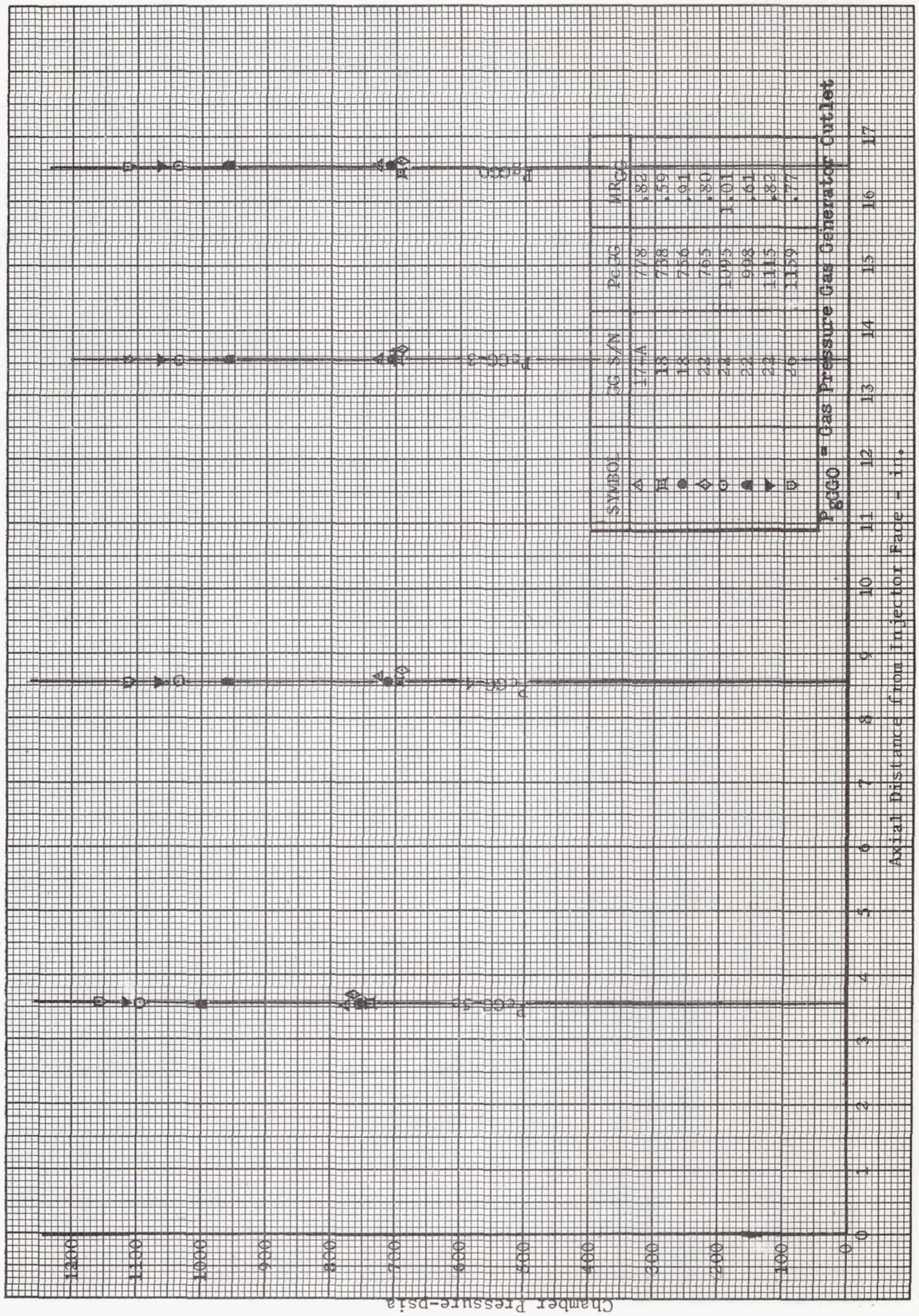

Figure 17

Gas Generator Chamber Pressure Versus

Axial Length of Chamber (Typical)

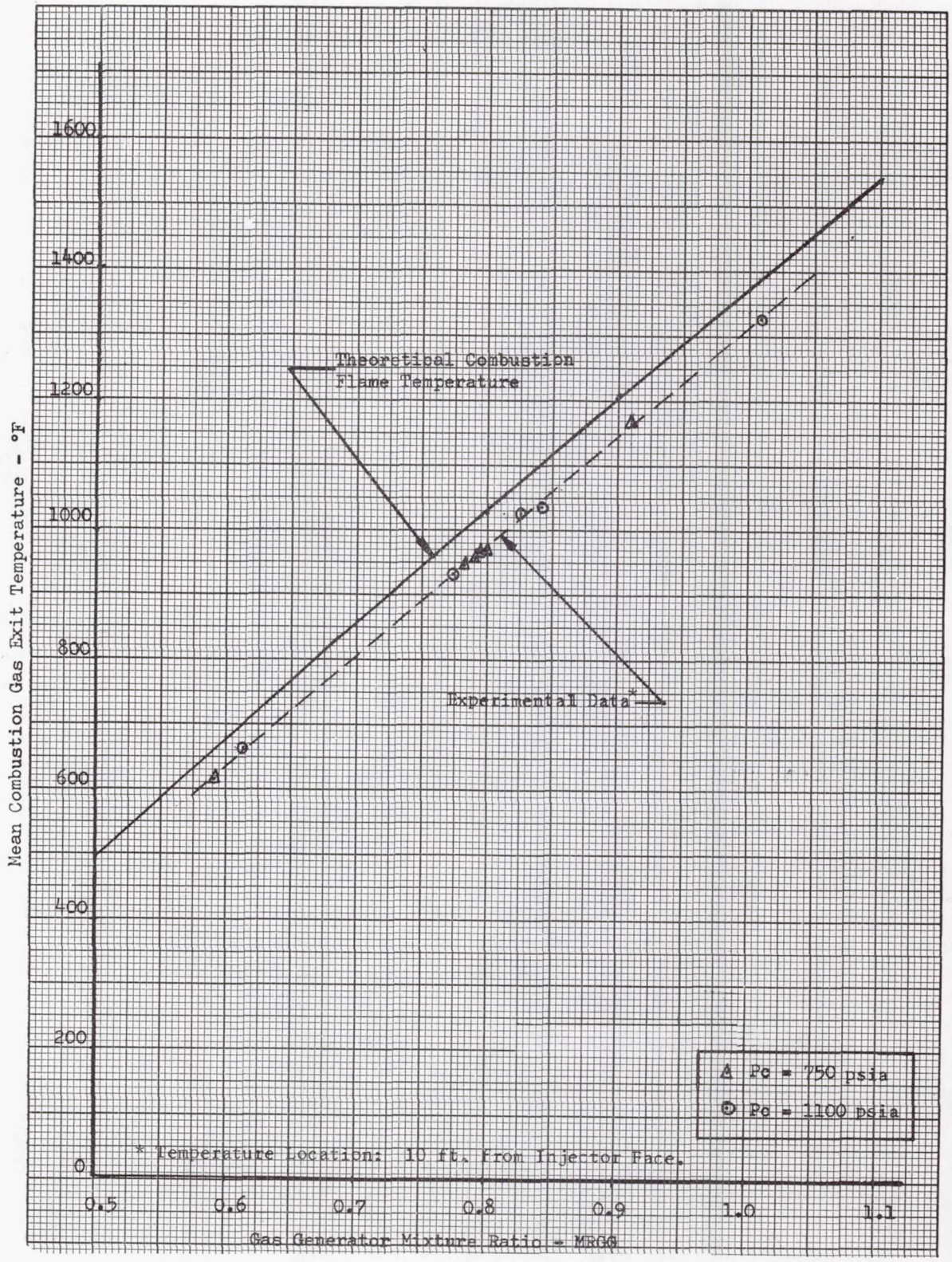

Figure 18

Mean Combustion Gas Exit Temperature Versus Gas Generator Mixture Ratio - Serial Number 022 Type Gas Generator Assembly

sufficient steady-state data (except for S/N 018 gas generator assembly), the results are not conclusive.

Serial No. 015 was the first M-1 coaxial gas generator assembly tested. With only 34 injection elements, the flowrate per element was the highest tested but performance was quite low. The injector pressure drops with S/N 015 were low (<100 psi) and chugging was encountered in one test. High frequency combustion instability occurred during the third test and is described in detail in Section III,E. Serial Number 015 was the only 34-element gas generator assembly tested.

One test was conducted with S/N 017 gas generator assembly using an acoustical liner. Low amplitude combustion oscillations occurred. The injection element had a blunt tip on the injector face side and several of the 68 element tips eroded (see Figure No. 10) from the inside of the oxidizer counterbore outward. The blunt tip could have eroded because of the flame holding effect or because the tip could no longer adequately conduct heat away from the element to the cryogenic injected propellant. The injector was reworked by enlarging the inside diameter of the element tip by counterboring the element to reduce the blunt tip effect.

Reworked injector S/N 017A was tested three times and low frequency combustion instability was encountered during all tests. Although further element tip erosion did not occur, chugging characteristics of the reworked elements were more predominate. Tests of both assemblies were conducted at the same test stand. The possible influence of lower oxidizer injection velocity upon chugging is discussed in Section III,E. Further development effort with this assembly was discontinued.

Six tests at 750 psia nominal chamber pressure were successfully conducted using S/N 018 gas generator assembly with injector baffles. Based upon the initial chugging of S/N 015 gas generator assembly, it was assumed that higher oxidizer injector pressure drop was required for S/N 018 injection element to avoid this chugging. Therefore, the oxidizer injection element hardening insert (see Figure No. 8) was installed and tack-welded to the oxidizer element tip to increase oxidizer injection ΔP. Relatively high oxidizer injection velocity was achieved because of the location of the insert. The normal combustion noise level of S/N 018 was lower ($\pm$ 1.2% of mean PcGG) than they encountered during testing of all the coaxial injector gas generator assemblies. This occurred either because of the proximity of the oxidizer ΔP to the combustion flame front detuning injection coupling from combustion feedback or the low injection velocity ratio. Injector baffles were used to prevent transverse high frequency combustion instability. Combustion gas temperature distributed just downstream of the gas generator was less favorable than for S/N 022. Although excellent stability and acceptable gas temperature distribution was demonstrated by S/N 018 gas generator assembly, progressive nibbling (erosion) occurred on the protruding insert tips (see Figure No. 12). None of the inserts were lost during the six tests but the possibility existed that if an insert was dislodged during a turbopump development test, extensive damage could be done to the turbine blades. Although the nibbling could have been eliminated by redesigning the S/N 018 oxidizer injection element, when S/N 022 gas generator assembly was

adequately demonstrated, no further effort was expended with S/N 018. No attempts were made to test S/N 018 at high chamber pressures (1145 psia).

Serial No. 020 gas generator assembly had 132 injection elements. All injector patterns from gas generator assemblies S/N 015 through 020 were designed before the decision was made to use baffles. The lack of adequate free paths on the S/N 020 injector pattern prevented the use of baffles. An acoustical liner was designed and installed to prevent first tangential combustion instability frequency. Combustion instability in the second tangential mode occurred during the start transient and is discussed in Section III,E. When S/N 022 was successfully tested, no further effort was expended to develop S/N 020.

Serial No. 022 gas generator assembly was designed for the purpose of incorporating all the latest information available from current technological studies and M-1 gas generator assembly test results to provide a stable high performance gas generator for M-1 oxidizer and fuel turbopump assembly development tests. Stable combustion, high combustion efficiency, and reasonably uniform combustion gas temperature distribution were adequately demonstrated during all gas generator development tests (see Figure No. 19). However, chugging occurred during the turbopump development tests. Chugging is discussed further in Section III,E.

Serial No. 025 and 026 were fabricated as backup hardware for S/N 022 gas generator assembly. Combustion performance characteristics were similar to those of S/N 022.

Mean combustion gas temperature data agreed very closely with the theoretical combustion flame temperature calculated from chemical equilibrium composition considerations (see Figure No. 18). The temperature was measured at a location 10 ft from the injector face immediately upstream of the flow nozzle. The data were not corrected for heat loss to the gas duct, which consisted of 100-in. in length of 8-in. schedule 80 corrosion resistant steel. No difference was noted in the effect of chamber pressure upon exit temperature. Throughout the range of gas generator mixture ratios tested, the combustion gas mixture is oxidizer lean to the extent that the reaction is driven to completion even at low chamber pressures. Oxidizer and free radical species, other than water and hydrogen, were negligible.

A radial thermocouple rake was located 2 ft from the injector face. The distribution of temperatures are tabulated in Figure No. 20 for typical tests with S/N 018 and 022 gas generator assemblies. Temperature variations still exist locally at this axial length but the maximum recorded temperatures are cooled sufficiently to preclude hardware erosion downstream of this point.

Typical gas temperatures for S/N 022 are plotted in Figure No. 21 against radial distance from the chamber axis irrespective of the thermocouple angular orientation to the oxidizer and fuel inlets. Because of the abundance of film cooling around the pentagonal injector baffle hub (see Figure No. 14) and the absence of oxidizer at the axis of the injector, relatively cool gases existed along the chamber

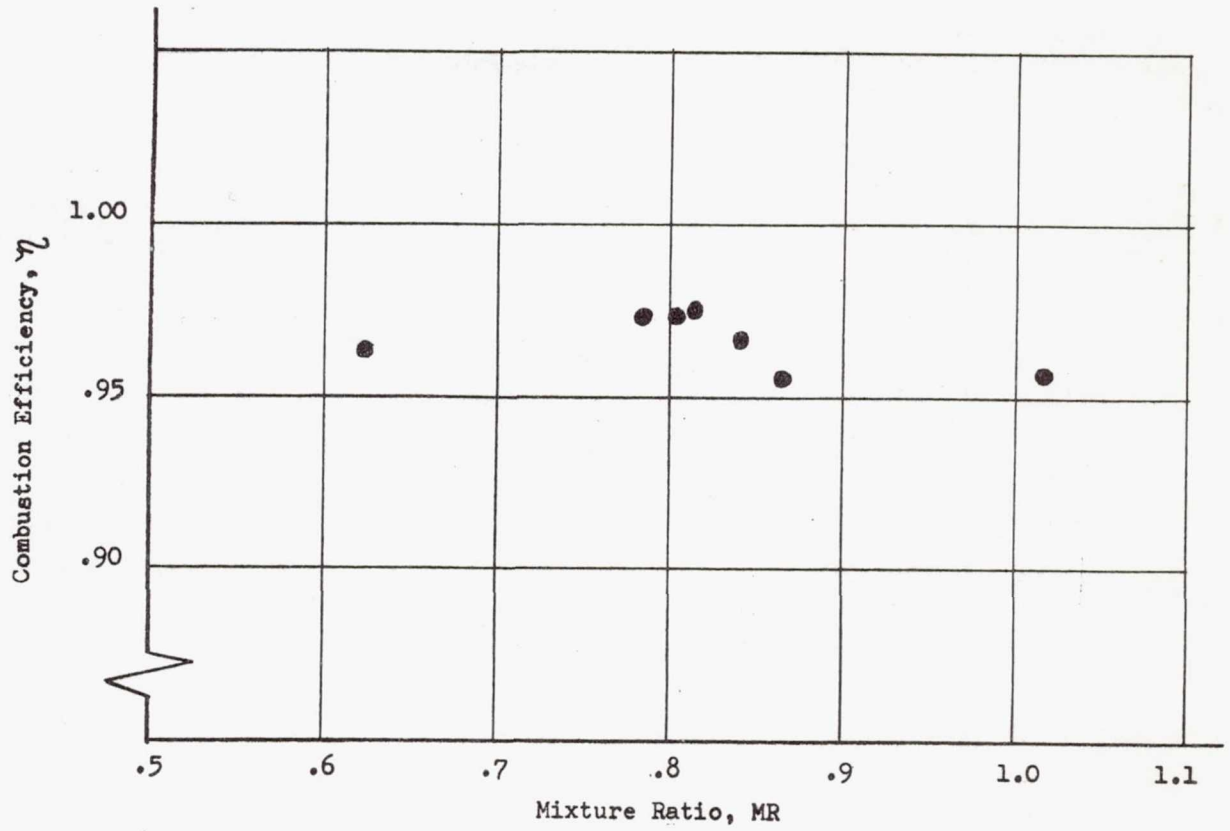

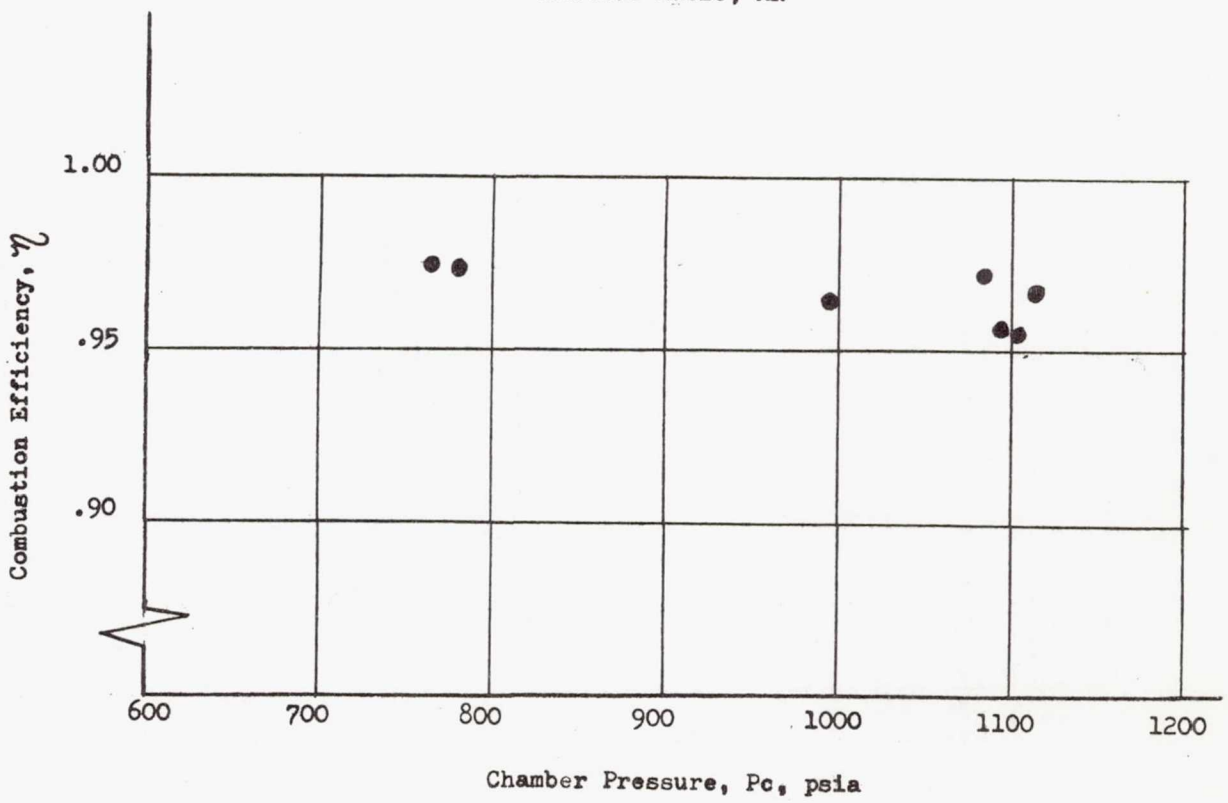

Figure 19

Combustion Efficiency of Serial Number 022 Gas

Generator Assembly Versus Mixture Ratio and Chamber Pressure

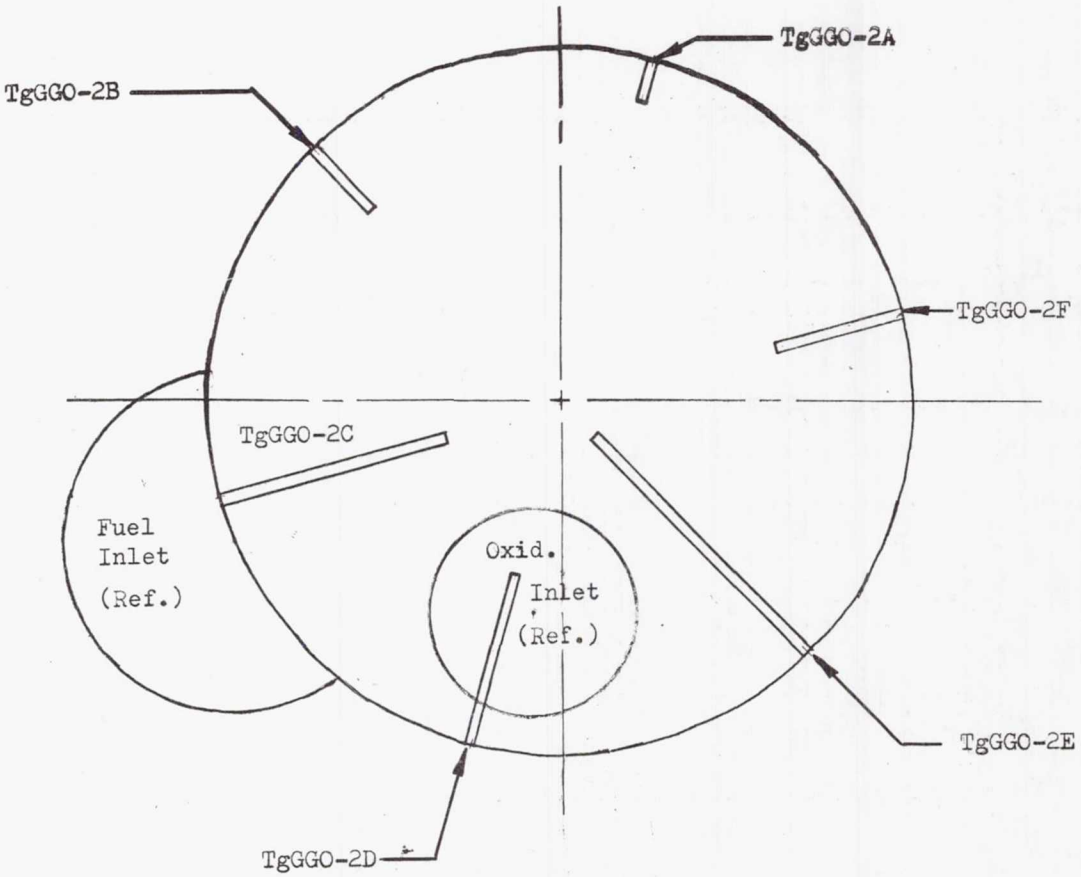

Gas Generator Exit Temperature Orientation
(24 in. from Injector Face)

		Exit Temperature, °F					
	GG S/N	18	18	22	22	22	22
	PcGG	738	756	781	1095	998	1115
	MRGG	.59	.91	.80	1.01	.61	.82
	Theoretical Comb. Flame Temp.	660	1222	1030	1390	695	1067
Parameter	Radial Distance From Chamber Axis, in.						
TgGGO-2A	3½	348	827	953	1319	580	967
-2B	3	559	1071	1258	1726	803	1303
-2C	1¼	703	1281	NI	NI	NI	NI
-2D	2	811	1590	912	1287	564	909
-2E	½	625	1326	NI	NI	NI	NI
TgGGO-2F	2½	587	1270	976	1455	713	1105

NI = Parameter not instrumented for Test.

Figure 20

Typical Gas Generator Assembly Exit Temperature Distribution

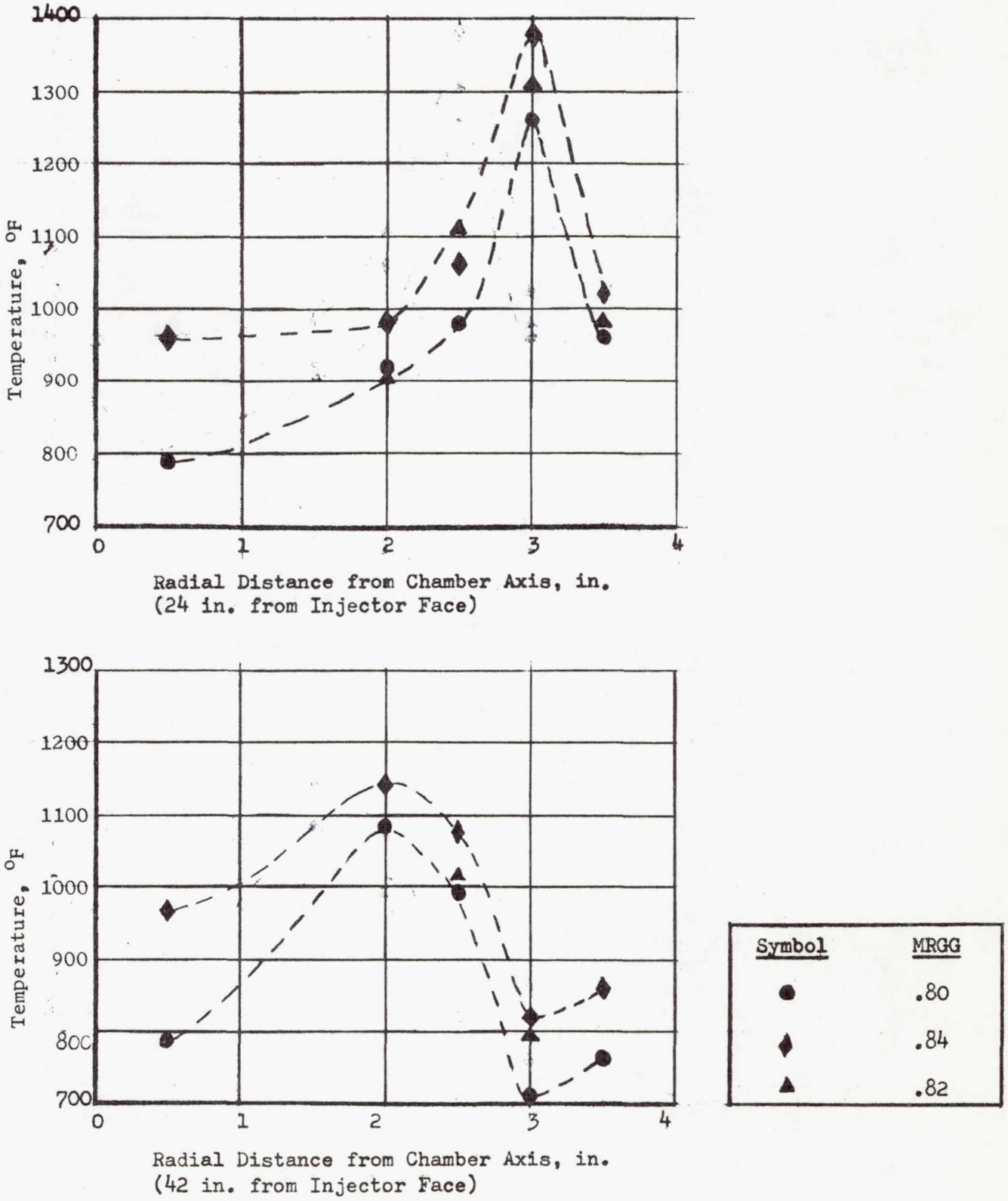

Figure 21

Typical Radial Combustion Gas Temperature Distributions

Downstream of Serial Number 022 Type Gas Generator Assembly

axis. Gases near the chamber wall were also cooler because of the chamber wall film cooling.

Approximately 7-1/2% chamber fuel film cooling was used for S/N 022 gas generator assembly. The chamber fuel film cooling was designed using a modified Hatch and Pappel Equation.[4] Variation of chamber film temperature along chamber axial length at variable mixture ratios is shown for some typical tests in Figure No. 15. All temperatures were recorded approximately 1/8-in. away from the chamber wall.

An interesting temperature distribution phenomena was noted during both the oxidizer and fuel turbopump development tests with gas generator drive. In these tests, turbine gas flow was tapped off approximately at a right angle to the gas flow from the gas generator outlet. The remaining gases were restricted downstream by the bypass orifice shown schematically in Figure No. 22. The oxidizer turbopump test facility was similar to that shown in Figure No. 22 except that approximately 10 ft of gas duct separated the point of the tap-off on the pentapus to the inlet of the turbine where the mean gas temperature was recorded.

During both turbopump test series, the mean turbine inlet temperature for a given gas generator mixture ratio was 100 to 300°F lower than the experimental data previously shown in Figure No. 18 for tests without turbopumps. To divert the gas flow in a right angle to the turbine, the bypass flow restrictor downstream must create a sufficient pressure gradient within the pentapus to change the direction of flow from the turbine gases. Because of the presence of the gas generator stabilizer nozzle, the Mach Number at the split-off point in the pentapus was subsonic but yet not negligible. Figures No. 20 and No. 21 show that complete thermal equilibrium is not achieved at a location 2 ft from the injector face. Therefore, on the average, the water molecules were at higher temperatures than the average hydrogen molecules. Thus, when an identical pressure gradient was exerted against both higher density, higher temperature water gas and lower density, lower temperature hydrogen gas, the lower momentum hydrogen was relatively easier to divert towards the turbine. Furthermore, the lower the percentage of turbine flowrate, the lower the average turbine inlet temperature was relative to its corresponding average combustion temperature.

Turbine inlet temperature thermocouples for fuel turbopump testing were recorded immediately upstream of the turbine inlet restrictor shown in Figure No. 22. The gas temperature measured near the top of the duct (low momentum, short flow radius of curvature) indicated only 200°F, whereas gas temperature near the bottom of the duct (high momentum, long flow radius of curvature) indicated approximately 850°F, thus substantiating the mathematical analysis. Average over-all combustion

---

(4) Hatch, W. E. and Papell, S. S., Use of a Theoretical Flow Model to Correlate Data for Film Cooling or Heating and Adiabatic Wall by Tangential Injection of Gases of Different Fluid Properties, NASA TN D-130, 1959.

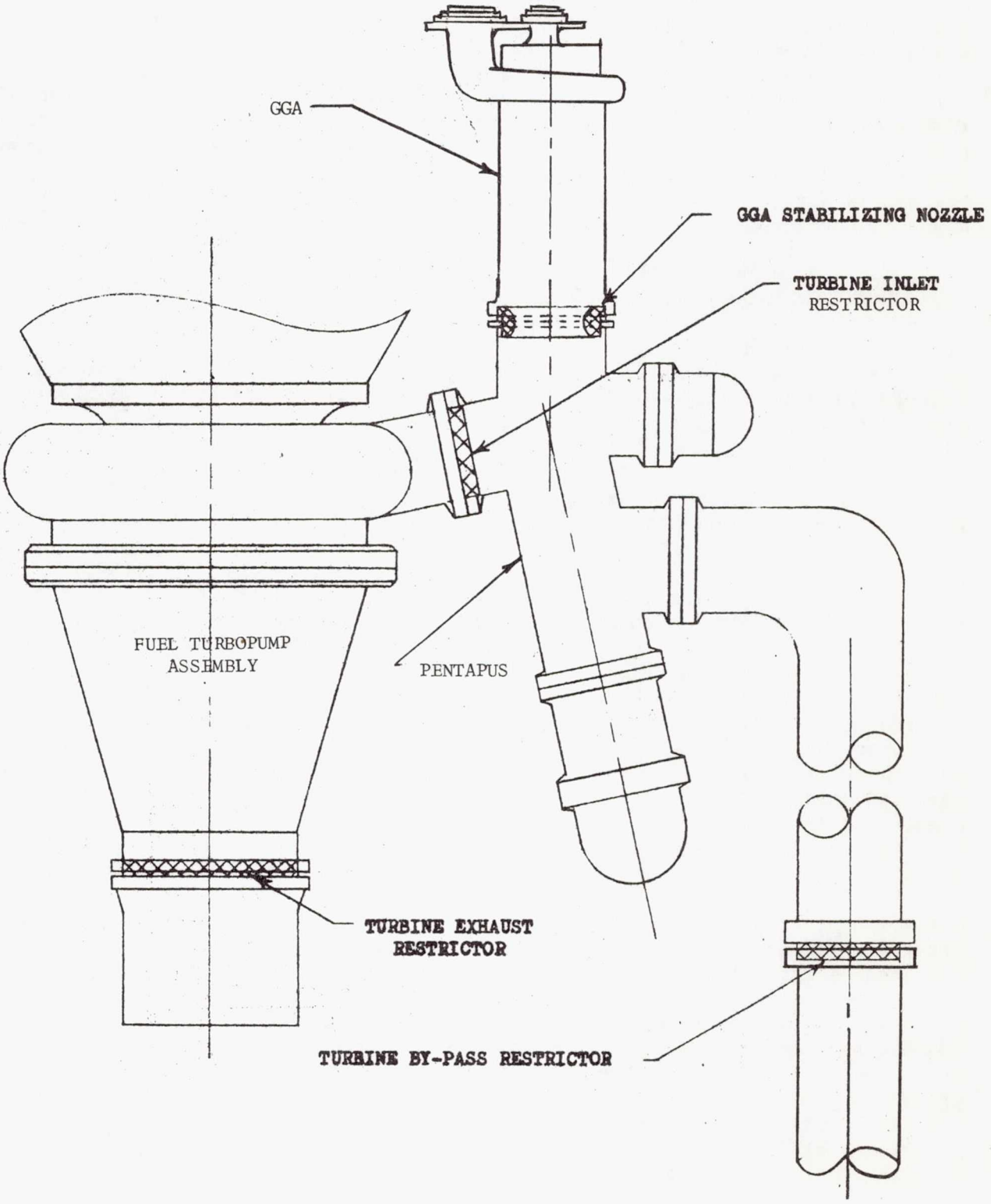

Figure 22

Fuel Turbopump Development Test Schematic with Gas Generator Drive

gas temperature, based upon the 0.78 gas generator mixture ratio for this test, should have been approximately 950°F. As a consequence, the effective turbine flow mixture ratio and gas temperature were lower than the average gas generator mixture ratio and gas temperature. Conversely, the bypass gas properties corresponded to a higher mixture ratio and gas temperature than that actually achieved with the gas generator. This point should be considered when designing the engine hot gas bypass lines if a "momentum separator" effect is not desired. To preclude this occurrence, the bypass tap-off point can be moved up to the same axial location and diversion angle as the turbine flow line.

E. HIGH FREQUENCY AND LOW FREQUENCY COMBUSTION STABILITY OF M-1 GAS GENERATOR ASSEMBLIES

Combustion instability considerations occur within two basic categories, high frequency combustion instability and low frequency combustion instability. Briefly, high frequency combustion instability (screeching) occurs when periodic chamber pressure oscillations take place without a perceptible change in propellant injection flowrates. Low frequency combustion instability (chugging) occurs when one or both propellant manifold pressures incur periodic oscillations, usually 180 degrees out-of-phase with chamber pressure, resulting in oscillatory injection flowrates as well as oscillatory chamber pressure. Both types of combustion instability were experienced by various M-1 gas generators.

High frequency combustion instability is attributed to organized combustion reaction rates associated with combustion chamber acoustic resonance frequencies. The occurrence of screeching has long been a recognized problem in rocket injector designs. Because screeching is associated with injector and chamber acoustic resonance frequencies, very small rocket injectors having acoustic resonance frequencies too high to support organized combustion reaction rates do not encounter the screeching problem. All large rocket injectors have a potential screeching problem. A partial and accepted solution to the screeching problem has been to install baffles in the injector combustion zone so that the resonance frequency within each baffle compartment is too high to permit screeching and a standing resonance within the over-all injector is dispersed. However, baffles are effective against transverse modes of high frequency combustion instability only and do not provide protection against longitudinal instabilities. Usually, gas generator designs do not have sufficiently large injector diameters to support transverse instability modes; therefore, baffles are not required. However, this was not true for the M-1 gas generator primarily because of its large size and high flow rate.

Four instances of high frequency combustion instability were encountered during the M-1 gas generator development program. Two tests with unbaffled multi-orifice injectors encountered the first tangential instability mode. One unbaffled coaxial injector also experienced first tangential instability. During the fourth test, second tangential instability was encountered with a coaxial injector having a chamber without baffles but with an acoustical liner designed to suppress first tangential instability. Descriptions and analyses for transverse

instability modes have been given by Reardon[5].

One of the more popular theories of high frequency combustion instability is the Sensitive Time Lag Theory[6]. An estimate of the M-1 gas generator assembly combustion instability zones based upon this theory is shown in Figure No. 23. The sensitive time lag (τ) is used to determine the possible frequencies at which combustion instability might occur and the interaction index (n) is used to determine the probability of combustion instability. For any given sensitive time lag, if the test operating point lies beneath the shaded zones of the corresponding instability modes, combustion is expected to be stable; however, if the operating point lies above the shaded zone, high frequency combustion instability is predicted. On the development test stand where all four unstable gas generator tests occurred, the sonic nozzle was 10 ft from the injector face (see Figure No. 16). The sixteenth longitudinal mode for this test configuration and the first tangential mode of high frequency combustion instability have approximately the same sensitive time lag and the same instability frequency. However, the interaction index of the first tangential mode (for unbaffled injectors) is lower and according to the best estimates, indicates the greater probability of its occurrence than the sixteenth longitudinal mode. This is particularly significant in the interpretation of stability data for S/N 018 and 022 gas generator assemblies. It is also worth noting that the interaction index of the higher harmonics of longitudinal modes are successively higher.

An analytical investigation of liquid oxygen droplet vaporization rates as a possible mechanism for high frequency combustion instability was conducted by Wieber of NASA/LeRC[7]. The particular propellant combination investigated was liquid oxygen/heptane but the assumptions made in the analysis for liquid oxygen vaporization rates appear equally applicable to liquid oxygen vaporization in the M-1 gas generator assembly. Although the gas generator mean combustion gas temperature is only 1000°F, the assumed combustion temperature (5000°R) in the local stoichiometric reaction zone where the liquid oxygen would vaporize is valid. To summarize, the results of this analysis indicates it is possible to heat liquid oxygen droplets to their critical temperature with little vaporization of mass for high chamber pressure rocket injectors. When the critical temperature is reached, any additional heating of the droplet results in a rapid vaporization rate (flashes) which releases considerable gaseous oxygen for combustion in a very short time. It is hypothesized that this may be the mechanism for high frequency combustion instability. What is even more significant is that Mr. Wieber calculated that the liquid oxygen droplet heating time to its critical temperature was approximately 0.12 millisec for a wide range of droplet sizes. The 0.12 millisec figure corresponds almost exactly to the required sensitive time lag for the M-1 gas generator assembly first tangential instability mode frequency indicated in Figure No. 23. It is yet

---

(5) Reardon, F. H., Investigation of Transverse Mode Combustion Instability in Liquid Propellant Rocket Motors, Princeton University, 1961

(6) Crocco, L. and Cheng, S. I., Theory of Combustion Instability in Liquid Propellant Rocket Motors, Butterworth's Scientific Publications, London, 1956

(7) Wieber, P. R., "Calculated Temperature Histories of Vaporizing Droplets to the Critical Point," AIAA Journal, December 1963

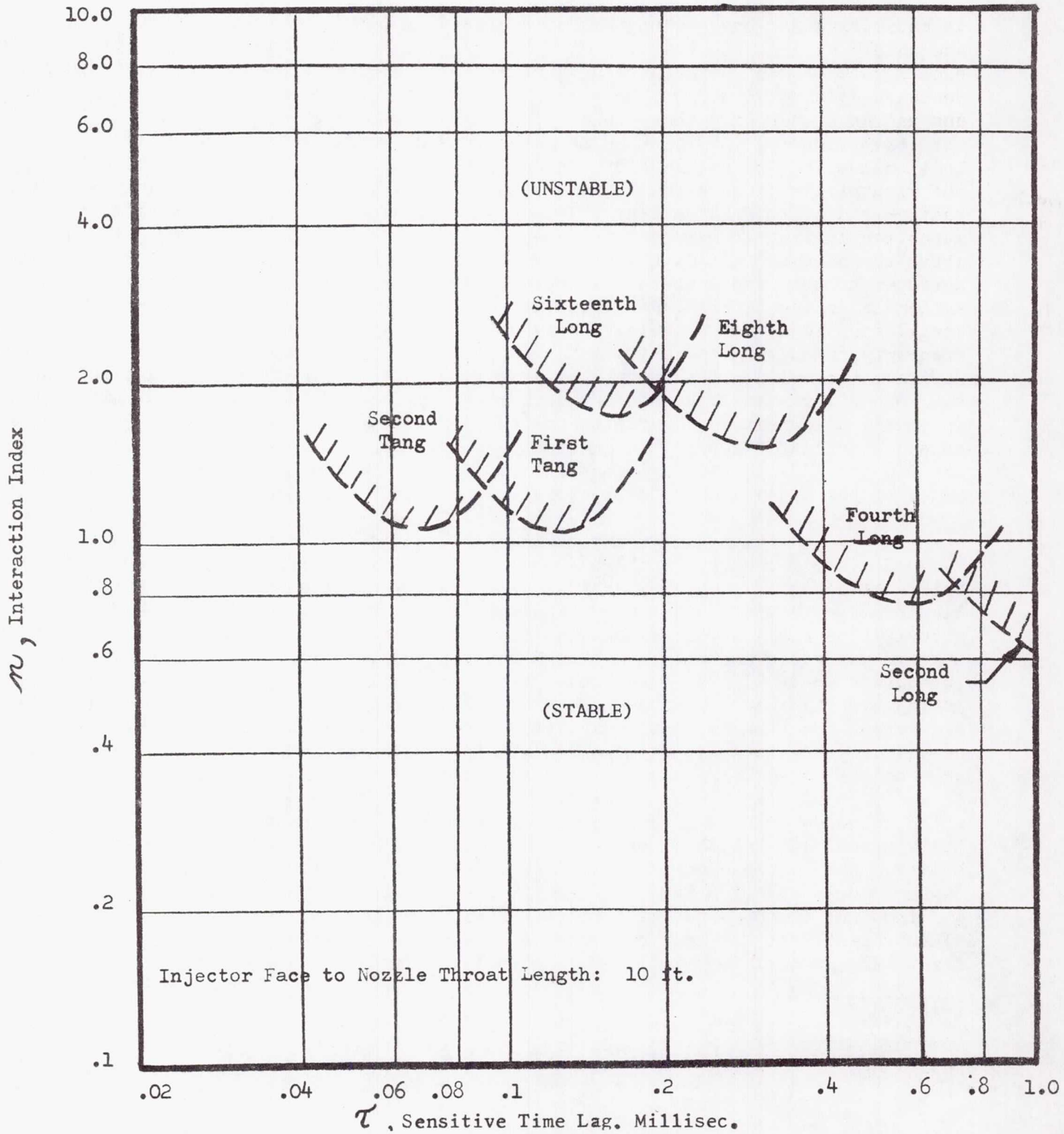

Figure 23

Estimated M-1 Gas Generator High Frequency Combustion Instability Zones

to be ascertained as to whether liquid oxygen vaporization rates can be used to adequately explain the occurrence of high frequency combustion instability or if the excellent agreement with the sensitive time lag theory is coincidence. If coincidence, no serious discrepancies could be found between the analytical assumptions and gas generator combustion conditions.

Initial multi-orifice gas generator assembly designs (Figures No. 3 and No. 4) utilized symmetrical four-legged injector baffles. However, the use of baffles did not permit uniform utilization of the available injector face area for injection orifices. Deep face erosion occurred because of combustion gas recirculation in the void injection areas; therefore, unbaffled injectors were tested during an interim period. It was during this testing of unbaffled injectors that first tangential combustion instability occurred in three tests. When it was firmly established that high frequency combustion instability was a problem, two types of stability aids were designed for existing injectors: baffles and acoustical liners. To install baffles within the existing injector patterns, the five-legged spider baffle was designed for S/N 017, 017A, and 018 (Figures No. 10, No. 11, and No. 12). In addition to baffles, some design and development effort was expended on acoustical liners as stability aids.

Basically, the acoustical liner operates on the theory of the Helmholtz type resonator.(8) The gas cavity in the annulus between gas generator chamber wall and liner must locally resonate at the same frequency as the combustion instability frequency. When this occurs, the resistance of the apertures in the liner wall should absorb sufficient energy generated by the combustion instability to decrease the feedback gain and prevent combustion instability from occurring. The serious drawback of using acoustical liners is that they are effective only near the design resonance frequency. The liner resonance frequency is affected by the local gas properties behind the liner wall as well as the liner configuration. If the liner cavity gas properties are known, the acoustical liner can be designed to suppress a given resonance design frequency. This means liners are effective if, for a given rocket injector, only one predominant mode of high frequency combustion instability is expected to occur.

Serial No. 020 gas generator assembly had 132 injection elements. The oxidizer injection element was recessed 1/4-in. back from the injector face. The recessed cup design was based upon J-2 coaxial injection element data which appeared to be more stable than the comparable flush cup design. Because of the numerous injection elements, there was inadequate spacing between elements on the existing injector pattern (Figure No. 13) for the installation of baffles. Therefore, an acoustical liner design was used to suppress instability. Serial No. 004A, 007, and 015 gas generator assemblies had all previously encountered first tangential instabilities (approximately 4000 to 4500 cps, depending upon the mixture ratio). At

(8) Ingard, U., "On the Theory and Design of Acoustic Resonators," The Journal of the Acoustical Society of America, November 1953.

that time, it seemed logical to design the liner of S/N 020 to prevent first tangential instability. This liner was designed and fabricated at Aerojet-General by scaling and extrapolating the design plots supplied by NASA/LeRC. These plots were based upon a Pratt and Whitney computer model used to assist in acoustical liner design predictions.

The acoustical liner was tested with S/N 020 gas generator assembly and the second tangential mode of high frequency combustion instability occurred during Test No. 1.2-04-EHG-011. It was the first instance of this mode of instability in an M-1 gas generator assembly.

Because the acoustical liner for S/N 020 gas generator assembly was designed to damp only the first tangential instability mode, this test could not be used as the basis for determining whether the acoustical liner had served its purpose. The acoustical liner could have provided sufficient damping to prohibit the first tangential instability mode and, as a consequence, the combustion instability frequency could have been shifted to its next higher tangential mode. The possibility also exists that stability was affected because the number of coaxial elements per injector was increased and the thrust per element was decreased or because the oxidizer element was recessed. The finer injection grid may have improved propellant mixing sufficiently to decrease the combustion sensitive time lag, or the recessed oxidizer cup may have increased the propellant mixing time before the propellant reached the combustion zone, thus decreasing the sensitive time lag. If this occurred, the combustion sensitive time lag could have been decreased sufficiently to cause S/N 020 gas generator assembly to be inherently unstable only at the second tangential instability mode rather than at the first tangential mode. Because S/N 020 gas generator assembly was not tested again without an acoustical liner to determine which tangential modes were predominant, no conclusions about stability could be made concerning the effectiveness of the liner. It was beyond the scope of the M-1 gas generator development program to investigate combustion instability from a basic research standpoint or to expend further effort on the development of acoustical liners.

The first three unstable gas generator assembly tests with unbaffled injectors that encountered first tangential instability, occurred from October 1963 through April 1964. The only recognized influence on liquid oxygen and liquid hydrogen high frequency combustion instability previous to this had been the effect of hydrogen temperature on stability. It had been noted that high frequency combustion instability was more likely to occur at colder hydrogen injection temperatures. One method for quantitatively determining the screech margin of an injector had been to test with successively colder hydrogen injection temperatures until screeching occurred spontaneously, assuming that all other variables (P_c, M.R., $\dot{w}_t$, etc.) were kept constant. This empirical observation was not useful to the M-1 gas generator development program because the M-1 engine was being designed for deep space applications and the gas generator assembly had to be designed to operate with cold hydrogen for engine operation. However, in mid-1964 it was disclosed that liquid oxygen/liquid hydrogen injector research being performed at NASA/LeRC with coaxial injection elements indicated a possible injection velocity ratio (V_f/V_o)

effect upon high frequency combustion instability. When this information was received at Aerojet-General, the velocity ratio characteristics of the three unstable gas generator tests were re-analyzed. A discussion of as well as the conclusions from this analysis follows:

In a typical start transient, the test is always started with a fuel lead to control the start transient temperature spike. Propellant tank pressures are fully pressurized for steady-state operation prior to the test. Until ignition occurs in the chamber, a high ΔP exists between tank pressures and chamber pressure resulting in high flowrates through the propellant valves until the injector manifolds are filled and chamber ignition occurs. The effect of the fuel lead just prior to main chamber ignition can be seen by examining PfJGG, PoJGG, and PcGG shown in Figure No. 24. The injector manifolds are at ambient temperature prior to the test. The temperature of the feed facility propellant lines are chilled down only to the area of the gas generator valves prior to the test. Therefore, when the gas generator fuel valve is initially opened, chilling of the injector manifolds to cryogenic temperatures begins. The initially-injected hydrogen is heated by the injector heat capacity and has very low density. When the oxidizer valve is opened, the high ΔP that exists between the oxidizer tank pressure and the chamber pressure causes a rush of liquid oxygen flow through the gas generator oxidizer valve. Approximately 100 ft of facility propellant lines exist between the feed tanks and gas generator assembly. Even after the liquid oxygen injector manifold is filled, the facility line pressure surges continue flowing liquid oxygen at a high flowrate through the injector because of the high liquid oxygen density and long lines (considerable line momentum). When the liquid oxygen injector manifold volume fills, a sharp rise in chamber pressure occurs. The fuel facility line surges are almost nonexistent at the time of gas generator ignition, partly because of the earlier fuel valve opening but mainly because of the lower hydrogen density (compared to liquid oxygen). The fuel injector manifold has been chilling throughout the above time interval and the hydrogen injection temperature has been decreasing. When the main chamber pressure rise occurs, the fuel ΔP across the injector is abruptly decreased, because of the higher chamber pressure, and fuel injection flowrate is decreased. This was the critical stage in the M-1 gas generator start transient concerning high frequency combustion instability. A higher than steady-state oxidizer flowrate exists shortly after ignition because of the feed line momentum (liquid oxygen "water-hammer") effect which creates oxidizer injection velocities higher than during steady-state combustion. The fuel flowrate at the same time is abruptly lessened because of the decrease in fuel injector ΔP caused by rising chamber pressure. Simultaneously with the change in injector flowrates (increasing $\mathring{w}_o$ and decreasing $\mathring{w}_f$), the fuel injector continues chilling to the steady-state temperature which results in increased fuel injection density. As the fuel injection density increases, the fuel injection velocity decreases. Therefore, at some time shortly after gas generator ignition, the injection velocity ratio reaches a minimum value (considerably lower than steady-state injection velocity ratio) before returning to its steady-state value. All combustion instabilities analyzed were initiated during this period.

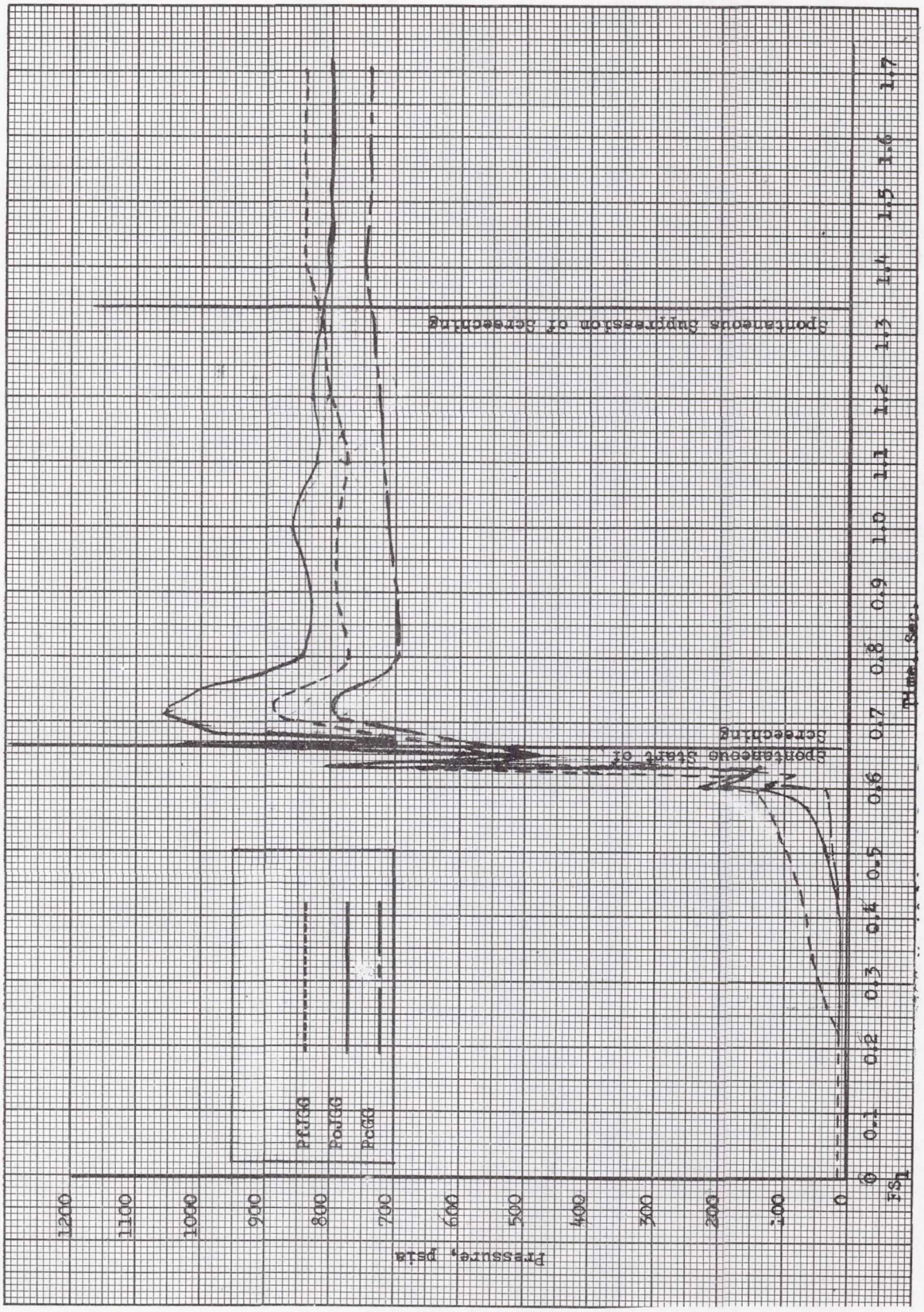

Figure 24

Injector Manifold and Gas Generator Chamber Pressure Versus Time for Test No. 1.2-03-EHG-003 with Serial Number 007 Multi-Orifice Gas Generator Assembly (Over-all Test)

Five successful tests with a cumulative component test duration in excess of 17 sec were conducted with S/N 007 multi-orifice gas generator assembly. During Test No. 1.2-03-EHG-003, the first tangential mode of high frequency combustion instability occurred. This combustion instability frequency was 4450 cps.

In Test No. 1.2-03-EHG-003, screeching was spontaneously initiated at FS_1 + 0.664 sec. At the time instability started, the injection velocity ratio was 2.2 and was still decreasing. Fuel injector manifold temperature at the start of instability was 59°R. The test was allowed to continue despite the instability. Analysis of the data indicated that erosion of the oxidizer injector faceplates began at approximately FS_1 + 1.1 sec and they continued eroding until approximately FS_1 + 1.6 sec. However, at FS_1 + 1.34 sec, all traces of screeching were spontaneously suppressed. It was calculated that at this time the injection velocity ratio was approximately 9.4 and the fuel injection temperature was 50°R. The injection velocity ratio was calculated based upon known propellant flowrates and injector pressure drops. The fuel faceplates were not eroded through at the end of the test; therefore, the fuel injection velocity was calculable.

The oxidizer injection velocity was calculated based upon the area of oxidizer faceplate that was eroded through at 1.34 sec. The latter was estimated by noting the progressive change in oxidizer injector pressure drop resistance during the test and noting the injection area available after the test. It is possible that the eroded oxidizer faceplate altered the liquid oxygen atomization characteristics and the latter suppressed the instability rather than the high injection velocity ratio; however, other examples will be given.

Serial No. 015 coaxial gas generator assembly encountered its first tangential high frequency combustion instability during Test No. 1.2-03-EHG-006. Screeching frequency was 4500 cps. The test sequence mechanics were identical to those previously explained in detail for S/N 007 gas generator assembly. A pressure plot of the over-all test is given in Figure No. 25. A detailed plot of injector manifold pressures, injection velocities, chamber pressure, and velocity ratio for the 15 millisec interval prior to the spontaneous start of combustion instability is shown in Figure No. 26. The injection velocity ratio at the start of instability was 3.4 at FS_1 + 0.5995 sec. Fuel injection temperature was 60°R at the start of instability. Figure No. 27 shows the same pressure and injection velocity parameters as Figure No. 26 except that the details are given for the 2 millisec time interval around the spontaneous suppression of high frequency combustion instability with coaxial gas generator S/N 015.

Because of a high amplitude pressure surge in PoJGG, the oxidizer manifold pressure dropped below PcGG for an interval of one-half millisec at FS_1 + 0.669 sec. It is assumed that the oxidizer flowrate momentarily ceased during the corresponding time interval. Thus, oxidizer injection velocity was zero and the injection velocity ratio was momentarily infinite. At FS_1 + 0.6691 sec, all trace of combustion instability was spontaneously and sharply terminated. Shortly thereafter, normal combustion resumed at a steady-state injection velocity ratio approximately equal to

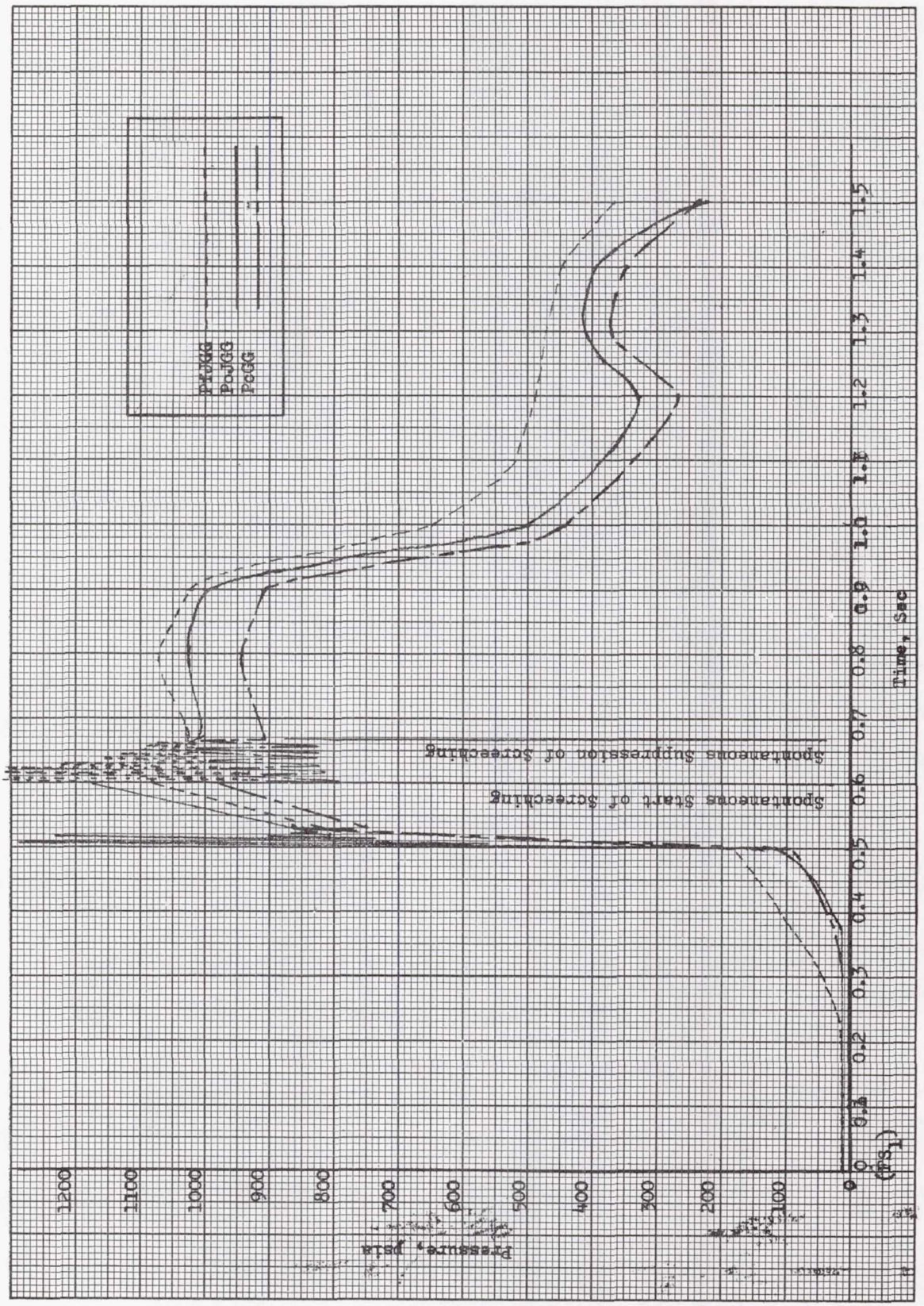

Figure 25

Injector Manifold and Gas Generator Chamber Pressure Versus Time for Test No. 1.2-03-EHG-006 with Serial Number 015 Coaxial Gas Generator Assembly (Over-all Test)

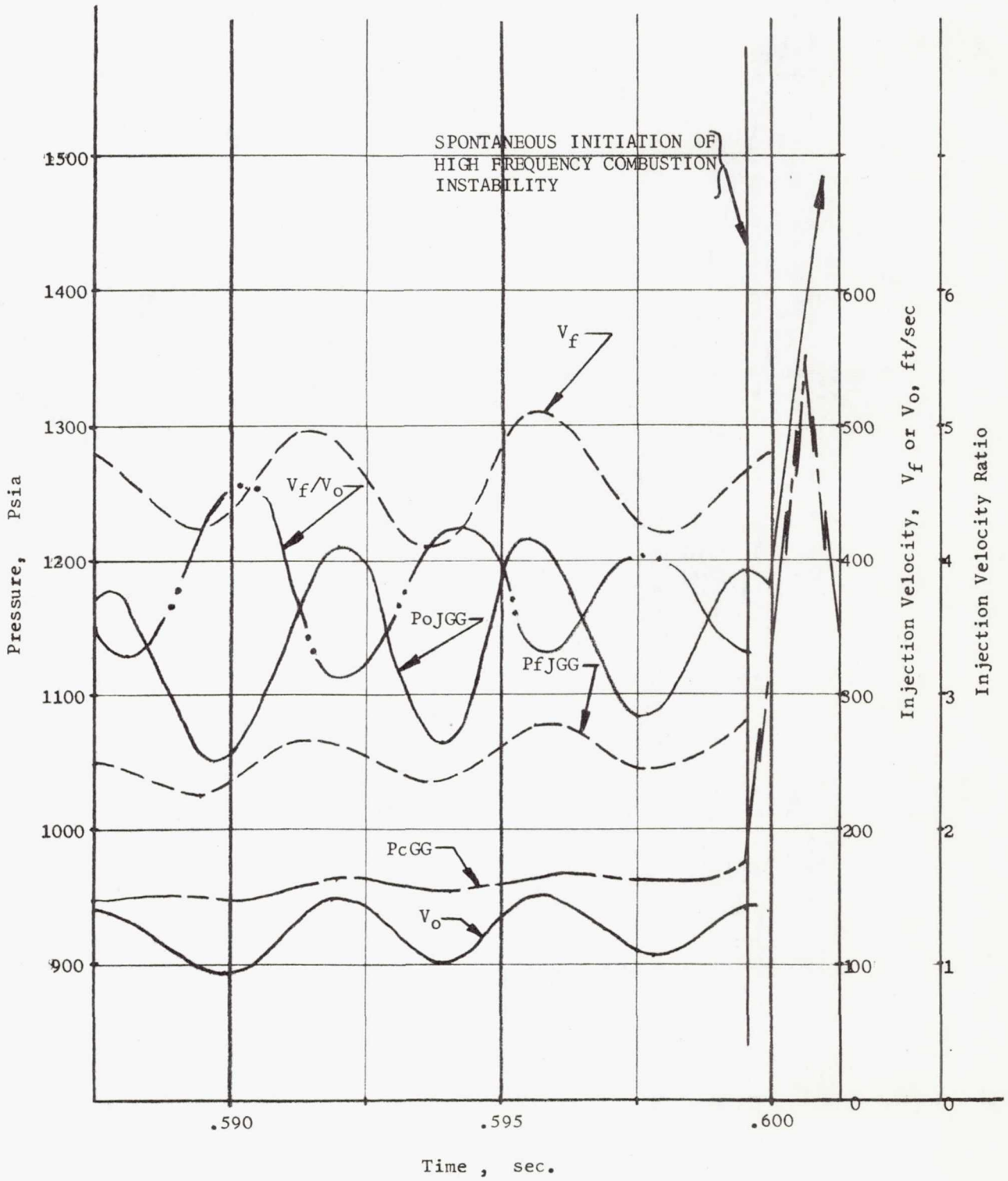

Figure 26

Pressures, Injection Velocities, and Velocity Ratio
Spontaneous Initiation of High Frequency Combustion
Instability of Serial Number 015 Coaxial Gas Generator
Assembly During Test No. 1.2-03-EHG-006 (Typical)

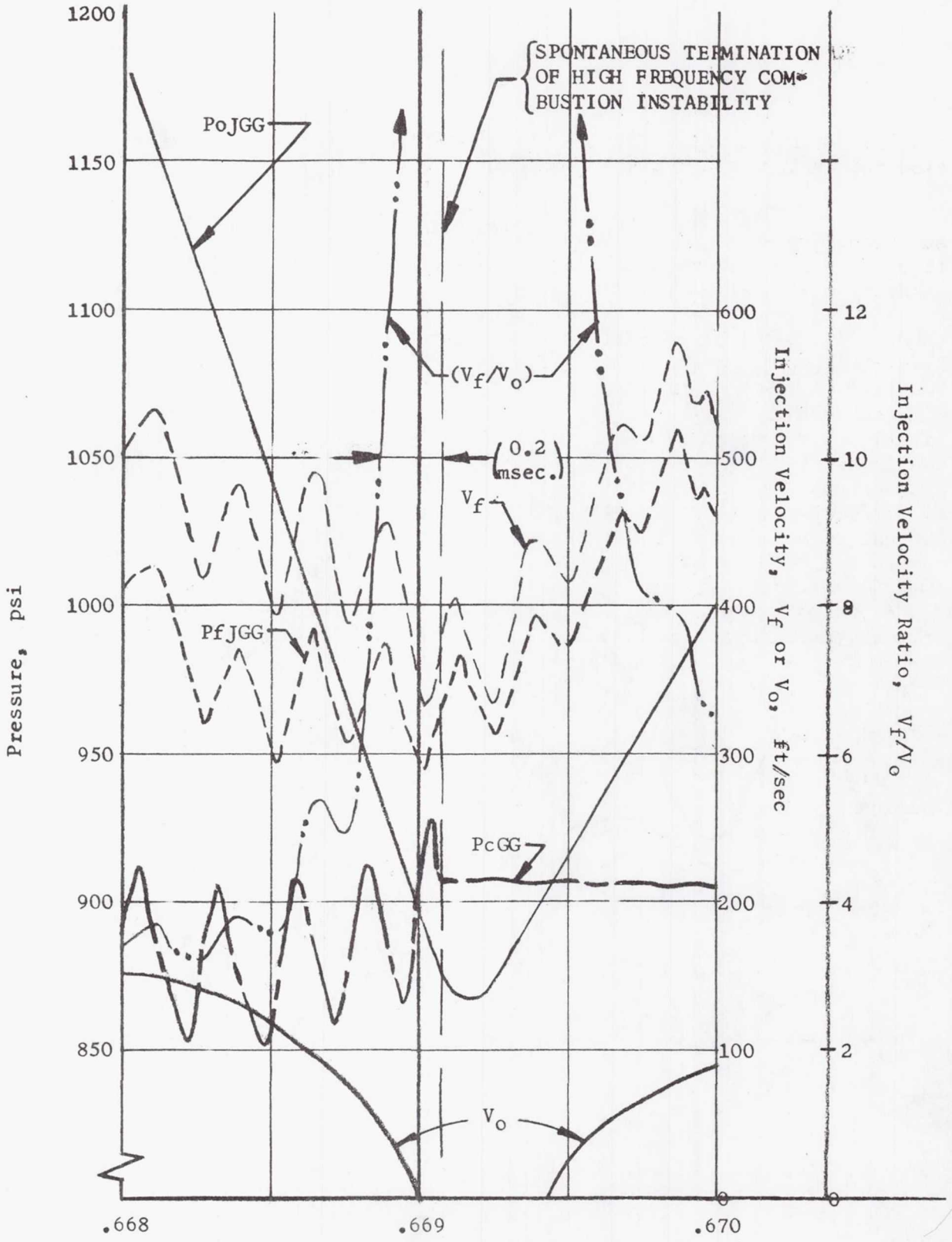

Figure 27

Pressures, Injection Velocities, and Velocity Ratio at Spontaneous Termination of High Frequency Combustion Instability of Serial Number 015 Coaxial Gas Generator Assembly During Test No. 1.2-03-EHG-006 (Typical)

5 with no further indication of high frequency combustion instability. Fuel injection temperature at 0.669 sec was 55°R.

It cannot be exactly determined at what velocity ratio instability was suppressed because of its abrupt rise. However, if a 0.2 millisec delay is assumed to have occurred between propellant injection and the quenching of instability, the velocity ratio was approximately ten.

One injection element was lost during this test because of an inadequate element-to-injector backplate joint design. It is not known at what point during the test or instability that the element was lost. The possibility has been considered that the loss of a single injection element (from 34 total elements) sufficiently disrupted the local injection flow pattern and combustion dynamics to quench the instability. However, this possibility appears unlikely because it has been stated that S/N 007 gas generator assembly encountered combustion instability at FS_1 + 0.664 sec. The oxidizer faceplates started to erode through at FS_1 + 1.1 sec, but was probably still intact until this point. The oxidizer faceplate erosion continued until FS_1 + 1.6 sec. After the test, post-fire injector face inspection revealed that approximately 60% of the total oxidizer injector face rings were completely eroded away. If it is assumed that a linear rate of oxidizer faceplate burn through occurred between 1.1 and 1.6 sec, at least 30% of the oxidizer face rings must have been eroded away before the instability was quenched at 1.34 sec. The effect of 30% of the total oxidizer faceplates being eroded through would be to disrupt the injection flow pattern to a greater extent than if only one of the 34 coaxial injection elements was lost. However, it was the former condition that was still unstable. It can also be shown analytically that if high frequency combustion instability is treated as a problem which satisfies the linear acoustic wave equation (for small pressure perturbations) for a cylindrical combustion chamber (which is very nearly the case for the M-1 gas generator assembly), then the solution for the first tangential instability mode is satisfied by the first order Bessel function of the first kind $\left[J_1 \left(\alpha_{1,0}\, r/R_o\right)\right]$.

Where:

$J_1 (x)$ = First order Bessel function of the first kind

$\alpha_{1,0} = 1.8413$

r = Local radius at which pressure perturbations are being calculated

R_o = Chamber radius

The injection element was lost from the innermost row of injection elements on S/N 015 gas generator assembly. Because of the nature of the first order Bessel function of the first kind, the pressure perturbation at the axis of the injector is negligible. The maximum pressure perturbation occurs at the chamber wall. Therefore, the loss of a single element in the innermost row should be expected to have the least effect in disrupting combustion gas dynamics because it occurs in a region

that experiences the least amplitude of pressure fluctuations than anywhere else on the injector face for the first tangential instability mode. It still appears that a high injection velocity ratio had a greater effect in spontaneously quenching high frequency combustion instability than the lost element in coaxial gas generator assembly S/N 015.

The first tangential mode of high frequency combustion instability occurred during Test No. 1.2-03-EHG-007 with S/N 004A multi-orifice gas generator assembly. The instability frequency was 4450 ± 150 cps. The variation in frequency occurred because the changing mixture ratio caused combustion gas acoustic velocity to vary and, as a consequence, the instability frequency varied. Pressures during the test are shown in Figure No. 28. Spontaneous screeching was initiated at FS_1 + 0.740 sec. At this time, the injection velocity ratio was 3.3 and still decreasing. Fuel injection temperature was 55°R. Because of the instability, the test was shut down (FS_2) at FS_1 + 0.780 sec. A fuel lead is used during start and a fuel lag is used for shutdown to prevent temperature spikes. When shutdown was signaled, the oxidizer valve began closing. The decreased oxidizer flowrate caused PoJGG to drop, as shown in Figure No. 28. Oxidizer injection velocity also decreased with decreasing oxidizer flowrate. At FS_1 + 1.01 sec (FS_2 + 0.23 sec), the injection velocity ratio had increased to 9.0, at which time the high frequency combustion instability ceased. Fuel injection temperature was approximately 48°R. Chugging started to occur beyond this point because of low oxidizer injector ΔP, but nevertheless, as regards high frequency combustion instability, the screeching stopped.

The last unstable test occurred with S/N 020 coaxial gas generator assembly. As mentioned previously, the possibility existed that the natural combustion sensitive time lag for S/N 020 gas generator assembly could have been less than with the three injector designs discussed above. The 132 injection elements on S/N 020 constituted nearly four times the number of elements used in S/N 015 and twice that used in S/N 022. Also, the oxidizer element recessed cup design was based upon J-2 thrust chamber data, indicating improved combustion stability characteristics. When S/N 020 coaxial gas generator assembly was tested with an acoustical liner but without baffles, second tangential (7200 cps) instability was encountered. Test parameters are shown in Figure No. 29. When ignition occurred at FS_1 + 0.72 sec, the injection velocity ratio was 5.0. Thereafter, the velocity ratio steadily decreased to 2.9 and was still decreasing when spontaneous screeching started at FS_1 + 1.19 sec. Fuel injection temperature was 55°R. Test termination was signaled at FS_1 + 1.223 sec because of instability and the oxidizer valve started closing. The decreased oxidizer flow caused P_oJGG and oxidizer injection velocity to decrease. The fuel valve remained nearly full open because of the required fuel lag during shutdown. Therefore, the relative proportion of fuel flowrate to oxidizer flowrate and injection velocity ratio increased. At FS_1 + 1.55 sec, the injection velocity ratio had increased to 5.7 and was still increasing when the second tangential high frequency combustion instability was spontaneously suppressed. The absolute value of injection velocity ratio at which instability was suppressed was lower with S/N 020 gas generator assembly than experienced during previous unstable tests. This could have been the result of mutual influence of both injection velocity ratio and oxidizer recess upon combustion stability. Two generalizations have been made concerning

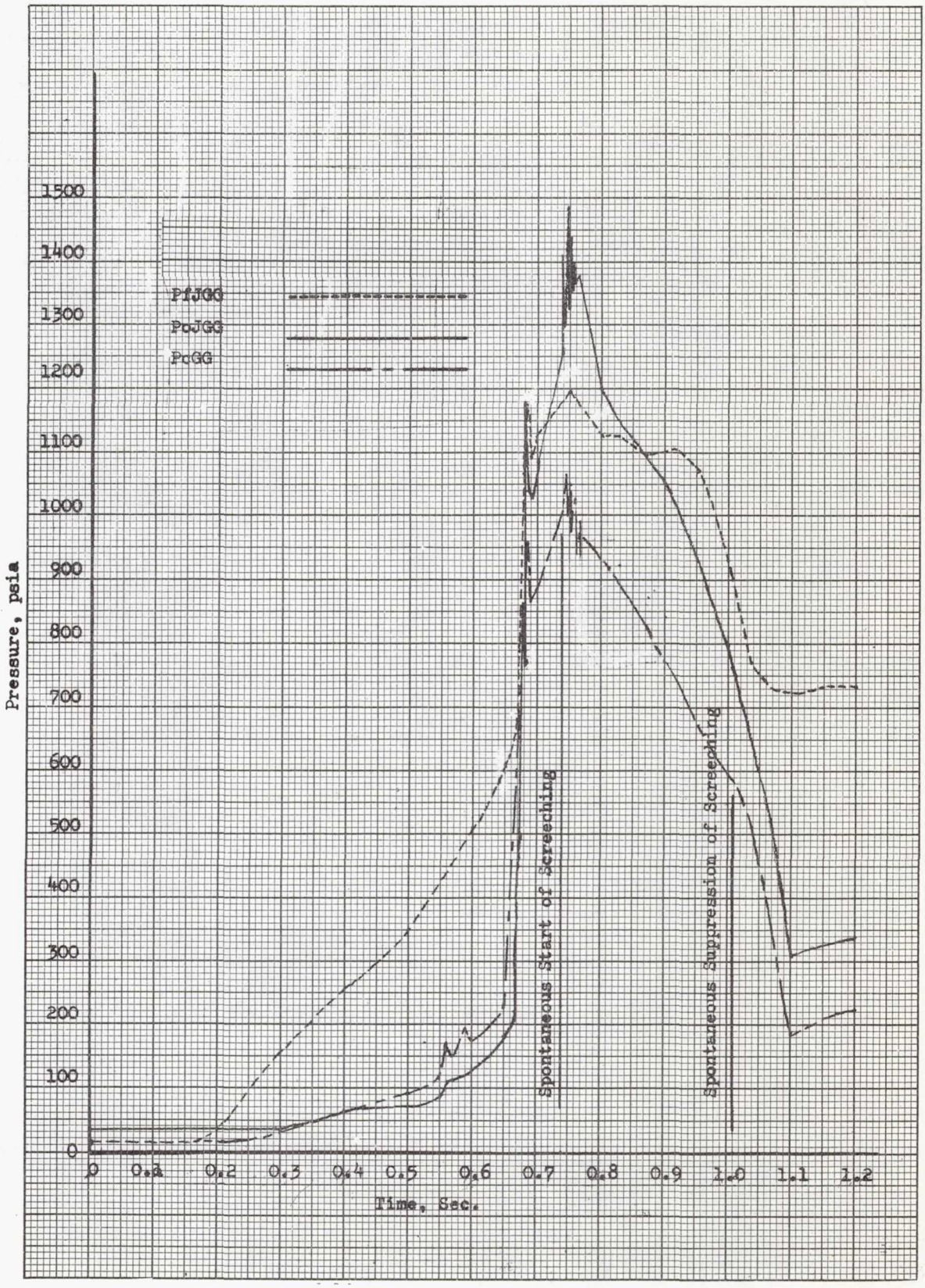

Figure 28

Injector Manifold and Gas Generator Chamber Pressure Versus Time for Test No. 1.2-03-EHG-007 with Serial Number 004A Multi-Orifice Gas Generator Assembly (Over-all Test)

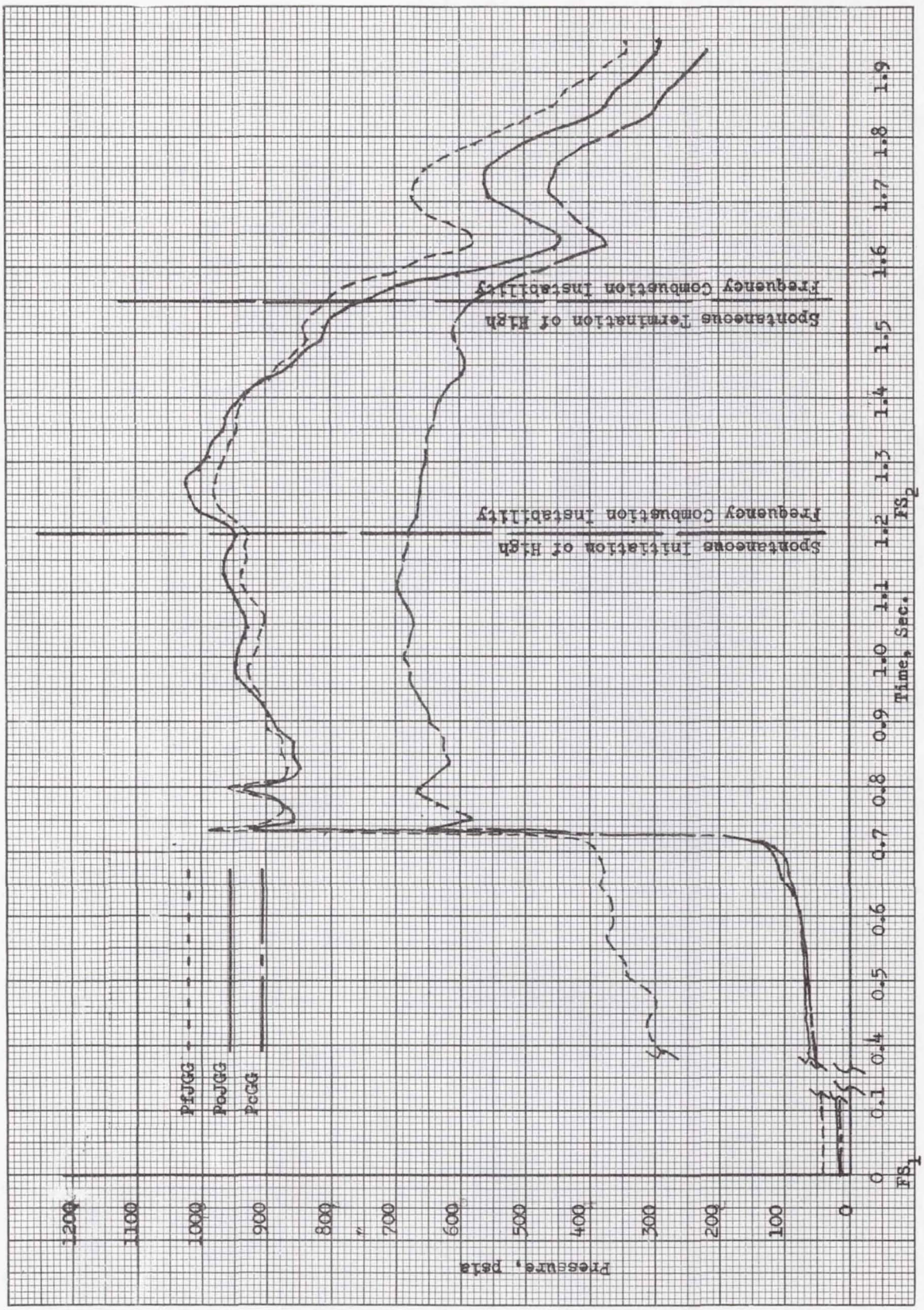

Figure 29

Injector Manifold and Gas Generator Chamber Pressure Versus Time for Test No. 1.2-04-EHG-011 with Serial Number 020 Coaxial Gas Generator Assembly (Over-all Test)

J-2 stability. One was that the greater the oxidizer recess, the greater the stability; the other was that the greater the injection velocity ratio, the greater the stability.

It is possible that the value of the injection velocity ratio required to suppress combustion instability changes with the sensitive time lag (i.e., the required velocity ratio to suppress second tangential instability may be less than that required to suppress the first tangential mode). Although the acoustical liner for S/N 020 was only designed to suppress first tangential instability, its effect on the second tangential mode may have been sufficient to permit stable combustion at a lower injection velocity ratio. In any case, it was indicated from S/N 020 coaxial gas generator assembly testing that even when operating within steady-state combustion instability conditions, when the injection velocity ratio increased, combustion was stabilized.

The fuel injection temperature and injection velocity ratio in all four unstable tests at the time of spontaneous initiation and spontaneous termination of high frequency combustion instability are shown in Figure No. 30. It was apparent in all four cases that combustion instability occurred at some lower injection velocity ratio and stabilized at another higher velocity ratio. This indicates there was a definite hysteresis loop in the velocity ratio versus stability criteria. Ignition occurred at some intermediate velocity ratio and the combustion was stable. Velocity ratio decreased because of the nature of the test conditions, and instability was probably caused by normal combustion noise at some point before a minimum velocity ratio was obtained. Once the instability occurred, the pressure perturbations were self-sustaining as velocity ratio increased and passed previously stable (when unimpulsed) regimes. But when the velocity ratio became sufficiently high, the instability could not be maintained even when combustion was pulsed from its own instability pressure perturbations and the instability was suppressed. There probably exists an intermediate velocity ratio at which instability would not be triggered by its own normal combustion noise. This intermediate value would have to be determined statistically from many repeated tests and was beyond the scope of the M-1 gas generator development program.

M-1 gas generator test data did not support liquid oxygen/liquid hydrogen stability criteria that combustion instability was more likely at colder hydrogen temperature. The influence of colder hydrogen temperatures probably had an indirect relationship to stability by causing an increase in fuel density and, thus, a lower injection velocity ratio for a fixed injector configuration. The correlation was probably recognized sooner because fuel temperature is a directly-recorded test parameter, whereas the injection velocity ratio is a calculated quantity.

The mechanism for improving stability by varying injection velocity ratio is probably the result of liquid phase mixing phenomena, although the details are not yet fully known. The occurrence of Free-Turbulence Shear Flows has been discussed by Rouse[9]. Briefly, he describes the relative cross-diffusion rates between

---

[9] Rouse, H., et al, Advanced Mechanics of Fluids, John Wiley and Sons, Inc., New York, 1959.

Figure 30

Fuel Injector Manifold Temperature and Injection Velocity Ratio Effect on High Frequency Combustion Instability

two hydraulic fluids injected in parallel concentric streams at two distinct injection velocities. The change in velocity gradient and fluid specie concentration with axial distance from the point of injection is related to the injection velocity ratio. This mathematically-derived analysis can make the empirically-observed relationship of injection velocity ratios and high frequency combustion stability more understandable.

Based upon over-all performance, stability, and combustion gas temperature distribution, S/N 018 and 022 type gas generator assemblies were the most successful. No conclusions regarding injection velocity ratio in relationship to high frequency combustion stability were possible upon the basis of the tests conducted with these assemblies. This was because both injectors had baffles. Serial No. 018 only had a design injection velocity ratio of 3.5 at steady-state (even lower during the start transients) and S/N 022 had a 10.0 velocity ratio. A low velocity ratio does not necessarily imply a longitudinal mode of instability should have been experienced by S/N 018 gas generator assembly. If the estimates of interaction index (n) for high frequency longitudinal modes are correct, and are higher than for transverse instabilities at the same frequencies (see Figure No. 23), the test results may indicate that only the transverse modes of unbaffled injectors are marginally unstable at low velocity ratios.

Serial No. 022 gas generator assembly was designed with a 10.0 injection velocity ratio. The showerhead oxidizer element was counterbored to decrease oxidizer injection velocity. The oxidizer element was recessed 0.200-in. because of a greater indicated stability with like J-2 element designs. Furthermore, because the injector pattern was not yet designed, it was decided to install injector baffles as added assurance of transverse combustion stability. A radial five-bladed baffle was designed.

Several variations of the prototype S/N 022 injection element were evaluated during single injection element tests at Aerojet-General. Because of the original concept that the higher the injection velocity ratio, the greater the high frequency combustion stability, the initial designs incorporated nominal injection velocity ratios of from 15 to 20. The basic element design was the same as the prototype element shown in Figure No. 8 with minor variations made in the annular fuel injection area and oxidizer injection area by chamfering or counterboring the oxidizer element tips. Severe chugging characteristics were exhibited during single injection element tests of these initial high velocity ratio elements. Some of the parameters pertinent to chugging characteristics are listed in Table IV for S/N 022 type injection elements. All numerical values were taken at steady-state chugging conditions.

The parameter $(4\pi^2 f^2 \frac{\Delta P_c}{\bar{P}_c})$ was selected to denote a quantitative measure of chugging. This parameter is plotted against injection velocity ratio, oxidizer injection velocity, and oxidizer injection element pressure drop in Figures No. 31, No. 32, and No. 33. This parameter was selected based upon the

TABLE IV

GAS GENERATOR SINGLE INJECTION ELEMENT CHUGGING DATA

Vo	Vf	Vf/Vo	M.R.	$\bar{P}_c$	f	ΔP_c	ΔP_o	ΔP_f	$4\pi^2 f^2 \left(\frac{\Delta P_c}{\bar{P}_c}\right)$
27.8	369	13.3	1.04	1121	50	90	111	79	7.91×10^3
23.2	366	15.7	0.95	1125	57	90	108	84	10.2
22.5	402	17.9	1.01	1121	55	165	107	83	17.6
18.3	369	20.2	0.72	1106	65	65	134	139	9.79
19.6	386	19.6	0.69	1157	90	55	188	131	15.2
47.9	564	11.8	0.88	1120	50	45	224	211	3.97
50.6	541	10.7	0.95	1096	55	50	213	205	5.46
51.4	807	15.7	0.73	1155	65	33	233	274	4.77
59.3	420	7.1	1.03	1093	60	22	252	139	2.86
55.7	431	7.7	0.93	1103	60	20	245	150	2.57×10^3

Where: Vo = Oxidizer Injection Velocity, fps

Vf = Fuel Injection Velocity, fps

$\bar{P}c$ = Mean Chamber Pressure, psia

f = Chugging Frequency, cps

ΔPc = Chamber Pressure Chugging Amplitude, psi

ΔPo = Oxidizer Injector Pressure Drop, psi

ΔPf = Fuel Injector Pressure Drop, psi

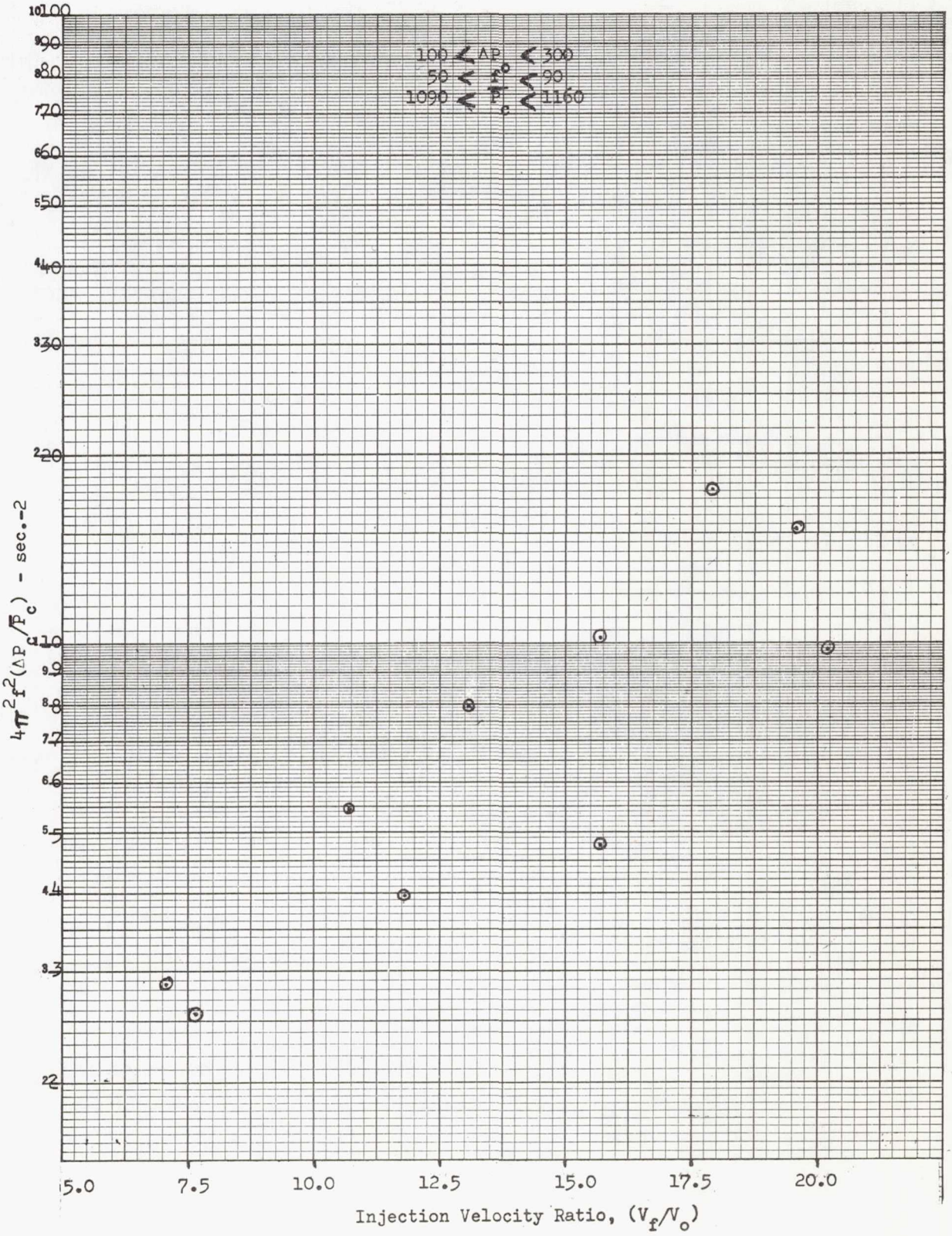

Figure 31

Injection Velocity Ratio Effect on Gas

Generator Single Injection Element Chugging

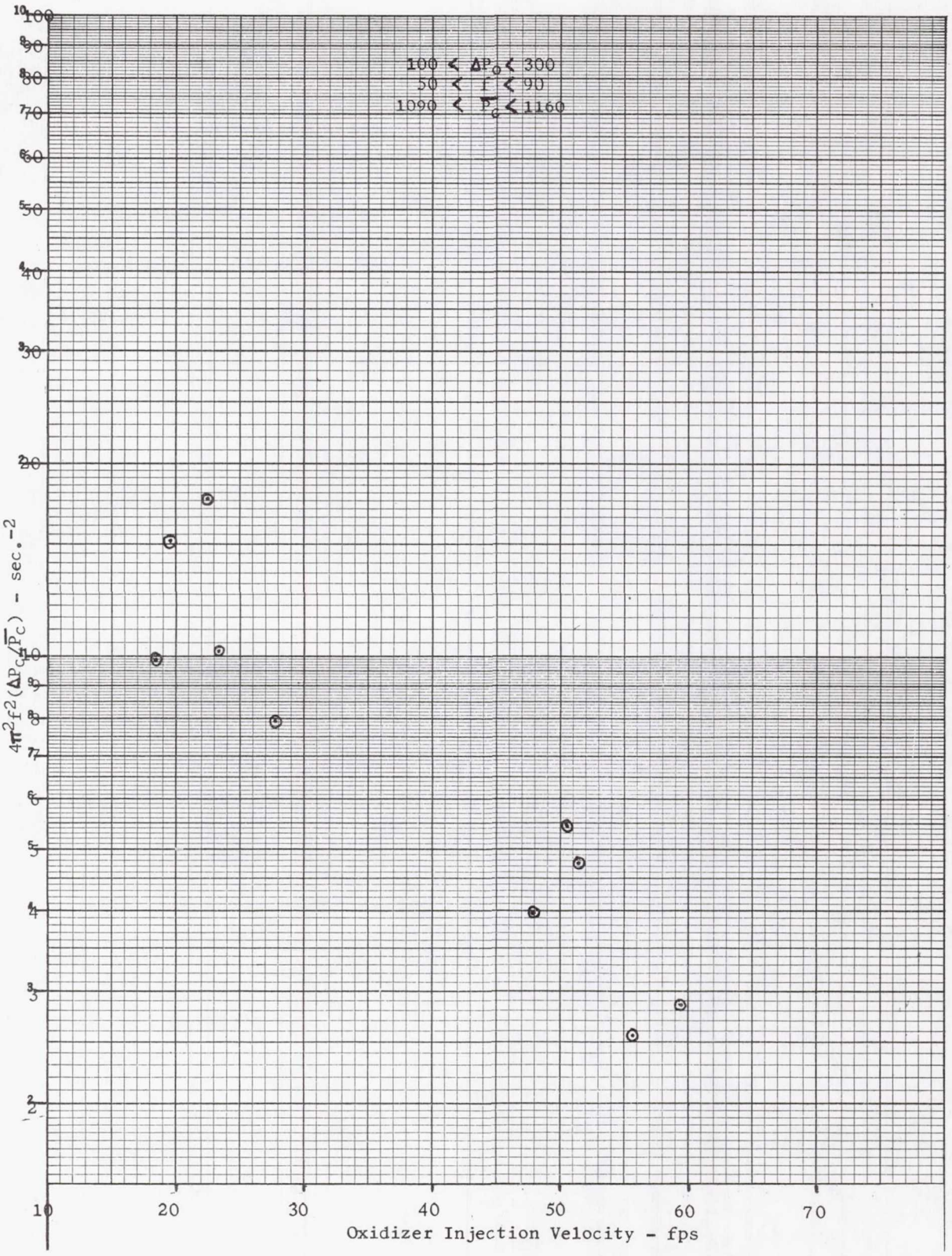

Figure 32

Oxidizer Injection Velocity Effect on Gas

Generator Single Injection Element Chugging

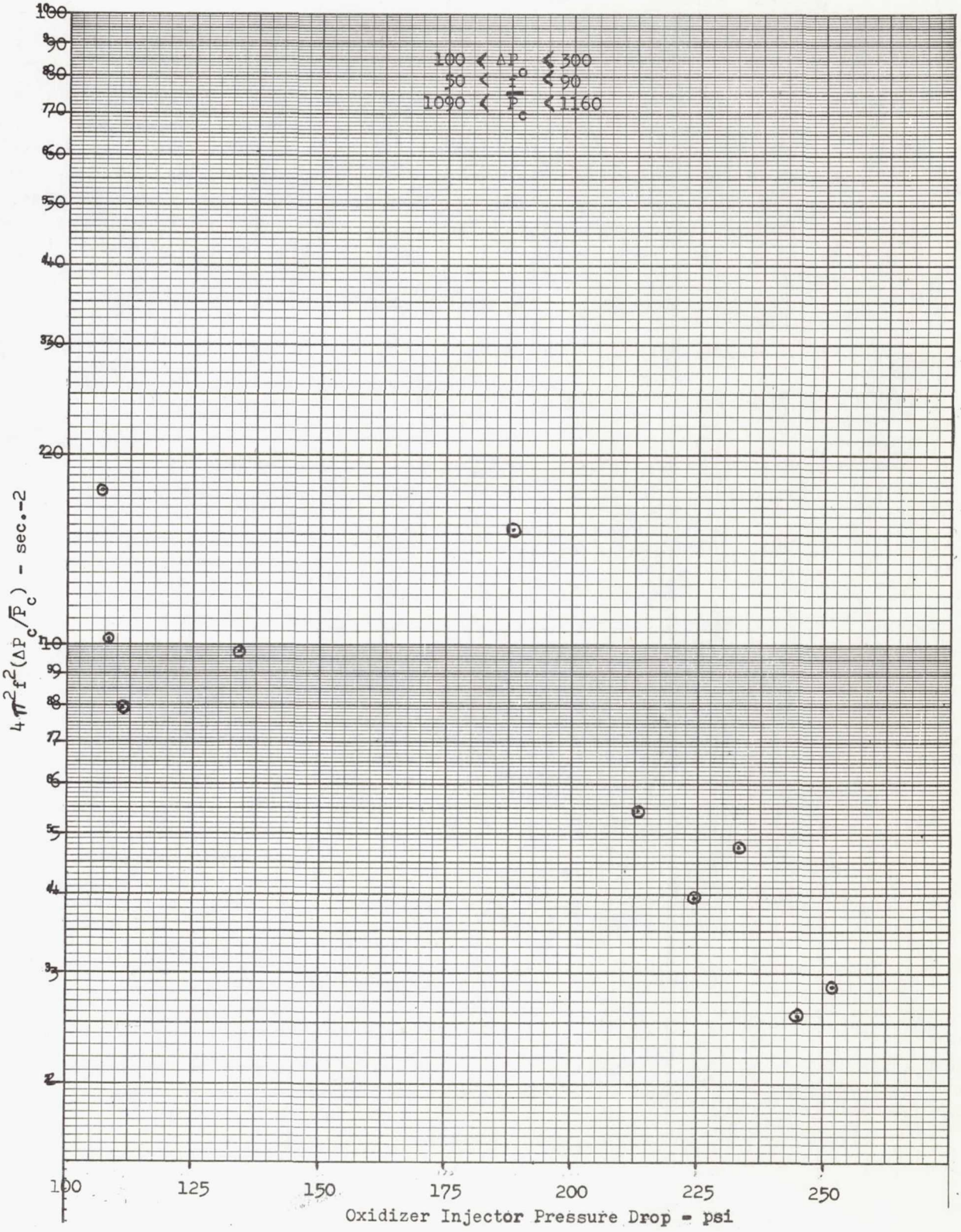

Figure 33

Oxidizer Injector Pressure Drop Effect on Gas

Generator Single Injection Element Chugging

following approximations.

$$P_c(\tau) = \bar{P}_c + \Delta P_c \sin 2\pi f \tau$$

is the assumed time variation in chamber pressure. The propellant injection flowrate for a simple lumped resistive flow system with constant pressurized feed tanks (for simplicity, both feed tanks were assumed to be at equal pressure) then becomes

$$\dot{W}_j(\tau) = K \sqrt{P_T - (\bar{P}_c + \Delta P_c \sin 2\pi f \tau)}$$

The nozzle flowrate of combusted gases is assumed to be

$$\dot{W}_n(\tau) = \left(\bar{P}_c + \Delta P_c \sin 2\pi f \tau\right) \frac{g A_T}{C^*}$$

and the mass (or weight) of combustion gases in the chamber is

$$W_c(\tau) = \frac{\left(\bar{P}_c + \Delta P_c \sin 2\pi f \tau\right) g(\mathrm{Vol})_c}{RT_c}$$

where: K = Hydraulic Flow Proportionality Factor

P_T = Propellant Feed Tank Pressure

R = Gas Constant

$(\mathrm{Vol})_c$ = Chamber Volume

W_c = Weight of Chamber Gases

$\dot{W}_n$ = Nozzle Flowrate

$\dot{W}_{comb}$ = Rate of Combustion

$\dot{W}_{css}$ = Steady-State Chamber Flowrate When $\Delta P_c = 0$

τ = Time Variable

σ = Combustion Dead Time

Other parameters are defined in Tables II and IV. The rate of gas combusted is assumed to be equal to the propellant injected at the prior dead time, σ,

$$\dot{W}_{comb.}(\tau) = \dot{W}_j(\tau - \sigma)$$

The rate of change of combustion gases in the chamber is

$$\frac{dW_c(\tau)}{d\tau} = \dot{W}_c(\tau) = \frac{g(Vol)_c}{RT_c}\left(2\pi f \Delta P_c \cos 2\pi f\tau\right)$$

But the rate of change of combustion gases in the chamber is the difference between the rate of gas combusted and nozzle outflow rate

$$\dot{W}_c(\tau) = \dot{W}_j(\tau - \sigma) - \dot{W}_n(\tau)$$

or

$$\dot{W}_c(\tau) = \frac{g(Vol)_c}{RT_c}\left(2\pi f \Delta P_c \cos 2\pi f\tau\right) = K\sqrt{P_T - \left[\bar{P}_c + \Delta P_c \sin 2\pi f(\tau-\sigma)\right]} - \frac{\bar{P}_c g A_T}{C^*}\left(1 + \frac{\Delta P_c \sin 2\pi f\tau}{\bar{P}_c}\right)$$

if no chugging occurs ($\Delta P_c = 0$), steady-state conditions indicate

$$\dot{W}_{css}(\tau) = 0 = K\sqrt{P_T - \bar{P}_c} - \frac{\bar{P}_c g A_T}{C^*}$$

therefore

$$\dot{W}_c(\tau) = \frac{g(Vol)_c}{RT_c}\left(2\pi f \Delta P_c \cos 2\pi f\tau\right) = \frac{\bar{P}_c g A_T}{C^*}\left[\sqrt{1 - \frac{\Delta P_c \sin 2\pi f(\tau-\sigma)}{P_T - \bar{P}_c}} - 1 - \frac{\Delta P_c \sin 2\pi f\tau}{\bar{P}_c}\right]$$

the next higher time derivative gives the maximum and the minimum for this unsteady flow condition

$$\ddot{W}_c(\tau) = -\frac{g(Vol)_c}{RT_c}\left(4\pi^2 f^2 \Delta P_c \sin 2\pi f\tau\right) = \frac{\bar{P}_c g A_T}{C^*}\left[\frac{2\pi f \Delta P_c \cos 2\pi f(\tau-\sigma)}{2(P_T - \bar{P}_c)\sqrt{1 - \frac{\Delta P_c \sin 2\pi f(\tau-\sigma)}{P_T - \bar{P}_c}}} - \frac{2\pi f \Delta P_c \cos 2\pi f\tau}{\bar{P}_c}\right]$$

Normalizing by $\bar{P}_c$

$$\frac{\ddot{W}_c(\tau)}{\bar{P}_c} = \left[\frac{4\pi^2 f^2 \Delta P_c}{\bar{P}_c}\right] \frac{g(Vol)_c}{RT_c} \sin 2\pi f \tau$$

Therefore, the term $4\pi^2 f^2 \frac{\Delta P_c}{\bar{P}_c}$ was interpreted as being indicative of the magnitude of oscillatory flowrate in defining the chugging limit cycle. It was desirable to minimize this quantity to improve the characteristic chugging stability of the M-1 gas generator. The chugging limit cycle may be a means of semi-quantitatively evaluating the relative negative gain margins based upon feedback gain analysis of chugging criteria[10]. The effect of oxidizer and fuel injector pressure drops relative to mean chamber pressure and injection velocity ratio effects have previously been analytically treated [11].

It is indicated from the data given in Figure No. 31 that the chugging is amplified for higher injection velocity ratios. Almost this same conclusion was reached in the testing of S/N 017 and 017A gas generator assemblies. One test of S/N 017 was conducted with an acoustical liner and mild low frequency combustion oscillations occurred. The oxidizer element tips were counterbored, thus decreasing oxidizer injection velocity and increasing velocity ratio. When S/N 017A gas generator assembly was retested, after being reworked, and without an acoustical liner, low frequency combustion characteristics were more predominate. Acoustic testing of the liner indicated its resonance frequency was in the approximate range of 10,000 cps and it was doubtful that it materially contributed to stabilize the low frequency oscillations (approximately 200 cps) of S/N 017 gas generator assembly. The data points in Figure No. 31 appear to fall on two separate lines. Generally, as can be seen from Table IV, points for the tests at higher mixture ratios fall near the upper curve and those at lower mixture ratios fall near the lower curve. Many other variables could have influenced chugging, and these were not considered. The data are aligned on a semi-logarithmic plot, which may either indicate that the negative gain margin function or the nonlinear loss effects for chugging with injection velocity ratio has an exponential relationship. The information in Figure No. 32 may indicate the chugging effect was caused by low oxidizer injection

---

(10) Wenzel, L. M. and Szuch, J. R., Analysis of Chugging in Liquid Bi-Propellant Rocket Engines Using Propellants with Different Vaporization Rates, NASA TN D-3080, 1965.

(11) Hurrell, H. G., Analysis of Injection-Velocity Effects on Rocket Motor Dynamics and Stability, NASA TR R-43, 1959.

velocities. The mixture ratio effect on the scatter of points is not as obvious in Figure No. 32 as it is in Figure No. 31. Chugging performance criteria incur considerably more scatter in the data when plotted against oxidizer injection element pressure drop, although the expected trend is still evident (i.e., increased chugging at low oxidizer pressure drops). The single datum point at 188 psi oxidizer $\triangle P_o$, which appears far out of line, may partly be because of its high (19.6) velocity ratio. It is not known which of these three parameters is the most important in eliminating chugging.

Based upon data from the single element tests, a nominal injection velocity ratio of 10 was selected for S/N 022 prototype gas generator assembly. Lower velocity ratios appeared to promise greater low frequency stability; however, they were thought to be less effective in suppressing high frequency instability, which was considered more important. Because 10 was the highest anticipated value required to suppress high frequency combustion instability, it was selected to achieve the most favorable low frequency combustion characteristics without compromising high frequency instability suppression capabilities.

In addition to the previously mentioned injection pressure drop and injection velocity effects, design mixture ratio also influences low frequency stability. At low mixture ratios, the combustion performance is more sensitive to oxidizer flowrate than to fuel (e.g., a 1 lb/sec change in oxidizer flowrate results in a significantly greater change in performance than the same change in fuel flowrate). Therefore, it was noted during M-1 gas generator testing that when chugging occurred it was usually caused by an interaction with the oxidizer injection pressures rather than with the fuel.

Besides the effect mixture ratio has upon performance, the probability of chugging increases at off-mixture ratio conditions for a given injector configuration because of changes in injector pressure drops. Because of the M-1 gas generator prototype valve flow characteristics, the ignition mixture ratio was approximately 0.35 and remained at a relatively low value for about approximately 1/2 sec before the steady-state design mixture ratio of 0.80 was achieved. The low mixture ratio decreased oxidizer injection $\triangle P$, which tended to induce chugging. Thus, at least the following four separate but simultaneous effects tended to induce instability at low mixture ratio: (1) lower mixture ratio increased combustion sensitivity to oxidizer flow; (2) low mixture ratio decreased oxidizer injection $\triangle P_o$ to P_c ratio, which lessened liquid oxygen chugging stability margins; (3) lower oxidizer flowrate decreased oxidizer injection velocity; (4) lower oxidizer injection velocity increased injection velocity ratio. All four effects are suspected of inducing low frequency combustion oscillations.

During M-1 gas generator assembly testing, an attempt was made to solve three of the four unstabilizing effects during the start transient. It had previously been determined that the injection of a third gaseous medium into one of the injector manifolds could prevent chugging[12]. This gaseous medium augmentation consisted of

[12] Morrell, G., Rocket Thrust Variation with Foamed Liquid Propellant, NASA RM 56K27, 1957.

injecting high pressure (approximately 1500 psia) ambient temperature gaseous helium into the oxidizer injector manifold during the start transient. The helium gas decreased the mean oxidizer injection density which resulted in an increase in the oxidizer injector pressure drop, an increase in the oxidizer injection velocity, and a decrease in the injection velocity ratio. Gaseous helium augmentation successfully damped the chugging in the first three gas generator development tests with prototype valves. Having successfully demonstrated the concept, turbopump development testing was initiated.

The hot gas test facility exhaust duct downstream of the sonic nozzle at the gas generator outlet was replaced with the turbine inlet test manifold. This was the only change made to either the test hardware or test facility. Gaseous helium augmentation was incorporated during the start transient. Nevertheless, chugging was encountered during the start transient. During some tests, the start transient chugging amplitude momentarily exceeded $\pm$200 psi at approximately 250 cps and 700 psi mean chamber pressure. The gas generator propellant tank pressures were ramped to more nearly duplicate the engine start transient and minimize turbine acceleration rates during turbopump development testing.

At ignition (lowest mixture ratio), the chugging frequency normally ranged from 280 to 250 cps. As mixture ratio increased, the chugging frequency steadily decreased to approximately 180 cps. Throughout most of this portion of the test the oxidizer injector manifold pressure was approximately 180 degrees out-of-phase with chamber pressure. Fuel injector manifold pressure was very nearly in phase with chamber pressure. At steady-state conditions, a low amplitude random in-and-out type of oscillation occurred at 100 to 120 cps with both injector manifold pressures and chamber pressure all in phase. The decrease in chugging frequency with increasing mixture ratio appears to exclude the possibility of hot gas acoustic resonance effects. The increasing mixture ratio should increase hot gas sonic velocity and if anything, increase resonance frequencies. When long, hot gas ducts become a part of the test facility or engine configuration, it is possible for hot gas acoustic resonance frequencies to reinforce low frequency combustion feedback gains at chugging frequency ranges (e.g., chugging of S/N 017A gas generator assembly at 200 to 220 cps corresponded to the first longitudinal mode of the 10-ft long development gas duct as well as low frequency combustion oscillations). Whatever the cause of chugging could have been, it was not known why the oscillation problem did not occur earlier during the development testing of gas generator assemblies when the helium augmentation appeared to be effective or why low frequency combustion instability occurred during later turbopump development tests when test conditions and procedures were duplicated. Some data indicate that the characteristic chamber length (L^* = chamber volume/nozzle throat area) affects low frequency combustion stability. Excellent low frequency stability was demonstrated during the initial tests with S/N 022 at the gas generator assembly development test stand at an L^* of approximately 250-in. Excellent stability was again demonstrated during the checkout test series at the oxidizer turbopump development test stand at an L^* of 50-in. when gaseous helium augmentation was incorporated. However, low frequency oscillations occurred at an L^* of 50-in. with gaseous helium augmentation during the oxidizer turbopump, fuel turbopump checkout, and fuel turbopump development test

series. When the gas generator assembly stabilizing nozzle was removed for one fuel turbopump test (see Figure No. 22) to effectively increase L*, the oscillation was greatly attenuated. Supposedly, the sonic nozzle at the gas generator outlet isolated the downstream gas geometry change from the gas generator combustion feedback system. Review of the average pressure data across the stabilizing nozzle indicated that the pressure ratio was adequate to maintain sonic flow. However, this does not necessarily preclude the possibility that the nozzle could not have been momentarily unchoked by adverse fluctuations in the pressure gradient across the throat.

When the oscillatory problem persisted, an oxidizer hardening orifice was installed between the oxidizer valve outlet and gas generator oxidizer manifold inlet. The combustion oscillations continued and the oscillatory frequency remained unchanged. However, the amplitude of oscillations was decreased to one third or one half of the original unorificed combustion oscillation amplitudes. Thus, the turbopump development test series were completed.

In retrospect, part of the low frequency combustion oscillation problem with S/N 022 gas generator assembly could have resulted from the attempt to assure an adequately high injection velocity ratio. Certain facts result from direct point-by-point comparison of test data for S/N 018 and 022 gas generator assemblies. A lower injection velocity ratio was designed for S/N 018. Although oxidizer injection $\triangle$Po was lower on S/N 018, the available drop was located at the injector face, whereas with S/N 022 element design the oxidizer pressure drop was taken 2-in. upstream of the injector face. However, S/N 018 was never tested at high (1145 psia) chamber pressures. No oxidizer element capacitance occurred downstream of S/N 018 oxidizer element $\triangle$P insert. The downstream oxidizer couterbore diameter of S/N 022 injection element is nearly twice its metering orifice diameter and 2-in. long. There is no real assurance that the counterbore cavity flowed full at the injection exit during all times or that the injection flowrate was steady. For future element designs, the effect of moving the injection pressure drop closer to the injector face should be investigated and the counterbore expansion ratio should be decreased to provide greater assurance of filling the counterbore and minimizing possible oxidizer flow fluctuations caused by variable wetting of the counterbore wall.

IV. CONCLUSIONS

The application of design criteria for the injection element design of coaxial elements obtained from systems operating at mixture ratios of approximately 5, resulted in a successful gas generator operating at a mixture ratio of 0.6 to 1.0.

Adequate temperature distribution and performance can be obtained with elements having a total flow of 1.7 lb/sec per element, with the oxidizer injection element recessed 0.200-in. and a hydrogen-to-oxidizer velocity ratio of 10.

The amplitude of low frequency pressure oscillations during transients can, in some cases, be reduced by adding gaseous helium to the injected oxidizer to maintain injection pressure drops while oxidizer flowrates are low.

V. RECOMMENDATIONS

The primary objective of the M-1 gas generator development program was to provide a 120,000 hp liquid oxygen/liquid hydrogen gas generator for development testing of turbopump assemblies for the M-1 engine. All testing and development efforts were directed toward the attainment of that goal. Any observations made concerning liquid oxygen/liquid hydrogen performance were taken from the available test data obtained during the pursuit of the primary objective. No effort was made to conduct special tests to either prove or disprove any premises. Should a research program be contemplated to more fully understand liquid oxygen/liquid hydrogen combustion phenomena, it is recommended that one field of endeavor be devoted to injection velocity ratio implications upon both high frequency and low frequency combustion instability.

Specifically, injection velocity ratio or differential injection velocity effects upon liquid phase mixing and oxidizer droplet vaporization phenomena should be examined. The effect of varying mixture ratio and propellant density over a wide range may alter the over-all picture of the phenomena now defined as injection velocity ratio. Interaction of velocity ratio and oxidizer element recess effects need to be studied.

For M-1 gas generator test conditions, 10 was the velocity ratio above which all screeching was spontaneously suppressed in unbaffled injectors. This value could change if operating conditions are altered. The effect that propellant transport properties have upon liquid phase propellant mixing, vaporization rates and combustion characteristics should be determined.

Limited test data indicated that chugging was more severe at high injection velocity ratios but it may have been caused by low oxidizer injection velocity and resultant low oxidizer Reynold's numbers and poor stream breakup.

If S/N 018 gas generator assembly had been tested without baffles and screeching occurred, and if S/N 022 gas generator assembly had been tested without baffles and screeching had not occurred, the injection velocity ratio hypothesis regarding high frequency combustion instability could have been either proven or disproven. Furthermore, if unbaffled S/N 022 gas generator assembly could be pulsed to induce screeching, it could be determined by observing its recovery characteristics whether it was significant that S/N 007, 004A, 015, and 020 all spontaneously suppressed screeching at high injection velocity ratios.

The development of the coaxial injector concept for future liquid oxygen/liquid hydrogen gas generators should be continued. Until results are available from the above recommended studies, it is suggested that design injection velocity ratios of approximately 10 be used. If high velocity ratio studies appear promising or if higher combustion performance is desired within a shorter combustor length, evaluation of unbaffled injector designs should be considered. Doing away with the baffles will allow the elimination of baffle film cooling, which will result in a more uniform gas temperature distribution. The coaxial injection element with the

fuel annulus outermost will offer the best injector erosion resistance because the excess fuel serves as a shield around the combustion gases. Coaxial elements should be designed for low thrust per element, (i.e., use many elements per injector). This allows better mixing and more uniform temperature distribution and thus, a higher design gas generator mixture ratio which, in turn, aids in eliminating chugging and improves over-all engine performance.

If chugging remains a serious problem, it may be necessary to compromise and design injection elements for lower injection velocity ratios than recommended above and use injector baffles to prevent transverse high frequency combustion instability. The injection element pressure drop should be located as close to the injector face as possible, consistent with a high injection velocity ratio design. This is especially necessary for the oxidizer circuit. By decreasing the propellant capacitance between the pressure drop and the combustion flame front to a minimum, maximum advantage is derived from the available pressure drop to prevent chugging.

It is essential that the oxidizer injector manifold volume be minimized consistent with uniform oxidizer injection distribution. The oxidizer manifold volume acts as a capacitance which tends to offset the effect of upstream feedline pressure drops in the prevention of chugging. If the feed system is too "soft", feedback gain may occur and increase the possibility of chugging. Furthermore, the residual oxidizer left in the manifold at the end of the test must be disposed of if post-test temperature spikes are to be avoided. Because of the radical difference in liquid oxygen and liquid hydrogen densities, unless the fuel manifold volume is considerably larger than that of the oxidizer, either a gaseous post-test injector manifold purge or a long fuel delay must be used to avoid an oxidizer-rich shutdown with high temperature spikes.

To prevent unwanted combustion temperature excursions or transient chugging phenomena, it may be desirable to achieve the constant design injection mixture ratio throughout the start transient, steady-state operation, and shutdown transient. Consideration must be given to the transient feed pressures, transient propellant densities, and injector manifold volumes when designing the gas generator valve to obtain the flow characteristics necessary to achieve a constant mixture ratio. A fuel lead during start and a fuel lag for shutdown is always necessary during the transients for fuel-rich gas generators. The valve should be designed to obtain flow characteristics and injector manifold volume ratio necessary to eliminate the requirement for gaseous helium augmentation and post-test injector manifold purges.

Chugging considerations should be of prime importance in the design of engine feed and hot gas systems. The over-all feed system and hot gas system resonances with their impedance effect upon feedback gain to the gas generator injector must be considered for the possible range of chugging frequencies.

BIBLIOGRAPHY

1. Bartz, D. R., A Simple Equation for Rapid Estimation of Rocket Nozzle Convective Heat Transfer Coefficients, Jet Propulsion, Journal of the American Rocket Society; January 1957

2. Crocco, L. and Cheng, S. I., Theory of Combustion Instability in Liquid Propellant Rocket Motors, Butterworths Scientific Publications; London, 1956

3. Hatch, J. E., and Papell, S. S., Use of a Theoretical Flow Model to Correlate Data for Film Cooling or Heating an Adiabatic Wall by Tangential Injection of Gases of Different Fluid Properties, NASA TN D-130; 1959

4. Hersch, M., Effect of Interchanging Propellants on Rocket Combustor Performance with Coaxial Injection, NASA TN D-2169, 1964

5. Hurrell, H. G., Analysis of Injection-Velocity Effects on Rocket Motor Dynamics and Stability, NASA TR R-43, 1959

6. Ingard, U., "On the Theory and Design of Acoustic Resonators"; The Journal of the Acoustical Society of America, November, 1953

7. Morrell, G., Rocket Thrust Variation with Foamed Liquid Propellant, NASA RM 56K27, 1957

8. Reardon, F. H., Investigation of Transverse Mode Combustion Instability in Liquid Propellant Rocket Motors, Princeton University, 1961

9. Rouse, H., et al, Advanced Mechanics of Fluids; John Wiley & Sons, Inc., New York, 1959

10. Sekas, N. J. and Acker, L. W., Design and Performance of a Liquid-Hydrogen, Liquid-Oxygen gas Generator for Driving a 1000-Horsepower Turbine, NASA TN D-1317; 1962

11. Wenzel, L. M. and Szuch, J. R., Analysis of Chugging in Liquid Bi-Propellant Rocket Engines Using Propellants with Different Vaporization Rates, NASA TN D-3080, 1965

12. Wieber, P. R., Calculated Temperature Histories of Vaporizing Droplets to the Critical Point, AIAA Journal, December 1963

W. F. Dankhoff (5 Copies)
NASA
Lewis Research Center
21000 Brookpark Road
Cleveland, Ohio 44135
Mail Stop 500-305

J. A. Durica (1 Copy)
Mail Stop 500-210

Patent Counsel (1 Copy)
Mail Stop 77-1

Lewis Library (2 Copies)
Mail Stop 3-7

Lewis Technical Information Division (1 Copy)
Mail Stop 5-5

W. E. Conrad (1 Copy)
Mail Stop 100-1

R. J. Priem (1 Copy)
Mail Stop 86-5

Office of Reliability and Quality
Assurance (1 Copy)
Mail Stop 500-203

W. W. Wilcox (1 Copy)
Mail Stop 500-305

A. Fortini (1 Copy)
Mail Stop 500-305

NASA (6 Copies)
Scientific and Technical Information
Facility
Box 5700
Bethesda, Maryland

NASA (1 Copy)
Library
Ames Research Center
Moffett Field, California 94035

Library (1 Copy)
NASA
Flight Research Center
P. O. Box 273
Edwards AFB, California 93523

Library (1 Copy)
NASA
Goddard Space Flight Center
Greenbelt, Maryland 20771

Library (1 Copy)
NASA
Langley Research Center
Langley Station
Hampton, Virginia 23365

Library (1 Copy)
NASA
Manned Spacecraft Center
Houston, Texas 77058

Library (1 Copy)
NASA
George C. Marshall Space Flight Center
Huntsville, Alabama 35812

Library (1 Copy)
NASA
Western Operations
150 Pico Boulevard
Santa Monica, California 90406

Library (1 Copy)
Jet Propulsion Laboratory
4800 Oak Grove Drive
Pasadena, California 91103

A. O. Tischler (1 Copy)
Code RP
NASA
Washington, D. C. 20546

J. W. Thomas, Jr. (5 Copies)
I-E-E
NASA
George C. Marshall Space Flight Center
Huntsville, Alabama 35812

E. W. Gomersall (1 Copy)
NASA
Mission Analysis Division
Office of Advanced Research and Technology
Moffett Field, California 94035

Major E. H. Karalis (1 Copy)
NASA
Lewis Research Center
AFSC Liaison Office
21000 Brookpark Road
Cleveland, Ohio 44135
Mail Stop 4-1

Dr. A. Acosta (1 Copy)
California Institute of Technology
1201 East California Street
Pasadena, California

Dr. E. B. Konecci (1 Copy)
National Aeronautics and Space Council
Executive Office of the President
Executive Office Building
Washington, D. C.

H. V. Main (1 Copy)
Air Force Rocket Propulsion Laboratory
Edwards Air Force Base
Edwards, California

Aerospace Corporation (1 Copy)
2400 East El Segundo Boulevard
P. O. Box 95085
Los Angeles, California 90045

J. Farrel (1 Copy)
R. Harvey (1 Copy)
Arnold Engineering Development Center
Arnold Air Force Station
Tullahoma, Tennessee

Bell Aerosystems Company (1 Copy)
P. O. Box 1
Buffalo, New York

Chemical Propulsion Information Agency (1 Copy)
John Hopkins University
Applied Physics Laboratory
8621 Georgia Avenue
Silver Spring, Maryland

Flight Propulsion Laboratory Department (1 Copy)
General Electric Company
Cincinnati, Ohio

General Dynamics/Astronautics (1 Copy)
Library and Information Services (128-00)
P. O. Box 1128
San Diego, California 92212

Technical Information Center (1 Copy)
Lockheed Missiles and Space Company
P. O. Box 504
Sunnyvale, California

Martin Denver Division (1 Copy)
Martin Marietta Corporation
Denver, Colorado 80201

North American Aviation, Inc. (1 Copy)
Space and Information Systems Division
Downey, California

Pratt and Whitney Aircraft
Corporation (1 Copy)
Florida Research and Development
Center
P. O. Box 2691
West Palm Beach, Florida 33402

Reaction Motors Division (1 Copy)
Thiokol Chemical Corporation
Denville, New Jersey 07832

Library Department 586-306 (1 Copy)
Rocketdyne
Division of North American Aviation
6633 Canoga Avenue
Canoga Park, California 91304

Space Technology Laboratories (1 Copy)
Subsidiary of Thompson-Ramo-Wooldridge
P. O. Box 95001
Los Angeles, California

Stanford Research Institute (1 Copy)
333 Ravenswood Avenue
Menlo Park, California 94025

Thompson-Ramo-Wooldridge, Inc. (1 Copy)
23555 Euclid Avenue
Cleveland, Ohio 44117

M. Sumnerfield (1 Copy)
L. Crocco (1 Copy)
Princeton University
Princeton, New Jersey 08540

Library-Documents (1 Copy)
Aerospace Corporation
2400 East El Segundo Boulevard
P. O. Box 95085
Los Angeles, California 90045

AEOIM (1 Copy)
Arnold Engineering Development Center
Air Force Systems Command
Tullahoma, Tennessee 37389

AFRSTD (1 Copy)
Headquarters, U. S. Air Force
Washington, D. C. 20339

Wright Patterson Air Force Base (1 Copy)
Dayton, Ohio 45433

U. S. Army Missile Command (4 Copies)
Redstone Scientific Information Center
Redstone Arsenal, Alabama 35808
Attn: Chief, Document Section

Dr. B. H. Goethert (1 Copy)
Chief Scientist
ARO, Incorporated
Arnold Engineering Development Center
Arnold AF Station, Tennessee 37389

T. Reinhardt (1 Copy)
Bell Aerosystems Company
P. O. Box 1
Buffalo, New York 14205

Technical Library (1 Copy)
Commander
U. S. Naval Missile Center
Point Mugu, California 93041

Library (1 Copy)
NASA
John F. Kennedy Space Center
Cocoa Beach, Florida 32931

M. J. Zucrow (1 Copy)
Purdue University
Lafayette, Indiana 47907

STL Tech. Lib. Doc. Acquisitions (2 Copies)
Space Technology Laboratory, Inc.
1 Space Park
Redondo Beach, California 90200